University of Southern Queensland

Faculty of Engineering and Surveying

Effect of Existing Cracks in Shear Strengthening of Concrete Girders with External Post-tensioning

A dissertation submitted by

Steven Luther

in fulfilment of the requirements of

Courses ENG4111 and 4112 Research Project

towards the degree of

Bachelor of Engineering (Civil)

Submitted: October, 2005

Abstract

Deteriorated bridges all around the world are in need of replacement, or repair and strengthening. This damage is commonly caused by the overloading of bridges, due to the increasing size of heavy vehicles using the bridges today. Full bridge replacement poses the problems of high cost and disruption to traffic, so suitable methods of repair and strengthening are required.

A common deterioration of these bridges is shear cracking. External post-tensioning is a method of shear strengthening girders, but existing shear cracks can limit the effectiveness of the external post-tensioning. Epoxy injection is a method of structurally repairing cracks, which could possibly be used to repair the shear cracks. If effective, this would allow the post-tensioning to effectively strengthen the member. This project is studying the shear strengthening of concrete girders using external post-tensioning, with existing shear cracks repaired with epoxy injection.

This research investigates the combined repair method with experimental testing of four rectangular beams. Two of the beams were preloaded to form shear cracks, with the first strengthened only with post-tensioning. The other preloaded beam had its shear cracks repaired with epoxy injection, and was then post-tensioned. After post-tensioning, both of these beams were loaded until ultimate failure. The results from these two beams were compared to a reinforced control beam, and a post-tensioned control beam. These comparisons were made to evaluate the effectiveness of the combined repair method.

The results from this testing indicate that applying post-tensioning alone to a shear cracked girder will not increase the member's capacity, as the cracks cause the post-tensioning to be ineffective. The testing did show that by combining external post-tensioning with epoxy injection of the existing cracks, a deteriorated girder will have a significant increase in shear capacity. Hence, this combined rehabilitation technique has been shown to be an effective method of shear strengthening.

University of Southern Queensland

Faculty of Engineering and Surveying

ENG4111 & ENG4112 *Research Project*

Limitations of Use

The Council of the University of Southern Queensland, its Faculty of Engineering and Surveying, and the staff of the University of Southern Queensland, do not accept any responsibility for the truth, accuracy or completeness of material contained within or associated with this dissertation.

Persons using all or any part of this material do so at their own risk, and not at the risk of the Council of the University of Southern Queensland, its Faculty of Engineering and Surveying or the staff of the University of Southern Queensland.

This dissertation reports an educational exercise and has no purpose or validity beyond this exercise. The sole purpose of the course pair entitled "Research Project" is to contribute to the overall education within the student's chosen degree program. This document, the associated hardware, software, drawings, and other material set out in the associated appendices should not be used for any other purpose: if they are so used, it is entirely at the risk of the user.

Prof G Baker
Dean
Faculty of Engineering and Surveying

Certification

I certify that the ideas, design and experimental work, results, analyses and conclusions set out in this dissertation are entirely my own effort, except where otherwise indicated and acknowledged.

I further certify that the work is original and has not been previously submitted for assessment in any other course or institution, except where specifically stated.

Steven Luther

Student Number: Q12216898

_____
Signature

_____
Date

Acknowledgements

The author would like to express sincere gratitude to his supervisor Dr. Thiru Aravinthan for his guidance and support throughout the course of this project.

This research involved a large portion of experimental investigation, and so required a great deal of assistance throughout. Many thanks are directed to Glen Bartowski, Bernhard Black, Dan Eising and Mohan Trada for their invaluable assistance during the construction and testing stages of this research.

The author also wishes to thank his fellow peers, Kumaran Sumakaran and Paul Harbour, for their kind assistance throughout the course of this project.

Mr Steven Luther
October, 2005.

Contents

List of Figures

List of Tables

Nomenclature

A_g = gross cross-sectional area

A_{pt} = cross-sectional area of prestressing steel

A_{sc} = cross-sectional area of compressive reinforcement

A_{st} = cross-sectional area of tensile reinforcement

A_{sv} = cross-sectional area of shear reinforcement

A_{sv-min} = cross-sectional area of minimum shear reinforcement

A_{sv-max} = cross-sectional area of maximum shear reinforcement

α_v = distance from load point to nearest support

b = width of rectangular cross-section

b_{ef} = effective width of the compression face

b_v = effective width of web for shear (equal to b for rectangular cross-sections)

C_c = compressive force in the concrete

C_s = compressive force in the compressive reinforcement

D = depth of section

d = depth to resultant force in tensile steel at M_u

d_n = depth to neutral axis in a section

d_o = distance from the extreme compressive concrete fibre to the centroid of the outer most layer of tensile reinforcement

d_p = depth to the prestressing steel

d_{sc} = depth to centre of compressive reinforcement

d_{st} = depth to centre of tensile reinforcement

e = eccentricity of prestressing force from the centroidal axis of the section

E_s = Young's modulus of steel

f'_c = characteristic compressive cylinder strength of concrete at 28 days

f_{py} = yield strength of prestressing steel

f_{sy} = yield strength of reinforcing steel

$f_{sy.f}$ = yield strength of shear reinforcement

I_g = second moment of area of the uncracked section

k_u = ratio of neutral axis depth to outer most layer of tensile steel depth

L = distance between supports

M_{dec} = decompression moment

M_u = ultimate moment capacity

P = prestressing force

P_u = theoretical ultimate load capacity of a beam

$P_{u.f}$ = theoretical ultimate flexural capacity load of a beam

$P_{u.s}$ = theoretical ultimate shear capacity load of a beam

P_{ue} = experimental ultimate load capacity of a beam

P_v = vertical component of prestressing force

s = spacing of shear reinforcement

T_p = tensile force in prestressing steel

T_s = tensile force in tensile reinforcement

V_{dec} = shear force at decompression moment

V_u = ultimate shear strength

V_{uc} = concrete component of ultimate shear strength

V_{us} = shear reinforcement contribution to ultimate shear strength

y_b = distance from centroidal axis to bottom fibre

$\beta_1 \beta_2 \beta_3$ = multiplying factors for determining V_{uc}

γ = ratio of the depth of the assumed rectangular compressive stress block to d_n at M_u

γ_{xy} = shear strain

ε_{max} = maximum principal strain

ε_{min} = minimum principal strain

ε_{sc} = strain in the compressive reinforcement

ε_{st} = strain in the tensile reinforcement

ε_u = extreme compressive fibre strain at ultimate strength in pure bending

θ_v = angle between the concrete compression strut and the longitudinal axis of the beam

$\sigma_{p.ef}$ = effective stress in the prestressing steel

σ_{pu} = ultimate stress in the prestressing steel

CHAPTER 1

INTRODUCTION

1.1   Background

Deteriorated bridges all around the world are in need of replacement, or repair and strengthening.   Full bridge replacement poses the problems of high cost and disruption to traffic, so suitable methods of repair and strengthening are required.

A common deterioration of these bridges is shear cracking. This is commonly caused by overloading of the bridges, due to the ever increasing size and number of heavy vehicles using the bridges today. These cracks lower a member's ultimate shear capacity, reduce its stiffness, and leave the reinforcement exposed to the weather. If these cracks are left long enough, the reinforcement can corrode away, further reducing the member's capacity, and therefore increasing the likelihood of ultimate failure. For these reasons, the cracks need to be repaired, and the member strengthened to avoid further cracking from the current or future loadings.

Epoxy injection appears a good way to structurally repair the cracks, and protect the reinforcement, as it has been used to seal concrete cracks where an impermeable surface is required.

Post-tensioning is a method being looked at to strengthen members, as repaired members will require higher capacities than originally designed for, due to the increased loading. Previous research has indicated that post-tensioning a member with existing shear cracks, may not increase the member's shear capacity. This is thought to be due to the lack of aggregate bond between the cracked surfaces, which may be overcome by epoxy injection of the cracks.

This project is specifically looking at the effect of existing cracks on shear strengthening of concrete girders with external post-tensioning. The use of epoxy injection of the cracks will be combined with external post-tensioning to evaluate the strength gained from this combined repair method.

1.2   Strengthening Techniques

The two strengthening techniques to be used in this research are external post-tensioning, and epoxy injection of cracks. This section will introduce what both techniques are.

1.2.1   External Post-tensioning

External post tensioning is the method of applying a compressive force to a member through tendons not attached to the member. The force in the tendons is transferred to the concrete member by the end anchorage, which are commonly plates bolted on the end. External post tensioning has commonly been used to increase the flexural and shear capacities of new reinforced beams. It has been found to be a versatile method of applying the compressive force, and has many advantages over internal stressing. The external tendons do not require grouting, and the applied force can be changed throughout a member's design life. The eccentricity of the post-tensioning force can also be adjusted at critical positions of the member, to maximise its effectiveness. Deviators can be used at critical locations along a beam to control the change in eccentricity. A disadvantage of external post-tensioning is if steel tendons are used, they need to be protected from the weather, to avoid corrosion. External post-tensioning also uses space around the concrete member, which is not always available. Overall, external post-tensioning can be an effective way to increase a member's capacity.

1.2.2   Epoxy Injection of Cracks

Epoxy injection is a method of structurally rebonding cracks in concrete. The epoxy is pressure injected into the cracks to form a bond with each concrete surface when set. It is good for structural repair, as it has tensile and compressive strengths greater than concrete. According to Epoxysystems (2001), epoxy used for bonding concrete cracks has a tensile strength of 34-55 MPa, and a compressive strength of 70-80 MPa. Due to the strong bond formed with concrete, and the high strength characteristics of epoxy, cracked members repaired with epoxy injection should regain their original strength.

1.3   Project Aim and Scopes

This project aims to investigate the shear strengthening of concrete girders using epoxy injection and external post tensioning. This will predominantly be done through experimental tests conducted on four model beams. It will also involve reviewing related research, and comparing the experimental data obtained to Australian Standard design procedures.

To achieve these aims, the following objectives had to be met:

1.   Research and review background information on the shear strengthening of concrete girders using epoxy injection and external post-tensioning.

2.   Design model test beams for experimental investigations, taking into account previous test results.

3.   Prepare model beams, and arrange testing devices.

4.   Conduct tests on the model beams, and record observed results.

5.   Evaluate and analyse the test results of the different model beams.

6.   Arrive at a conclusion for the project, which will better explain the shear behaviour of rehabilitated girders using epoxy injection and external post-tensioning.

1.4   Structure of Dissertation

The investigation of the shear strengthening of concrete girders using external post-tensioning and epoxy injection of cracks will involve reviews of related studies, experimental testing, and analysis of results. This section outlines the structure of the dissertation.

Chapter 2 contains reviews of previous research conducted on shear strengthening of concrete members with external post-tensioning and epoxy injection of cracks. As little research has been done on this combined strengthening method, research on both strengthening methods is also reviewed individually. The AS3600 shear strength prediction equations are also shown in this section.

Chapter 3 contains the design of the specimens to be used for the experimental testing.

Chapter 4 explains the methodology used for the experimental testing. This involves the construction of the test specimens, the loading setup and procedure, the application of the external post-tensioning, and the method used for epoxy injection of the cracks.

Chapter 5 involves the analysis and discussion of results. It also compares the experimental results to AS3600 predictions, to analyse the validity of the prediction equations for strengthening applications.

Chapter 6 provides a summary of the research project conducted, and the conclusions gained from it. Recommendations are given on the use of the strengthening method, and areas for further related research are highlighted.

The appendices provide supporting material to the research. These include the project specification, the end anchorage plate capacity check, strain gauge data sheets, material data sheets for the epoxy, and a risk assessment for testing.

1.5 Summary

Due to the increasing number of deteriorated bridge structures around the world, cost effective methods of rehabilitation are needed. For the specific problem of concrete girders with shear cracking, combining epoxy injection of cracks with external post-tensioning is a possible option. This research project will conduct experimental testing to evaluate this repair and strengthening technique.

CHAPTER 2

LITERATURE REVIEW

2.1 Problem That Exists

Many concrete bridges around the world are in need of repair. Most of these bridges
have cracking that renders them unserviceable, and subsequently have reduced
ultimate load carrying capacity.   These bridges need to be either replaced, or
repaired and strengthened to adequately service the traffic loading.

Klaiber et al (1989) reports that over 200,000 bridges in the USA are in need of
repair. Most of these bridges have either flexural or shear cracks that need to be
repaired to protect the reinforcement from corrosion, and reduce deflections to
below serviceable limits. This has occurred due to increased number and size of
heavy vehicles using the bridges. These bridges would have been designed for
smaller loadings, so the serviceability design loads are frequently being exceeded.
Pisani (1999) reports that some bridges are frequently being loaded to near their
ultimate design load. This first occurred in military areas, but is now occurring more
on general roads. This type of loading causes cracking to occur.

Totally replacing a bridge is a measure that is usually put off as long as possible.
This is due to the major disruption to traffic flow it causes, and the high costs
involved. This is why shear strengthening of bridge members is important, and why
epoxy injection and external post tensioning appears an attractive solution. It would
require minimal traffic closures, and would be significantly cheaper. For these
reasons, the effectiveness of this method should be assessed.

Little research has been done on shear strengthening of beams using epoxy injection
combined with external post tensioning. The small amount of research conducted in

this area has been carried out at USQ in 2003 and 2004. For this reason, the research on the combined strengthening method will be reviewed, as well as research on either method individually.

2.2   Epoxy Injection Combined with External Post-tensioning

Alam (2004) studied the effect of epoxy injection on the shear strengthening of small scale concrete girders. The specimens used in this research were rectangular in cross section, 250mm x 100mm. The small size of the specimens was found to have a large effect on the capacity of the beams. Premature failure occurred during the testing of a number of the beams, due to the small section size and low amount of cover. This amounted to some of the beams failing due to compressive rupture at the top face, instead of a pure shear failure. This research also highlighted how the strength of the concrete greatly influences the capacity of the girders, as the ordered ready-mix concrete for each of the specimens varied greatly in strength. Due to the large variation in concrete strengths, an assessment of the shear strengthening technique was unable to be concluded definitively. The research did indicate increased shear capacity may be gained from the combined strengthening technique.

Woods (2004) conducted model testing of a bridge headstock repaired by epoxy injection and external post-tensioning. He found that by repairing the existing shear cracks with epoxy injection, and then post-tensioning, significant increases in ultimate capacity and stiffness were achieved. He also strengthened one of the cracked model headstocks with just post-tensioning, with a slight increase in capacity found.

Jobling (2004) conducted model testing on the same bridge headstocks. He also used epoxy injection to rehabilitate the shear cracks, but used a fibre wrap for the external post-tensioning. He found this too was an effective way to shear strengthen the headstocks.

This research aims to find whether the strength increase in headstocks gained from the combined repair technique, can be translated to girders, which have a larger span to depth ratio.

2.3   External Post-tensioning

There has been extensive research into the flexural strengthening of concrete bridges using external post tensioning, but little on shear strengthening.

Pisani (1999) found that applying post tensioning to a beam without shear cracking, increases the shear capacity of the beam. This points towards post tensioning increasing a damaged member's shear capacity, if the shear cracks are successfully repaired with epoxy.

Haraji (1993) studied the strengthening of concrete beams by external prestressing. Through flexural testing of 16 beams, he found up to 146% increase in flexural strength, and deflections reduced by up to 25%, due to prestressing. He reported that external prestressing is an effective way to control cracks and re-establish service load deflections. Members subject to external prestressing also had a prolonged fatigue life, by reducing the stress levels in the internal tensile reinforcement. He also reported that straight tendons were less effective in increasing flexural resistance, compared to tendons with a deviated profile.

Tan and Ng (1997) found that deviators and tendon configuration heavily affect the behaviour of externally prestressed beams. Without deviators, the tendons are free to move and change eccentricity when under load, thus inducing second order effects. The reduced eccentricity of the applied prestressing causes a reduction in flexural capacity. He reported that one deviator is sufficient for a beam with a span-to-depth ratio of up to 15, to minimise second order effects. The only effect this has on this research project is that the flexural capacity of the beams may be less than the predicted, as rods with no deviators will be used for post tensioning. To ensure

the beams fail in shear, the shear capacity load of the beams will be significantly less than the predicted flexural capacity load.

Tan and Ng (1998) also studied the effect of shear in externally prestressed beams. They found that if deviators were not used, significant second order effects were found, resulting in the beam's shear capacity reducing. If deviators are used, the beam's behaviour follows that of a prestressed beam with internally unbonded tendons. If second order effects are minimised, the strength and failure mode can be predicted using the strut-and-tie model.

Tan and Naaman (1993) proposed a model based on the strut-and-tie method, to define a safe domain of loading for simply supported, externally prestressed beams. They used the model to predict the failure mode, either crushing of the diagonal concrete compression strut, yielding of the shear reinforcement, yielding of the internal tensile reinforcement, or yielding of the external prestressing. The first two modes are shear type failures, while the last two are flexural failures. The prediction of failure mode was based on the shear span to depth ratio, ratio of the loading platen width to beam depth, longitudinal reinforcement, shear reinforcement, ratio of effective depths of reinforcement to beam depth, and the path of the external prestressing. The major point from this research is that the application of external prestressing to strengthen an existing structure may result in a mode of failure different to what is expected from the original structure. This is important, as shear type failures are brittle while flexural failures are more ductile.

AS3600 Clause 8.1.6 states that for a beam with a span-to-depth ratio of 35 or less, the stress in a tendon not yet bonded at ultimate strength, shall be determined from

$$\sigma_{pu} = \sigma_{p.ef} + 70 + \left(\frac{f'_c \cdot b_{ef} \cdot d_p}{100.A_{pt}} \right) \leq \sigma_{p.ef} + 400$$

and for a beam with a span-to-depth ratio of greater than 35

$$\sigma_{pu} = \sigma_{p.ef} + 70 + \left(\frac{f'_c \cdot b_{ef} \cdot d_p}{300.A_{pt}} \right) \leq \sigma_{p.ef} + 200$$

Where,

$\sigma_{p.ef}$ = effective prestress

f'_c = 28 day concrete compressive strength

b_{ef} = effective width of the compression face

d_p = depth to prestress tendons

A_{pt} = Area of prestressing tendon

In both cases, σ_{pu} is not to be taken greater than the tendon yield strength, f_{py}. These equations are used to select the prestressing tendon size for each application.

2.4   Epoxy Repairing

There has been little research done on the shear strengthening of girders using epoxy injection, but there have been a number of related studies done in other applications. These include flexural strengthening, and repair of concrete joints.

Chung (1975) conducted tests on reinforced concrete beams which had flexural cracks repaired with epoxy injection. He found that the capacity gained was the same or slightly higher than the original beams. He also noted the cracks reformed away from the previous cracks that were repaired, but the permanent deflection the beams had could not be eliminated by the repair.   This study showed the effectiveness of bonding cracks with epoxy, and that the tensile bond strength was higher than the surrounding concrete. As the permanent deflection could not be eliminated, adding post tensioning to the process may be beneficial.

Chung and Liu (1977) conducted tests on the shear strength of epoxy-repaired concrete joints. They used epoxy injection to bond two concrete surfaces (1 smooth, 1 rough), then loaded the specimen to create a shearing effect along the plane of the joint. They found the repaired joint had increased shear resistance. The joints showed no sign of distress with 5 MPa shear stress applied, but the surrounding

concrete did fail in shear. This indicates an epoxy bonded crack would have greater shear strength than the surrounding concrete.

French, Torp and Tsai (1990) conducted tests on the epoxy repair of a beam-column sub assemblage damaged from a moderate earthquake. They compared the pressure injection technique with the vacuum impregnation technique for applying the epoxy. They found both methods were effective in repairing the cracked region, but the vacuum impregnation technique was more effective for large regions of cracks. This is because it can fill offshoot cracks where the other method is unable to. This enables the vacuum impregnation technique to fill whole regions at once, where as the pressure injection method needs to be applied to each crack. The testing of the sub assemblage showed:

- The repaired structures were 2.5-3 times stiffer than the damaged structure, and had 85 percent of the original structures stiffness.
- The bond between the reinforcement and the concrete which had originally failed was restored.
- As in other studies, repaired cracks did not reform, instead new cracks formed adjacent to them.

2.5   Shear Capacity Predictions

AS3600 Clause 8.2.2 states the design shear strength of a beam shall be taken as φV_u
Where,

$$V_u = V_{uc} + V_{us}$$

φ = 0.7 (strength reduction factor used for shear strength in limit state design)

Here,

V_{uc} = Shear resisted by concrete and longitudinal bars

V_{us} = Shear resisted by ligatures

The shear force resisted by the ligatures is the same for both reinforced beams and post tensioned beams. For perpendicular shear reinforcement, Clause 8.2.10 of AS3600 states

$$V_{us} = \left(\frac{A_{sv} \cdot f_{sy.f} \cdot d_o}{s} \right) \cot \theta_v$$

Where,

s = centre to centre spacing of shear reinforcement

θ_v = angle between the axis of the concrete compression strut and the longitudinal axis of the member, taken as varying linearly from 30° when $V^* = \varphi V_{u.min}$ to 45° when $V^* = \varphi V_{u.max}$

A_{sv} = cross sectional area of shear reinforcement

$f_{sy.f}$ = yield strength of shear reinforcement

2.5.1 Reinforced Concrete Beam

For a reinforced concrete beam, clause 8.2.7.1 of AS3600 states

$$V_{uc} = \beta_1 \cdot \beta_2 \cdot \beta_3 \cdot b_v \cdot d_o \left(\frac{A_{st} \cdot f'_c}{b_v \cdot d_o} \right)^{\frac{1}{3}}$$

Where,

$$\beta_1 = 1.1 \times \left(1.6 - \frac{d_o}{1000} \right) \geq 1.1$$

β_2 = 1, generally for members without significant axial force; or

$$= 1 - \left(\frac{N^*}{3.5 A_g} \right) \geq 0 \text{, for members subject to significant axial tension;}$$

or

$$= 1 + \left(\frac{N^*}{14 A_g} \right) \text{ for members subject to significant axial compression.}$$

This factor illustrates the effect of axial force on the propagation of shear cracks. A compressive force reduces crack propagation, and therefore increases the shear resisted by the concrete. Conversely, axial tension encourages the shear cracks to form.

β_3 = 1; or may be taken as –

$$= 2 \times \frac{d_o}{\alpha_v}$$ but not greater than 2, provided that the applied loads and the support are orientated so as to create diagonal compression over the length α_v.

b_v = width of the section

d_o = distance from top edge to centre of bottom longitudinal reinforcement

f'_c = 28 day concrete compressive strength

A_{st} = cross sectional area of longitudinal reinforcement

A_g = gross cross sectional area

N^* = design axial force

α_v = shear span, the distance from the section being considered to the face of the nearest support.

2.5.2   Externally Post-tensioned Concrete Beam

For a post tensioned beam, clause 8.2.7.2 (a) of AS3600 states that for flexure-shear cracking

$$V_{uc} = \beta_1 \cdot \beta_2 \cdot \beta_3 \cdot b_v \cdot d_o \left(\frac{\left(A_{st} + A_p \right) f'_c}{b_v \cdot d_o} \right)^{\frac{1}{3}} + V_o + P_v$$

Where,

β_1, β_2, β_3 and A_{st} are the same as for reinforced beams except that in determining β_2, N* is taken as the value of axial force excluding prestress

A_{pt} = cross-sectional area of prestressing steel

P_v = vertical component of prestress force

V_o = the shear force which would occur at the section when the bending moment at the section was equal to the decompression moment (M_o)

$$= \frac{M_o}{\left(\dfrac{M*}{V*}\right)} \quad \text{for simply supported conditions, where } M* \text{ and } V* \text{ are}$$

the bending moment and shear force respectively, due to the same design loading

$$M_o = \left(\frac{P}{A_g} + \frac{P \cdot e \cdot y_b}{I_g}\right)\frac{I_g}{y_b}$$

Where,

P = prestressing force

e = eccentricity from the centroid of the section

y_b = distance from the centroid to bottom edge

I_g = second moment of area of the uncracked section

A_g = gross cross-sectional area

For web-shear cracking, AS3600 clause 8.2.7.2 (b) states:

$$V_{uc} = V_t + P_v$$

Where,

V_t = the shear force, which in combination with the prestressing force and other action effects at the section, would produce a principle tensile stress of $0.33\sqrt{f'_c}$ at either the centroidal axis or the intersection of flange and web, whichever is more critical.

P_v = vertical component of prestress force

2.6 Summary

This section has given an overview of the problem that exists in deteriorating bridge structures, and background on research conducted on epoxy repairing of cracks and post-tensioning. With only limited research having been conducted on combining epoxy injection with external post-tensioning to shear strengthen concrete members, both repair methods were also looked at individually. The AS3600 prediction

equations for the shear capacities of reinforced and post-tensioned beams were also looked at.

The previous research conducted at USQ by Woods and Jobling on the model headstocks, indicated that concrete members could be shear strengthened with external post-tensioning combined with epoxy injection of cracks. Whether this strengthening ability translates to girders is unclear, as the research conducted by Alam on small scale girders was inconclusive. As previously mentioned, this was due to wide ranging strengths of concrete used, and the small section size and low amount of cover, which caused premature failure in the specimens to occur. For these reasons, further testing on the combined strengthening technique applied to girders is required. This research project will involve the experimental testing of larger scale girders, to evaluate the shear strengthening of girders using external post-tensioning combined with epoxy injection of existing shear cracks.

CHAPTER 3

DESIGN METHODOLOGY

3.1   Introduction

This chapter presents an overview of the design work undertaken for the model beams to be experimentally tested. The four beams included a reinforced control beam, a shear cracked beam to be repaired only with post-tensioning, a beam to have its existing shear cracks repaired with epoxy injection and then post-tensioned, and finally a post-tensioned control beam. The two beams to be rehabilitated were to be preloaded to the same level, to form significant shear cracks. The control beams were tested to assess the effectiveness of both strengthening techniques. For this testing, the model beams needed to be designed as both a reinforced beam, and a post-tensioned beam.

The selection of loading position, specimen design and post-tensioning requirements are shown in this chapter. The design of the specimens includes the determination of cross-section, longitudinal reinforcement and shear reinforcement. The post-tensioning system design includes the selection of initial tensioning level, tendon capacities, and end anchorage.

For the ease of constructing the formwork and reinforcement cages, a rectangular cross-section was chosen for the specimens. The rectangular cross-section also gives a good representation of industry needs, as rectangular cross-sections are commonly used for bridge girders and concrete building beams. The section chosen was 300mm high by 150mm wide. This model size was selected as it was believed it would be adequate to exhibit the same failure characteristics as larger bridge girders used in practical applications. Having similar failure characteristics would

enable the conclusions formed from this research to be applied to full size bridge girders.

The selection of loading position and span were made to ensure shear failure over flexural failure. Four point loading was chosen to cause shear failure in both ends of the beam. This type of loading also causes a lower design moment compared to midspan loading, which will encourage shear failure over flexural failure. To cause shear failure in both ends of the beam, the shear span was set at 2.5. Having a beam depth of 300mm, this equates to a distance of 750mm between the load and the support. A 500mm separation between the two applied loads was also set. The total span for the beam was 2000 mm, with an overhang of 300 mm at each end. This equates to a total length of 2600 mm for the design specimens. The 300 mm overhang at each end was required to secure the end anchorage for the post-tensioning, and so idealised pin supports could be set. The specimen size and loading points are shown in Figure 3.1.
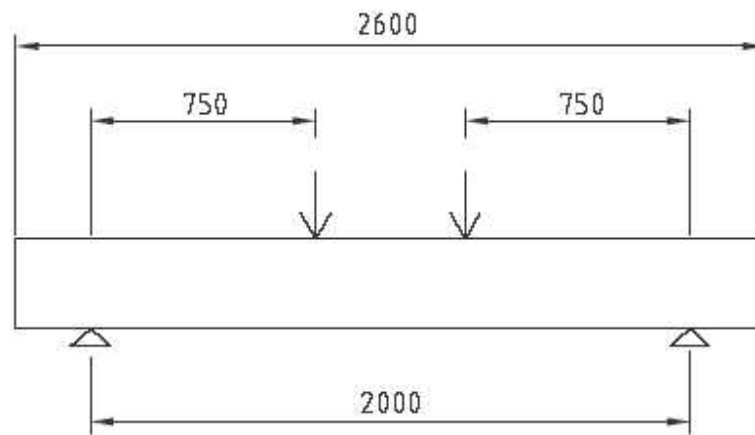
Figure 3.1: Specimen Size and Loading Position

The free body diagram, bending moment diagram, and shear force diagram for the four point loading is shown in Figure 3.2.
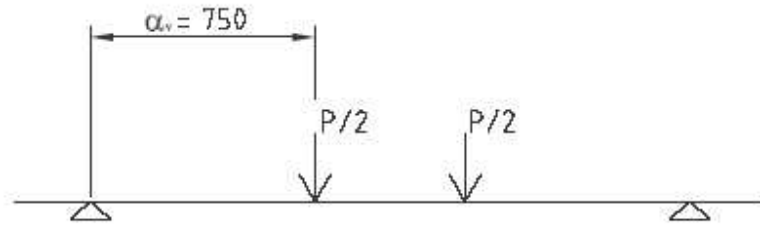
Figure 3.2 (a) – Free Body Diagram

Figure 3.2 (b) – Shear Force Diagram
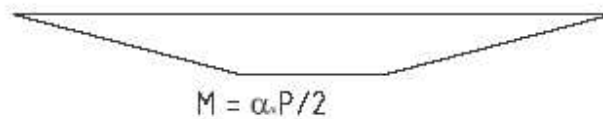
Figure 3.2 (c) – Bending Moment Diagram

Figure 3.2: Free Body Diagram, Shear Force Diagram and Bending Moment Diagram

The maximum design shear force is between the supports and the loading points, while the maximum design moment is between the loading points. This is to be expected, as shear failures usually occur between the support and the loading point, while flexural failures occur midspan. Between the supports and the loading points, the design shear force is half the applied load.

To ensure shear failure, the beam was designed to have at least a 40% higher flexural failure load than its shear failure load. This was done through the spacing and size of the shear ligatures. R6 (round) bars were chosen for the ligatures, as these were readily available in the laboratory, and would be small enough to bend with a simple jig. A spreadsheet was used to find an acceptable spacing for the ligatures.

The ultimate moment capacity, M_u, and the shear capacity, V_u, for the design specimen will be calculated for before and after post-tensioning. The corresponding ultimate loads, P_u, found for each will also be shown in the following sections.

3.2   Preliminary Design

The cross section of the design specimen is shown in Figure 3.3. The depth of the beam was 300 mm, and the width 150 mm.
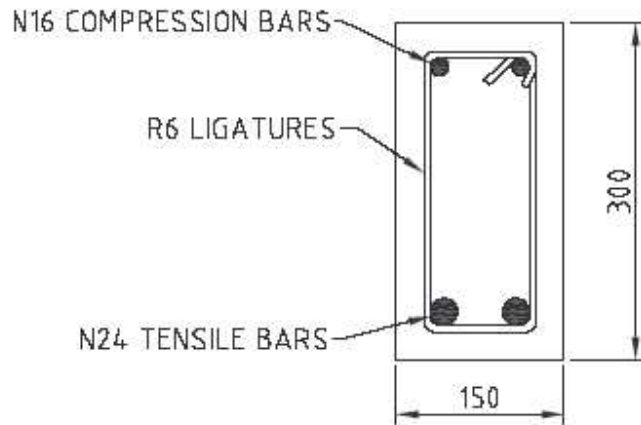
Figure 3.3: Cross Section of the Design Specimen

The section is doubly reinforced with 2 N24 tensile bars at the bottom, and 2 N16 compression bars at the top. R6 bars were used for the ligatures, with a spacing of 250 mm. These sizes were used so the beam had a higher flexural capacity than shear capacity. This was found using a spreadsheet to analyse the capacities of a number of different reinforcement layouts. The spacing of the ligatures was reduced to 60 mm in the overhang sections of each beam, to cope with the localised compressive stresses exerted from the post-tensioning.

3.3   Design of Reinforced Beam

The ultimate moment capacity, M_u, and the shear capacity, V_u, for the design specimen before post-tensioning are calculated in this section.

3.3.1   Flexural Capacity

The flexural capacity load of the beam was calculated to ensure it was substantially higher than the beam's shear capacity load.

In a doubly reinforced section at ultimate moment capacity, the resultant tensile force in the bottom steel, T_s, is equal to the compressive force in the concrete, C_c, plus the compressive force in the top steel, C_s. Once the forces and their points of action are known, the moment capacity can be found by taking moments about the bottom tensile steel. The internal strains, stresses, and forces in the section are shown in Figure 3.4, and the calculations to find the specimen's flexural capacity are shown below.
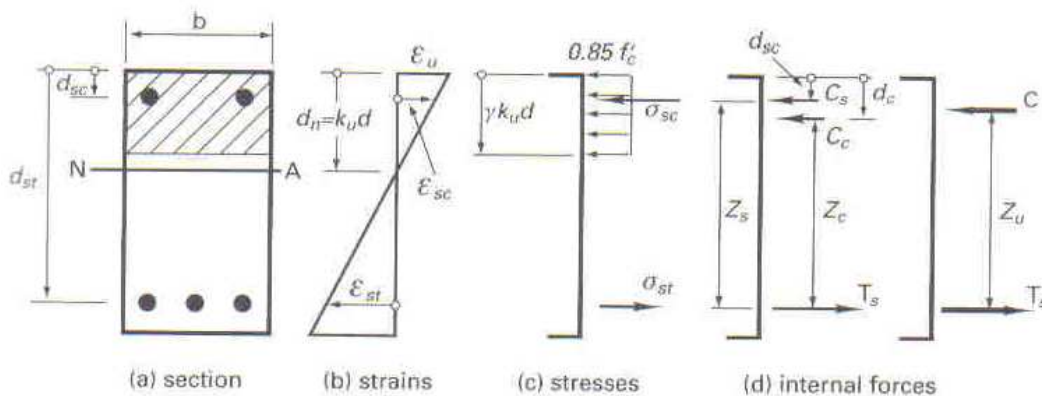
Figure 3.4: Doubly Reinforced Section at Ultimate Moment

(Source: Warner et al, 1998)

Section Properties

$$f'_c = 32MPa$$

$$\gamma = 0.85 - 0.007(f'_c - 28)$$
$$= 0.85 - 0.007(32 - 28)$$
$$= 0.822$$

Reinforcing Properties

$$f_{sy} = 500MPa$$

Depth to compression steel:

$$d_{sc} = 25 + 6 + \frac{16}{2} = 39mm$$

Depth to tensile steel:

$$d = 300 - 25 - 6 - \frac{24}{2} = 257mm$$

Area of compression steel:

$$A_{sc} = 400mm^2$$

Area of tensile steel:

$$A_{st} = 900mm^2$$

Initially assume all reinforcement yields before M_u, therefore;

Tensile steel force:

$$T_s = f_{sy} \cdot A_{st}$$
$$= 500 \times 900$$
$$= 450 \times 10^3 N$$

Compression steel force:

$$C_s = f_{sy} \cdot A_{sc}$$
$$= 500 \times 400$$
$$= 200 \times 10^3 N$$

Concrete compressive force:

$$C_c = 0.85 f'_c \cdot \gamma \cdot b \cdot d_n$$
$$= 0.85 \times 32 \times 0.822 \times 150 \times d_n$$
$$= 3353.76 d_n$$

As the sum of the forces equals zero:

$$3353.76d_n + 200\times10^3 = 450\times10^3$$
$$d_n = 74.5mm$$

Checking the compressive reinforcement has yielded:

$$\varepsilon_{sc} = \varepsilon_c\left(\frac{d_n - d_{sc}}{d_n}\right)$$
$$= 0.003\times\left(\frac{74.5 - 39}{74.5}\right)$$
$$= 0.0014$$

As $\varepsilon_{sc} < 0.0025$, the assumption that the compressive reinforcement had yielded is incorrect. The compressive forces will be recalculated knowing the compressive reinforcement is in the elastic range, with:

$$C_s = E_s \cdot \varepsilon_u \cdot \left(\frac{k_u \cdot d_{st} - d_{sc}}{k_u \cdot d_{st}}\right)A_{sc}$$

By equating the sum of the forces to zero, the neutral axis depth is found using a quadratic equation to find k_u:

$$k_u^2 + u_1.k_u - u_2 = 0$$

Where,

$$u_1 = \frac{\varepsilon_u \cdot E_s \cdot A_{sc} - f_{sy} \cdot A_{st}}{0.85 f'_c \cdot \gamma \cdot b \cdot d_{st}}$$

$$u_2 = \frac{\varepsilon_u \cdot d_{sc} \cdot E_s \cdot A_{sc}}{0.85 f'_c \cdot \gamma \cdot b \cdot d_{st}^2}$$

Therefore,

$$u_1 = \frac{0.003 \times 200 \times 10^3 \times 400 - 500 \times 900}{0.85 \times 32 \times 0.822 \times 150 \times 257}$$
$$= -0.245$$

$$u_2 = \frac{0.003 \times 39 \times 200 \times 10^3 \times 400}{0.85 \times 32 \times 0.822 \times 150 \times 257^2}$$
$$= 0.0425$$

This gives the quadratic equation:

$$k_u{}^2 - 0.245 \times k_u - 0.0425 = 0$$

Solving the quadratic equation:

$$k_u = \frac{-b \pm \sqrt{b^2 - 4a.c}}{2a}$$
$$= \frac{0.245 \pm \sqrt{(-0.245)^2 - 4 \times 1 \times -0.0425}}{2 \times 1}$$
$$= 0.362 \text{ or } -0.117$$

Taking the positive value:
$$k_u = 0.362$$

Therefore, the neutral axis depth:
$$d_n = k_u \cdot d$$
$$= 0.362 \times 257$$
$$= 93.1 mm$$

The force in the tensile steel is the same as previously, but the compressive forces in the concrete and compressive reinforcement need to be recalculated.

Tensile steel force:

$$T_s = 450 \times 10^3 \, N$$

Compression steel force:

$$C_s = 200 \times 10^3 \times 0.003 \left(\frac{0.362 \times 257 - 39}{0.362 \times 257} \right) 400$$

$$= 140191 N$$

Concrete compressive force:

$$C_c = 3353.76 d_n$$

$$= 312198 \, N$$

Therefore, the ultimate moment capacity of the beam:

$$M_u = C_s (d_{st} - d_{sc}) + C_c (d_{st} - 0.5\gamma \cdot k_u \cdot d_{st})$$

$$= 140191 \times (257 - 39) + 312198 \times (257 - 0.5 \times 0.822 \times 0.362 \times 257)$$

$$= 98.85 kN.m$$

The force required to produce the ultimate moment, M_u, is found from:

$$P_1 = \frac{M_u}{\alpha v}$$

Where,

$P_1 = $ Load from one loading point

$\alpha v = $ Distance between the support and loading point

Therefore,

$$P_1 = \frac{98.85}{0.75}$$

$$= 131.8 kN$$

As four point loading is used, the ultimate flexural load capacity of the beam, $P_{u.f}$, is calculated as:

$$P_{u.f} = 2 \times P_1$$

$$= 2 \times 131.8$$

$$= 263.6 kN$$

This moment capacity load can now be used to ensure the beam has a lower shear capacity than flexural capacity, to ensure the beams fail in shear.

3.3.2   Shear Capacity

The ultimate shear capacity, V_u, of the reinforced concrete beam is determined in this section.

$$V_u = V_{uc} + V_{us}$$

The ultimate shear strength of the concrete, V_{uc}, is:

$$V_{uc} = \beta_1 \cdot \beta_2 \cdot \beta_3 \cdot b_v \cdot d_o \left(\frac{A_{st} \cdot f'_c}{b_v \cdot d_o} \right)^{\frac{1}{3}}$$

Where,

$$\beta_1 = 1.1 \times \left(1.6 - \frac{d_o}{1000} \right) \geq 1.1$$
$$= 1.1 \times \left(1.6 - \frac{257}{1000} \right) \geq 1.1$$
$$= 1.48$$

$$\beta_2 = 1 \text{ (as there is no axial load present)}$$

$$\beta_3 = 1$$

Therefore,

$$V_{uc} = 1.48 \times 1 \times 1 \times 150 \times 257 \times \left(\frac{900 \times 32}{150 \times 257} \right)^{\frac{1}{3}}$$
$$= 51.77 kN$$

The ultimate shear strength of the shear reinforcement, V_{us}, is:

$$V_{us} = \left(\frac{A_{sv} \cdot f_{sy.f} \cdot d_o}{s} \right) \cot \theta_v$$

Where,

$$\theta_v = 30^o + 15^o\left(\frac{A_{sv} - A_{sv.\,min}}{A_{sv.\,max} - A_{sv.\,min}}\right)$$

Where,

A_{sv} = cross sectional area of shear reinforcement

$$= 2 \times \pi \times 3^2$$
$$= 56.5mm^2$$

$A_{sv.\,min}$ = cross sectional area of minimum shear reinforcement

$$= \frac{0.35b_v \cdot s}{f_{sy.f}}$$
$$= \frac{0.35 \times 150 \times 250}{250}$$
$$= 52.5mm^2$$

$A_{sv.\,max}$ = cross sectional area of maximum shear reinforcement

$$= \frac{b_v \cdot s\left(0.2 f'_c - \frac{V_{uc}}{b_v \cdot d_{st}}\right)}{f_{sy.f}}$$
$$= \frac{150 \times 250 \times \left(0.2 \times 32 - \frac{51770}{150 \times 257}\right)}{250}$$
$$= 758.6mm^2$$

Therefore,

$$\theta_v = 30^o + 15^o\left(\frac{56.5 - 52.5}{758.6 - 52.5}\right)$$
$$= 30.09^o$$

Therefore, the ultimate shear strength of the shear reinforcement, V_{us}, is:

$$V_{us} = \left(\frac{56.5 \times 250 \times 257}{250}\right)\cot(30.09)$$
$$= 25.09kN$$

Calculating the reinforced concrete beam's ultimate shear capacity:

$$V_u = V_{uc} + V_{us}$$
$$= 51.77 + 25.09$$
$$= 76.86 kN$$

As four point loading is used, the ultimate shear capacity load, $P_{u.s}$, is calculated as:

$$P_{u.s} = 2 \times 76.86$$
$$= 153.72 kN$$

The beam's shear capacity load, $P_{u.s}$ (153.72kN) is lower than the beam's flexural capacity load $P_{u.f}$ (263.6kN), so the beam should fail in shear.

3.4   Design of Externally Post-tensioned Beam

The ultimate moment capacity, M_u, and the shear capacity, V_u, for the design specimen after post-tensioning are calculated in this section.

3.4.1   Selection of Post-tension Force

The post-tension force to be used on the beams has been selected as 150kN, with an eccentricity of 50mm towards the bottom. This force has been determined taking into account the increase in member strength, ensuring the beam still fails in shear, and the available equipment. The eccentricity of the force was chosen to maximise the effectiveness of the post-tensioning, but was kept within the middle third of the section to ensure no tensile stresses were induced on the top face of the beams due to the post-tensioning. The positioning of the post-tensioning rods can be seen in Figure 3.5.
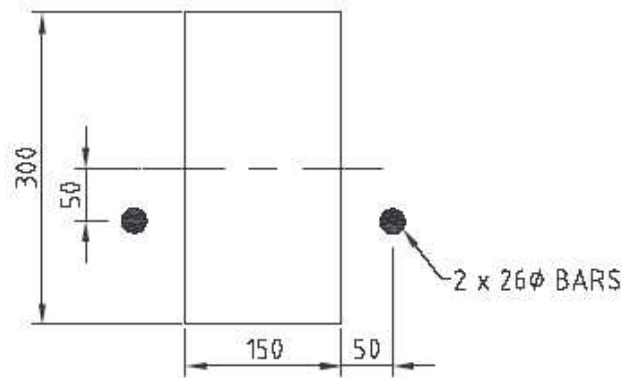
Figure 3.5: Positioning of Post-tensioning Bars

The available post-tensioning rods were 26mm high tensile Maceloy bars, with a yield strength of approximately 900MPa. The tensile strength, T_p, of these bars is:

$$T_p = A_p \cdot f_p$$
$$= \left(\pi \times 13^2\right) \times 900$$
$$= 478 kN$$

Therefore, these bars can easily handle the 75kN initial post-tension force on each of the two bars. 150C10 sections were used as end plates to transfer the post-tension force to the beams. The calculations to check for adequate capacity in these sections are shown in Appendix B.

3.4.2   Flexural Capacity

The flexural capacity of the beam after post-tensioning needs to be less than the beam's shear capacity after post-tensioning. The calculations for the beam's flexural capacity after post-tensioning are shown below.

The parameters of the initial post-tensioning are:

Post-tensioning force:

$$F = 150 kN$$

Depth to post-tensioning steel:

$$d_p = 200mm$$

Area of post-tensioning steel:

$$A_{pt} = 2 \times \frac{\pi D^2}{4}$$
$$= 2 \times \frac{\pi \times 26^2}{4}$$
$$= 1061.9 mm^2$$

Effective post-tensioning stress:

$$\sigma_{p.ef} = \frac{F}{A_{pt}}$$
$$= \frac{150 \times 10^3}{1061.9}$$
$$= 141.3 MPa$$

To find the stress in the post-tensioning rods, Clause 8.1.6 of AS3600 is used. For a beam with a span-to-depth ratio of less than 35 (2000/300 = 6.67), the ultimate stress in the rods is:

$$\sigma_{pu} = \sigma_{p.ef} + 70 + \left(\frac{f'_c \cdot b_{ef} \cdot d_p}{100.A_{pt}} \right) \leq \sigma_{p.ef} + 400$$
$$= 141.3 + 70 + \left(\frac{32 \times 150 \times 200}{100 \times 1061.9} \right) \leq 141.3 + 400$$
$$= 220.3 MPa$$

The flexural capacity of the post-tensioned beam is calculated in a similar way as for the reinforced beam, except the tensile force of the post-tensioning rods is added to the balancing equation.

Initially assume all reinforcement yields before M_u, therefore;

Tensile steel force:

$$T_s = f_{sy} \cdot A_{st}$$
$$= 500 \times 900$$
$$= 450 \times 10^3 \, N$$

Compression steel force:

$$C_s = f_{sy} \cdot A_{sc}$$
$$= 500 \times 400$$
$$= 200 \times 10^3 \, N$$

Concrete compressive force:

$$C_c = 0.85 f'_c \cdot \gamma \cdot b \cdot d_n$$
$$= 0.85 \times 32 \times 0.822 \times 150 \times d_n$$
$$= 3353.76 d_n$$

Post-tensioning steel tensile force:

$$T_p = \sigma_{pu} \cdot A_{pt}$$
$$= 220.3 \times 1061.9$$
$$= 233930 N$$

As the sum of the forces equals zero:

$$3353.76 d_n + 200 \times 10^3 = 450 \times 10^3 + 233930$$
$$d_n = 144.3 mm$$

Checking the compressive reinforcement has yielded:

$$\varepsilon_{sc} = 0.003 \times \left(\frac{144.3 - 39}{144.3} \right)$$
$$= 0.0022$$

As $\varepsilon_{sc} < 0.0025$, the assumption that the compressive reinforcement had yielded is incorrect. The compressive forces will be recalculated knowing the compressive reinforcement is in the elastic range.

Checking the tensile reinforcement has yielded:

$$\varepsilon_{st} = \varepsilon_c \left(\frac{d_{st} - d_n}{d_n} \right)$$

$$= 0.003 \times \left(\frac{257 - 144.3}{144.3} \right)$$

$$= 0.00234$$

As $\varepsilon_{st} < 0.0025$, the assumption that the tensile reinforcement had yielded is incorrect. The tensile forces will be recalculated knowing the tensile reinforcement is in the elastic range:

$$T_s = E_s \cdot \varepsilon_{st} \cdot A_{st}$$

As ε_{st} is dependent on the neutral axis depth, d_n, the forces will be solved by trial and error knowing both the compressive and tensile reinforcement are in the elastic range.

From the trial and error, $d_n = 143.98mm$

The strains equal:

$$\varepsilon_{sc} = 0.003 \times \left(\frac{143.98 - 39}{143.98} \right)$$

$$= 0.002187$$

$$\varepsilon_{st} = 0.003 \times \left(\frac{257 - 143.98}{143.98} \right)$$

$$= 0.002355$$

The forces equal:

$$C_s = E_s \cdot \varepsilon_{sc} \cdot A_{sc}$$

$$= 200 \times 10^3 \times 0.002187 \times 400$$

$$= 174960N$$

$$C_c = 0.85 f'_c \cdot \gamma \cdot b \cdot d_n$$

$$= 0.85 \times 32 \times 0.822 \times 150 \times 143.98$$

$$= 482874N$$

$$T_s = E_s \cdot \varepsilon_{st} \cdot A_{st}$$
$$= 200 \times 10^3 \times 0.002355 \times 900$$
$$= 423900N$$

$$T_p = \sigma_{pu} \cdot A_{pt}$$
$$= 220.3 \times 1061.9$$
$$= 233930N$$

Therefore, taking moments about the tensile reinforcement, the ultimate moment capacity is:

$$M_u = C_s(d_{st} - d_{sc}) + C_c(d_{st} - 0.5\gamma \cdot d_n) - T_p(d_{st} - d_p)$$
$$= 174960 \times (257 - 39) + 482874 \times (257 - 0.5 \times 0.822 \times 143.98) - 233930 \times (257 - 200)$$
$$= 120.33 kN.m$$

The force required to produce the ultimate moment, M_u, is:

$$P_{u.f} = 2 \times \frac{120.33}{0.75}$$
$$= 320.9 kN.m$$

3.4.3   Shear Capacity

The ultimate shear capacity, V_u, of the post-tensioned beam is again determined from:

$$V_u = V_{uc} + V_{us}$$

The ultimate shear strength of the shear reinforcement, V_{us}, is as for the reinforced concrete beam, but the ultimate shear strength of the concrete, V_{uc}, is:

$$V_{uc} = \beta_1 \cdot \beta_2 \cdot \beta_3 \cdot b_v \cdot d_o \left(\frac{(A_{st} + A_{pt}) f'_c}{b_v \cdot d_o} \right)^{\frac{1}{3}} + V_o + P_v$$

Where,

β_1, β_2, β_3, b_v, d_o, f'_c, and A_{st} are the same as for the reinforced beam

$P_v = 0$, as the post-tensioning rods are horizontal

$V_o =$ the shear force which would occur at the section when the bending moment at the section was equal to the decompression moment (M_o)

$$= \frac{M_o}{\left(\dfrac{M*}{V*}\right)}$$ for simply supported conditions, where $M*$ and $V*$ are the

bending moment and shear force respectively, due to the same design loading

$$M_o = \left(\frac{P}{A_g} + \frac{P \cdot e \cdot y_b}{I_g}\right)\frac{I_g}{y_b}$$

Where,

P = post-tensioning force

   = 150kN

A_g = gross cross-sectional area

   = b.D

   = 150 x 300

   = 45000mm^2

e = eccentricity from the centroid of the section

   = 50mm

y_b = distance from the centroid to bottom edge

   = 150mm

I_g = Second moment of area of the uncracked section

$$= \left(\frac{b \cdot D^3}{12}\right)$$

$$= \left(\frac{150 \cdot 300^3}{12}\right)$$

$$= 3.375 \times 10^8 \, mm^4$$

Therefore, the decompression moment is:

$$M_o = \left(\frac{150 \times 10^3}{45000} + \frac{150 \times 10^3 \times 50 \times 150}{3.375 \times 10^8}\right) \times \frac{3.375 \times 10^8}{150}$$

$$= 15 kNm$$

$$\frac{M*}{V*} = \frac{\left(\dfrac{\text{Distance Between Load and Support} \times \text{Load}}{2}\right)}{\left(\dfrac{\text{Load}}{2}\right)}$$

$$= 0.75$$

Therefore, the shear force where decompression occurs is:

$$V_o = \frac{15}{0.75}$$

$$= 20 kN$$

The ultimate shear strength of the concrete, V_{uc}, is:

$$V_{uc} = \beta_1 \cdot \beta_2 \cdot \beta_3 \cdot b_v \cdot d_o \left(\frac{(A_{st} + A_p)f'_c}{b_v \cdot d_o}\right)^{\frac{1}{3}} + V_o + P_v$$

$$= 1.477 \times 1 \times 1 \times 150 \times 257 \times \left(\frac{(900 + 1061.9) \times 32}{150 \times 257}\right)^{\frac{1}{3}} + 20 \times 10^3 + 0$$

$$= 86.99 kN$$

Therefore, the ultimate shear capacity of the post-tensioned beam is:

$$V_u = 86.99 + 25.09$$

$$= 112.08 kN$$

Therefore, the ultimate shear capacity load, $P_{u.s}$, is calculated as:

$$P_{u.s} = 2 \times 112.08$$

$$= 224.16 kN$$

The post-tensioned beam's shear capacity load, $P_{u.s}$ (224.16kN) is lower than the post-tensioned beam's flexural capacity load $P_{u.f}$ (320.9kN), so the beam again should fail in shear. After applying the post-tensioning, the beam's shear capacity load has increased from 153.72 kN to 224.16 kN, which equates to an increase of 45.8%.

3.5   Anchorage of Tensile Reinforcement

To ensure the tensile reinforcement did not slip out when the shear cracks formed, the development length required at the support was checked. The length required was found at the support, as the shear crack was expected to propagate through the tensile reinforcement in this general area.

Warner et al (1998, p297) argue that in regions of high shear force, strut-and-tie modelling can be used for a beam. This entails the tensile reinforcement being taken as the bottom chord, and the concrete forming a strut between the loading point and the support, as shown in Figure 3.6. This is the simplest arrangement of the strut-and-tie model, but will provide a conservative estimate of development length required.
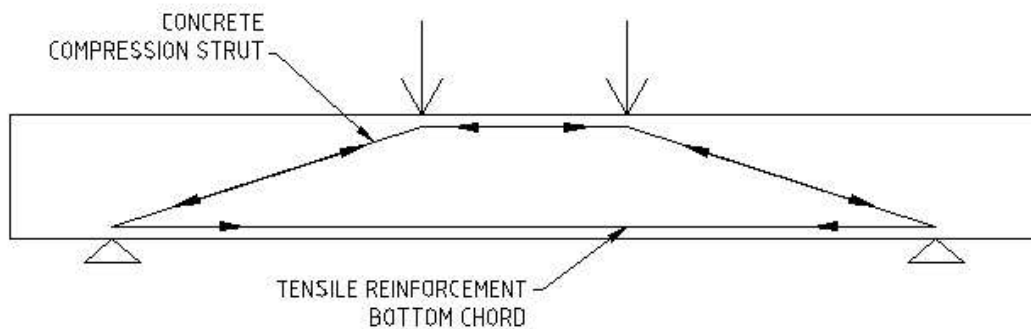
Figure 3.6: Strut-and-tie Model of Beam

The development length required for the tensile reinforcement was found using the ultimate shear capacity load for the reinforced beam (154 kN), as found in section 3.3.2. The maximum load from the reinforced beam was used instead of the load from the post-tensioned beam, as the tensile reinforcement in these beams was placed in compression before loading. This meant a lower ultimate tensile force at the support was expected in these beams. Analysing one end of the beam, the applied load is 77 kN. The force in the tensile reinforcement is found using simple statics from Figure 3.7.
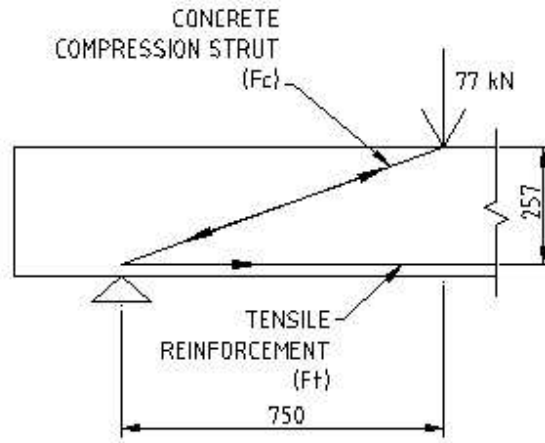
Figure 3.7: Statics of Strut-and-tie Model

Concrete compression strut force:

$$Fc = \frac{77}{257} \times \sqrt{\left(257^2 + 750^2\right)}$$
$$= 238kN$$

Tensile reinforcement force:

$$Ft = \frac{77}{257} \times 750$$
$$= 225kN$$

As there are two tensile reinforcement bars, the force in each bar is 112.5 kN (225 ÷ 2). The development length required for a bar at less than yield strength is found from Clause 13.1.2.2 of AS3600;

$$L_{st} = \frac{L_{sy.t} \times \sigma_{st}}{f_{sy}}$$

Where,

$$\sigma_{st} = \text{tensile stress in reinforcement}$$
$$= \frac{Ft}{A_b}$$
$$= \frac{112.5 \times 10^3}{450}$$
$$= 250 \, MPa$$

$$f_{sy} = 500\,\text{MPa}$$

$$L_{sy.t} = \frac{k_1.k_2.f_{sy}.A_b}{(2a + d_b).\sqrt{f'_c}}$$

Where,

$k_1 = 1.0$

$k_2 = 2.2$

$d_b = $ bar diameter

$\quad = 24\,\text{mm}$

$A_b = $ cross - sectional area of the reinforcing bar

$\quad = 450\,\text{mm}^2$

$2a = $ twice the cover to the deformed bar or the clear distance between adjacent

parrallel bars developing stress, which ever is less

$\quad = 52\,\text{mm}$

Therefore,

$$L_{sy.t} = \frac{1.0 \times 2.2 \times 500 \times 450}{(52 + 24) \times \sqrt{32}}$$

$$= 1151\,\text{mm}$$

$$L_{st} = \frac{1151 \times 250}{500}$$

$$= 576\,\text{mm}$$

As 576 mm of development length is required, but the end overhang sections of the beam are only 300 mm long, a cog will be placed at the end of each tensile bar to get the required development. Clause 13.1.2.4 of AS3600 states that the development length of a standard hook shall be taken as $0.5L_{sy.t}$. This will allow the required reinforcement to fit in the end overhang sections of the beam. Clause 13.1.2.5 of AS3600 states that the straight extension of the cog must be at least $4d_b$, so this section will be at least 96 mm. Figure 3.8 shows the cog to be used at the end of each tensile reinforcement bar, to ensure the bars do not slip once the shear cracks form.

3.6   Design Summary

The design of the specimens to be used for this testing is shown in Figure 3.8.
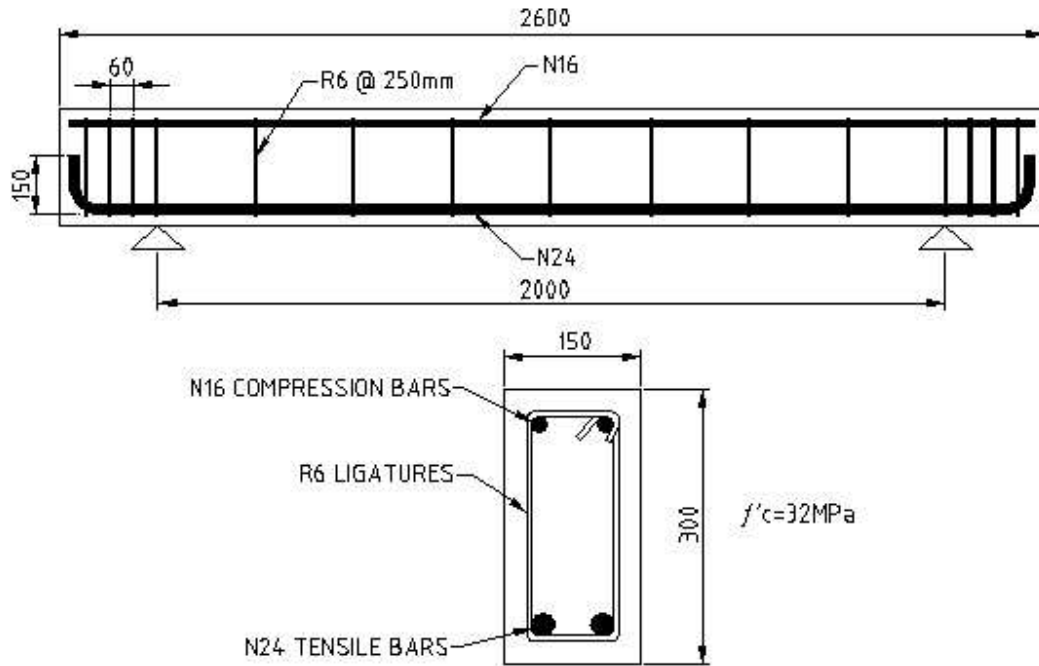
Figure 3.8: Specimen Design

The model beams have been designed to ensure they fail in shear over flexure. This has been done for both the reinforced control beam, and the post-tensioned beams. A summary of the design capacities can be seen in Table 3.1. The flexure/shear ratios shown indicate that both the reinforced beam and post-tensioned beams should fail in shear over flexure, as their flexural capacities are 71% and 43% higher than their shear capacities respectively.

Table 3.1: Summary of Design Capacities

	Shear Capacity Load, $P_{u.s}$ (kN)	Flexural Capacity Load, $P_{u.f}$ (kN)	Flexure/Shear Ratio
Reinforced Beam	154	264	1.71
Post-tensioned Beam	224	321	1.43

CHAPTER 4

EXPERIMENTAL METHODOLOGY

4.1   Introduction

This section will outline the procedures used in the construction and testing of the model beams.

4.2   Construction Methodology

Four test specimens were constructed using the design discussed in the previous chapter. The four beams were cast at once to ensure similar concrete strengths when testing for each beam. The four beams were tested between 28 and 40 days. As concrete gains almost all of its strength in the first 28 days, the concrete strength for each beam when tested were very similar.

4.2.1   Formwork

The formwork was constructed by university staff from 12 mm ply and 75 mm x 38 mm pine. The formwork was constructed to have the four beams side by side to minimise the material used. Three separator boards were used to stabilise the middle formwork ply, until the concrete had been filled on both sides of the ply.

The formwork was greased and the edges sealed with silicone before the beams were cast, to ensure they could easily be removed. Figure 4.1 shows the formwork and three separator boards.

Figure 4.1: Formwork to Cast Beams

4.2.2   Reinforcement

The reinforcement used in the beams was obtained from a local supplier, with the N24 tensile bars being cut and bent to order, as bending this size bar was beyond the university bending machine's capability. The N16 compression bars were cut to a length of 2500 mm, to allow 50 mm of space at either end for the ferrules, which were needed to position the end anchorage for the post-tensioning. The R6 ligatures were cut using bolt cutters, and bent using a jig to suit the required cage. The cage was designed to have 25 mm cover from the outside of the ligatures. The bending jig used is shown in Figure 4.2.

Figure 4.2: Bending Jig

The reinforcement cages were positioned in the formwork using 25 mm high mortar blocks. These were made five days before casting the beams from a water, cement and sand mix. Each block had a tie wire cast in, so the blocks could also be tied to the cages and used for lateral positioning. A constructed reinforcement cage positioned in the formwork using the mortar blocks is shown in Figure 4.3.

Figure 4.3: Positioning of Reinforcement Cages

Lifting hooks made from R6 reinforcement were made for each end of the beams. The bent bars were tied to the reinforcement cage in the strengthened end sections. They were placed in this section so they would not be in the effective span, and therefore would not affect the shear capacity of the beams.

Four ferrules were secured to the formwork using M10 bolts on either end of each beam, to be used to fasten the end plates during post-tensioning. A piece of N8 reinforcement was placed through the hole of each ferrule to ensure the ferrules did not slip during post-tensioning. These ferrules can be seen in Figure 4.3.

4.2.3   Steel Strain Gauges

The steel strain gauges were attached to the reinforcement to find the varying strains in the reinforcement when the beams were loaded. The strain gauges used were TML FLA-2-11, which are designed for use on metal. The data sheets for these gauges can be seen in Appendix C.

Ten steel strain gauges were used for each beam. Two of the gauges were placed on the midspan tensile reinforcement, and eight were placed on the shear ligatures in the shear span. The positioning of the steel strain gauges can be seen in Figure 4.4, with each marker representing a strain gauge on either side.
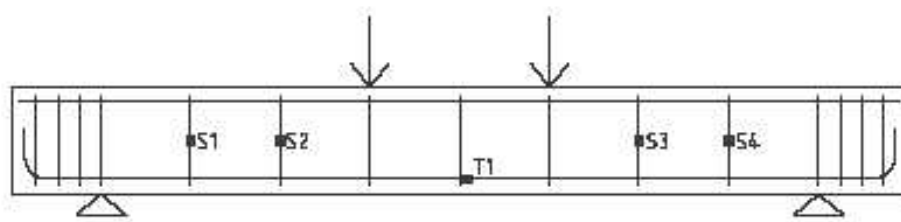
Figure 4.4: Positioning of Steel Strain Gauges

Before the gauges were attached, the steel surfaces were smoothed and cleaned. The ligatures were smoothed using emery paper, while the ribs of the tensile

reinforcement were smoothed off using a grinder. The smoothed surfaces were cleaned with acetone to remove any dust particles. The gauges were then glued to the steel using CN Adhesive, with finger pressure being applied to the gauge for approximately one minute. The data sheet for the CN adhesive is shown in Appendix C. Wax was melted over the gauge to form a watertight cover. The gauges were also wrapped with VN tape, to ensure the gauges were not damaged when the concrete was poured. A multimeter was used to check each gauge was operating correctly. All the gauges showed the required 120Ω resistance, indicating they were working correctly. Figure 4.5 shows a steel strain gauge that has been attached and covered.

Figure 4.5: Steel Strain Gauge

4.2.4   Pouring the Concrete

The concrete used to construct the test beams was obtained from a local supplier. The concrete that was ordered was 32MPa strength, 80mm slump and 20mm nominal aggregate size. The actual properties of the concrete were similar to this, and are shown in Chapter 5.

The concrete was placed in the formwork using a wheelbarrow and shovels. A poker vibrator was then used to compact the concrete, with care being taken around the steel strain gauges. After the concrete had been compacted, the surface was screeded off, and a trowel was used to finish smoothing the surface. The concrete surface was then covered with plastic to avoid excessive moisture loss, with the surface being regularly sprayed with water. This was done to avoid shrinkage cracks caused by drying to quickly. Figure 4.6 shows the freshly cast beams.

Figure 4.6: Freshly Cast Beams

During pouring of the beams, a number of cylinders were also cast, to be used for compressive strength tests when the beams were tested. A sample of these cylinders can be seen in Figure 4.7.

Figure 4.7: Freshly Cast Concrete Test Cylinders

4.2.5   Stripping, Moving and Curing

The formwork was stripped from the beams three days after they were cast. The side piece of the formwork was initially removed to allow access to the first beam. The beams were removed one at a time using the university's forklift, with a chain attached to the lifting hooks of each beam. The beams were then stacked together, covered with a plastic sheet, and left to cure until they were tested. The test cylinders were also removed from their moulds at this time, and were left to cure in the same conditions as the test beams. The beams and cylinders were continued to be sprayed with water daily for a further week to facilitate hydration and avoid shrinkage cracks occurring. Figure 4.8 shows the beams and test cylinders after removal from the formwork and moulds.

Figure 4.8: Beams and Test Cylinders after Stripping

4.2.6   Concrete Strain Gauges

The concrete strain gauges were attached to the beams to find the varying strains in the concrete at key locations when the beams were loaded. The strain gauges used were TML PFL-30-11, which are designed for use on concrete. The data sheets for these gauges can be seen in Appendix C.

The concrete strain gauges were attached to the beams just prior to loading. Ten concrete strain gauges were used for each beam. Four of the gauges were used at the midspan of the beam, with one being on the top face, and three being on the side face. The other six gauges were used as two sets of rosettes, with one set in either shear span. The positioning of the concrete strain gauges can be seen in Figure 4.9.
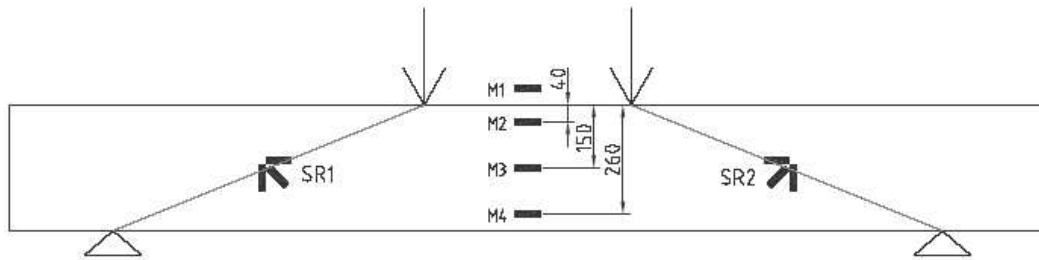
Figure 4.9: Positioning of Concrete Strain Gauges

Before the gauges were attached, the concrete surface was cleaned using a wire brush. To create a perfectly smooth surface where the gauges were to be attached, a layer of PS Adhesive, a two part concrete bonding agent, was covered over the areas. The data sheets for PS adhesive are also shown in Appendix C. A small piece of firm plastic which would not stick to the PS Adhesive, was placed firmly against the adhesive. Once the adhesive had dried, the plastic was removed, leaving a smooth surface for the gauges to be attached to. The gauges were then glued to the smooth surface using the CN adhesive, as used for the steel strain gauges. Figure 4.10 shows a concrete strain gauge rosette attached to the surface.
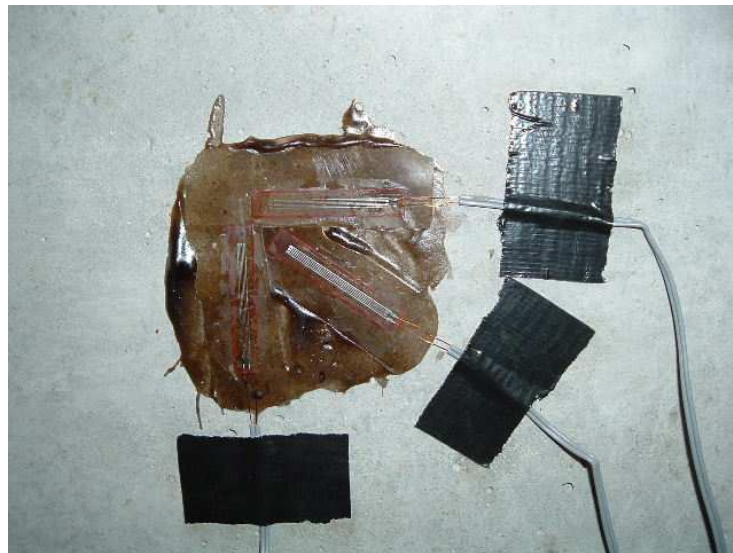
Figure 4.10: Strain Gauge Rosette

4.2.7   Post-tensioning

This section will explain about the post-tensioning system used for the test beams. It will include the elements involved in the setup, and the process used to tension the beams.

4.2.7.1   Prestressing Rods

The prestressing rods used for the post-tensioning were 26 mm high tensile threaded rods. The two rods were tensioned to 75 kN each using a hollow core hydraulic jack. The rods were tensioned by jacking the system between the end anchorage plate, and a nut and plate positioned behind the jack. A housing arrangement was used around the nut against the anchorage plate, to allow the nut to be tightened once the jack had tensioned the rod. As only one jack was available for the post-tensioning, each tendon was stressed in increments of 20 to 25 kN, to ensure both rods were carrying approximately the same load. This was done to ensure the tensile stress in the end anchorage bolts was not excessive, which could have caused the end plates to be pulled off. After each increment of tensioning, the nut in front of the jack was tightened to hold the increased force. The load applied in each rod was measured using a hollow load cell which was positioned at the end of each rod. The load cells were connected to the data logger, where the force applied during tensioning was monitored from. The jack used to stress the post-tensioning rods can be seen in Figure 4.11.

Figure 4.11: Stressing of Rods

4.2.7.2   End Anchorage

End anchorage was used to transfer the post-tensioned force in the rods to the beam. The end anchorage setup can be seen in Figure 4.11. The end anchorage was made up of an 10x150mm C-section, with a 15mm thick high strength steel plate behind it, as shown in Figure 4.11. These bearing plates had small lugs welded on the top and bottom to hold them in position. The C-sections were held in position with four M10 bolts which were screwed into four ferrules that had been cast in each end of the beams. The force from the rods was transferred through high strength nuts to the bearing plates and C-section, then to the beam.

4.2.8   Epoxy Repairing

The crack repair of the beams involved pressure injecting a two part epoxy, Nitofill LV. As the epoxy was required to be pressure injected, an impermeable seal on the surface of the beam along the crack lines was required. This was done using a two part epoxy crack sealant, Lokfix E. The application process for the Nitofill LV and

Lokfix E are discussed below, and the data sheets relating to these products are shown in Appendix D.

4.2.8.1   Lokfix E

Lokfix E is a two part epoxy sealant for use on concrete structures. It is used to give a member impermeability, and reduce the chance of reinforcement corrosion.

The Lokfix E was obtained in two cartridges connected together, for use with a double barrel corking gun. The cartridges were sized to automatically apply the correct proportions of the two parts of the epoxy. The two parts of the epoxy were mixed together when extruded, using a specially supplied mixing tube that was connected to the end of the cartridges.

Before the sealant was applied, the crack surface was cleaned using a wire brush, and any loose pieces of concrete were removed. Small holes were then drilled along the crack line, and injection nozzles for the Nitofill LV were glued to the concrete over the holes. The holes were needed to allow the Nitofill LV to freely enter the cracks. The Lokfix E was then extruded over the crack lines, and spread over a 5cm strip using a knife. Care was taken to ensure all cracks were covered and a tight seal was obtained around the flange of the nozzles. Figure 4.12 shows the positioning of the injection nozzles, and the sealing of the cracks using the Lokfix E. The sealant was left to dry for four days after it was applied before the Nitofill LV was injected.

Figure 4.12: Sealing of Cracks Using Lokfix E

Before the Nitofill LV was injected, the impermeability of the sealant was tested by pressure injecting water into the cracks. Leakage occurred around some of the injection nozzles, so these were repatched with Lokfix E to form an impermeable seal. The beam was then left for a day before the Nitofill LV was injected, to ensure the crack surfaces had dried.

4.2.8.2   *Nitofill LV*

Nitofill LV is a two part epoxy resin designed to rebond cracked concrete surfaces. It has very low viscosity, and is therefore ideally suited to being pressure injected into fine cracks.

The Nitofill LV was obtained in two cartridges connected together, for use with a double barrel corking gun. The cartridges were sized to automatically apply the correct proportions of the two parts of the epoxy. Like the Lokfix E, the two parts of the epoxy were mixed together when extruded, using a specially supplied mixing tube. The end of the tube was attached to the injection nozzles using a connector,

and the resin was injected using the corking gun. The injection process started at the lowest most nozzle, with all the nozzles being left open. This was to show when the resin had reached all parts of the crack. As the resin began to flow out of a nozzle, it was then closed. Once only the nozzle being used for injection was open, and the pressure on the corking gun was noticeably higher, the final nozzle where the injection was occurring was closed. The increase in pressure indicated the entire crack had been filled. The Nitofill LV was then left to cure for seven days before the beam was reloaded.

Before the beam was reloaded, the Lokfix E sealant was removed with a grinder, to allow the initial crack lines to be seen. This was so a comparison of the initial crack lines and the crack formed after repair could be made.

4.3   Testing Methodology

4.3.1   Introduction

This section outlines the experimental testing that was involved in this research. As previously stated, four beams were tested under varying conditions, which can be seen in Table 4.1.

Table 4.1: Test Conditions for Specimens

Specimen	Preloaded	Post-tensioned	Epoxy Repaired
B1	No	No	No
B2	Yes	Yes	No
B3	Yes	Yes	Yes
B4	No	Yes	No

This research focused on the effect of existing cracks on shear strengthening of concrete girders using external post-tensioning. The experimental tests involved looking at the repair methods needed to strengthen a member with existing shear cracks. Two of the test beams were preloaded, and then strengthened, while the

other two test beams were control beams used for comparisons. Specimen B1 was used as a control beam to find the failure load of the reinforced concrete beam. Specimen B2 was preloaded to form a shear crack, then post-tensioned and loaded until failure. The level of preloading was determined by visually determining when the maximum crack width was 2mm. Specimen B3 was preloaded to the same level as specimen B2, but it had its shear cracks repaired with epoxy injection. It was then post-tensioned and loaded to failure. Specimen B4 was the post-tensioned control beam. It was post-tensioned before any loading, and was loaded until failure. This beam was used as a comparison to specimens B2 and B3. It was used to find what fraction of the new post-tensioned member's shear strength, either strengthened member gained. The results from these tests can be seen in Chapter 5.

4.3.2   Test Configuration

The test configuration used to load the specimens can be seen in Figure 4.13. This example shows the test setup for the post-tensioned beams. The setup for the beams without post-tensioning did not require the post-tensioning rods, end anchorage or post-tensioning load cells.
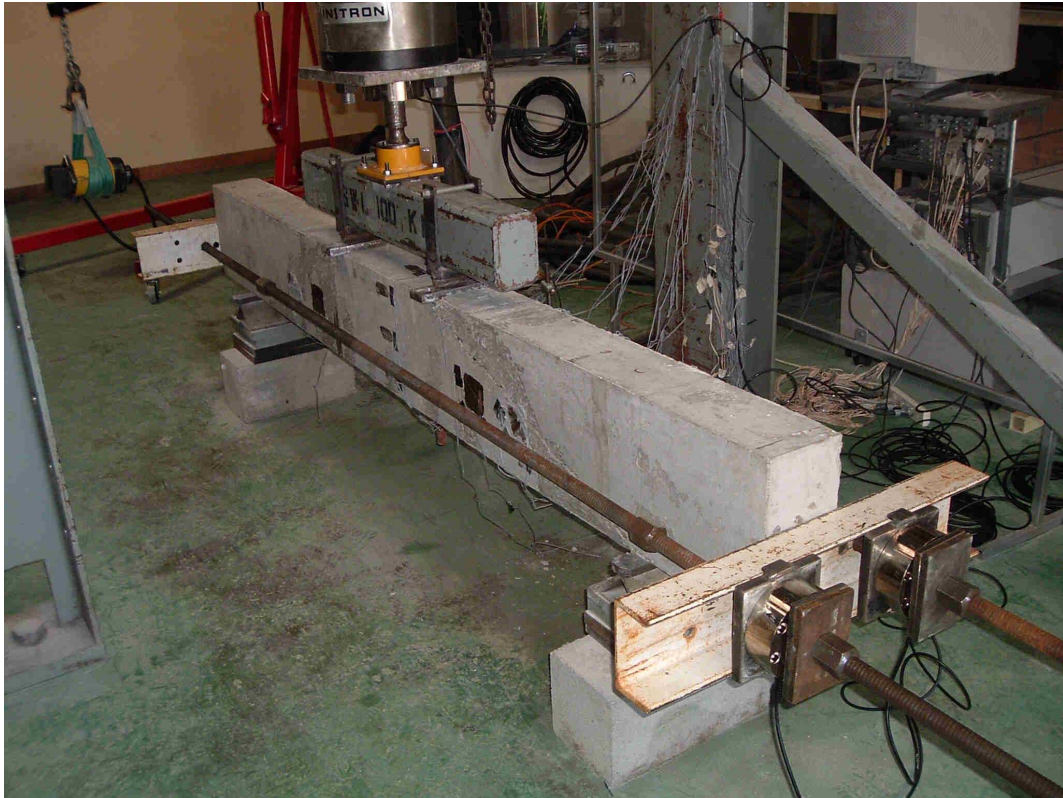
Figure 4.13: Test Configuration

To simulate pin supports as the beams were modelled for, the supports for the beam were made up of triangular shape steel blocks. A 30mm wide steel plate was positioned on top of each triangular block to avoid local cracking around the support. A concrete block and a number of steel plates were positioned under the triangular supports to adjust the height of the beam relative to the loading frame. The setup of the supports for the test beams can be seen in Figure 4.14.

Figure 4.14: Test Beam Supports

Figure 4.13 show how the beams were tested with four point loading. A single 500kN Instron loading ram, with a maximum travel of 150mm, was used to apply the load. The loading ram was supported by the loading frame, which had been adjusted to the correct height for the test beam setup. The load was transferred evenly to the beam at two points via the spreader beam. The spreader beam was connected to the loading ram with a ball and socket joint, and the two loading points were set 500 mm apart.

The force being applied from the loading ram was measured by a load cell that was positioned directly under the ram. Two load cells were also used to measure the force in the post-tensioning rods when they were being stressed, as well as when the load was being applied. The data gathered from the load cells was stored by the system 5000 data logger.

The midspan deflection of the test beams when loaded was measured by a load variable displacement transducer (LVDT). The data gathered from the LVDT was stored by the system 5000 data logger. Figure 4.15 shows the setup of the LVDT measuring the midspan deflection.

Figure 4.15: LVDT Measuring Midspan Deflection

4.3.3   Data Logging

The data measured from the load cells, LVDT and strain gauges during testing was collected using the system 5000 data logger. Each of the measuring devices was allocated a channel on the system 5000, and a reading of each channel was recorded every five seconds during testing. Three of the channels were used for the load cells, one for the LVDT, and 20 for the strain gauges.

4.3.4   Loading

The test beams were loaded at a constant rate of 0.5mm per minute using the Instron loading ram. This loading rate was able to be achieved as the loading ram was computer sensor controlled.

4.3.5   Material Testing

Material testing was conducted on the concrete and shear ligatures to find their exact properties. These were needed to accurately compare the practical results with AS3600 predictions equations.

4.3.5.1   Concrete Compressive Strength Tests

To find the compressive strength of the concrete, 20 cylinders, 100mm diameter by 200mm high, were cast when the beams were poured. These were left to cure in exactly the same conditions as the test beams. On the day of testing for each of the beams, five of the test cylinders were compression tested. The results from these tests can be seen in Chapter 5.

4.3.5.2   Reinforcing Steel Tensile Tests

Tensile tests were conducted on a number of pieces of the R6 steel that was used for the shear ligatures. The specimens were loaded until failure, and the load at yielding was noted. The results from these tests can be seen in Chapter 5. The bars used for the tensile and compressive reinforcement were not tested, as these bars did not reach yielding during any of the testing.

4.4   Safety

As this research involved predominantly experimental testing, there were a number of safety issues involved. These issues concerned the construction and loading of the specimens, post-tensioning, and the application of epoxy resins.

Simple safety measures were observed for the construction and loading of the specimens, and no hazardous incidents occurred. Steel capped boots were worn at all times, and hard hats were worn when the specimens were loaded. Other pieces of personal protective equipment (PPE) were worn for specific activities during the

construction. These included safety glasses when cutting reinforcement with a cutting wheel, and a dust mask when grinding the sealant off the beam.

The post-tensioning in this research involved applying considerable force to the rods, so a number of safety precautions were taken. These involved not standing behind either end of the rods during stressing or loading, in case of slipping or breakage. Warning signs were also erected to advise of stressing in progress.

The epoxy resins used in this testing are toxic if swallowed, and can cause skin and eye irritation. Before these resins were used, the Material Safety Data Sheets (MSDS) were consulted, so the safety issues involved were known. When the epoxy resins were applied, gloves were used and care was taken to avoid contact with the skin.

A risk assessment was prepared for this research, and is shown in Appendix E.

4.5   Summary

This chapter has outlined the procedures used in the construction and testing of the model beams. The testing phase of this research has involved the loading of the specimens, logging of data, applying external post-tensioning, and repairing cracks with epoxy injection. The safety issues involved in the experimental testing have also been covered.

CHAPTER 5

RESULTS AND DISCUSSION

5.1   Introduction

This section will outline the results that were obtained from the experimental testing conducted. It also includes discussion on why the results have occurred, and the implication they have on the research. The results discussed in this section include material strengths, data logged during loading, test observations, and comparisons of theoretical and experimental section capacities.

5.2   Material Tests

To accurately compare the experimental results with prediction equations, the exact properties of the materials had to be found. This is because the ordered compressive strength of concrete, and the stated yield strength of steel, can be largely different to the actual strengths.

5.2.1   Concrete Slump

Prior to the four beams being poured, a slump test was conducted to get an indication of the concrete's workability. A 70 mm slump was found for the concrete, which was close to the 80 mm slump that was ordered. As this is quite a dry mix, a poker vibrator was used to ensure the concrete was properly compacted.

5.2.2   Concrete Compressive Strength

The strength of the specimens is heavily dependent on the concrete strength. For this reason, one batch of concrete was used for all of the beams, and a number of

cylinders were cast on the day of pouring. The testing of the beams was conducted over a number of days, so on each test day, the concrete's compressive strength was found by doing compression tests on a number of cylinders. Figure 5.1 shows the compression test for a cylinder.

Figure 5.1: Cylinder Compression Test

The concrete strength at the time of testing for each beam is shown in Table 5.1. The sample cylinders for beam 3 preloading and beam 4 have been grouped together, as these tests were conducted on the same day.

Table 5.1: Concrete Compressive Strengths

Beam No.	Cylinder No.	Maximum Load (kN)	Compressive Strength, *ƒ*'c (MPa)	Average *ƒ*'c (MPa)
1	1	317	40.4	39.9
	2	318	40.5	
	3	300	38.2	
	4	317	40.4	
	5	316	40.2	
2	6	322	41.0	40.3
	7	312	39.7	
	8	308	39.2	
	9	317	40.4	
	10	322	41.0	
3 (Preloading) and 4	11	319	40.6	40.4
	12	314	40.0	
	13	305	38.8	
	14	315	40.1	
	15	333	42.4	
3 (After Epoxy Repair and Post-tensioning)	16	312	39.7	40.4
	17	308	39.2	
	18	317	40.4	
	19	319	40.6	
	20	331	42.1	

The concrete was ordered for 32 MPa, but the actual strength was considerably higher. The concrete did not gain much strength over the testing period, as the testing was conducted over a short period of time. The testing did not begin until 28 days after pouring, so the concrete had gained the majority of its strength by this stage. As the concrete strengths at each test time were so similar, the compressive strength of the concrete for all beams was taken as 40 MPa.

In Chapter 3, the theoretical capacities of the beams were found assuming 32 MPa concrete. To compare the experimental results with the prediction equations, the theoretical capacities of the beams are re-calculated later in this chapter, using the concrete strength found.

5.2.3   Reinforcing Strengths

Tensile tests were conducted on the R6 shear ligature steel to find the actual yield strength of the steel. This was compared to the theoretical yield strength of 250 MPa. Four sample pieces of the steel were used for the testing, with a summary of the results shown in Table 5.2.

Table 5.2: Ligature Steel Tensile Strength

Test Specimen	Actual Diameter (mm)	Yield Load (kN)	Yield Stress (MPa)
1	6.0	10.4	368
2	6.0	10.3	364
3	6.0	10.4	368
4	6.1	10.5	359
		Average	**365**

The yield strength of the R6 steel found from the testing was 365 MPa, which is considerably higher than the theoretical strength of 250 MPa. This strength is used later in this chapter, when recalculating the theoretical section capacities with actual material properties.

5.3   Crack Observation

The crack pattern for each of the test beams was observed as they were being loaded. The maximum crack widths at important load levels have also been noted.

5.3.1   Specimen B1

The shear cracking in the reinforced control beam formed as expected, starting from the support and propagating towards the loading point. The first shear crack was observed at 125 kN load near the tension face at the support. The crack propagated towards the loading point as the load was increased. At the maximum load of 196 kN, the maximum crack width was 2.5 mm. At this load, a second shear crack

formed parallel to the main crack, approximately 80 mm away towards the middle of the beam. The shear cracking in Specimen B1 can be seen in Figure 5.2.

Figure 5.2: Failure Crack in Specimen B1

Small flexural cracks formed in the midspan of the beam at approximately 60 kN. These stayed as fine cracks throughout the loading, as the tensile steel did not reach its yield point. These cracks stopped increasing in size when the shear cracks began to form around 125 kN load.

5.3.2   Specimen B2

Specimen B2 was preloaded to form a shear crack with a maximum width of approximately 2 mm. A load of 181 kN was required to form this crack. The initial shear cracking in the specimen formed in the same way as Specimen B1, with the first shear cracks forming at 117 kN. The cracking began around the support, and propagated towards the loading point as the load was increased. The initial crack formed in Specimen B2 can be seen in Figure 5.3.

Figure 5.3: Initial Crack in Specimen B2

Small flexural cracks formed in the midspan of the beam at approximately 50 kN. These again stayed as fine cracks throughout the loading, and stopped increasing in size when the shear cracks began to form around 127 kN load.

After the 150 kN of post-tensioning was applied, the maximum crack width reduced to 1 mm. Once the loading was reapplied, the cracks began to steadily reopen. At the maximum load of 194 kN, the maximum crack width was 3 mm. The crack continued to open as the load was applied, with the maximum crack width at failure being 8 mm. As with Specimen B1, a second shear crack formed parallel to the main crack, at approximately the maximum load taken. The failure crack of Specimen B2 can be seen in Figure 5.4.

Figure 5.4: Failure Crack in Specimen B2

5.3.3   Specimen B3

Specimen B3 was preloaded to form a shear crack with a maximum width of approximately 2 mm. A load of 183 kN was required to form this crack, which was approximately equally to that for Specimen B2. The initial shear cracking in the specimen formed in the same way as the previous specimens, with the first shear crack forming at 115 kN. The cracking began around the support, and propagated towards the loading point as the load was increased. The initial crack formed in Specimen B3 can be seen in Figure 5.5.

Figure 5.5: Initial Crack in Specimen B3

Small flexural cracks formed in the midspan of the beam at approximately 55 kN. These again stayed as fine cracks throughout the loading, and stopped increasing in size when the shear cracks began to form around 115 kN load.

After preloading, the shear cracks were repaired by epoxy injection, and the beam was post-tensioned. The initial cracks were completely repaired, as the new crack lines formed away from the initial cracks. Once the loading was reapplied, a new set of shear cracks began to form at 220 kN. The onset of the shear cracks was at a much higher load than for the reinforced control beam, as the post-tensioning caused the beam to be in compression. This meant a much higher load was required to form the flexural crack around the support, needed to initiate the shear crack. Just before the maximum load of 310 kN, the maximum crack width was 1.5 mm. After the maximum load of 310 kN was reached, the beam exhibited a shear-compression failure, with a large increase in crack width evident. The maximum crack width at this point was 7 mm. The failure crack of Specimen B3 can be seen in Figure 5.6. The initial crack line of this beam has been highlighted in green, showing how the shear crack formed away from the epoxy repaired crack. The failure crack formed

directly between the support and the applied load, cutting the initial crack at approximately half the beam's depth.

Figure 5.6: Failure Crack in Specimen B3

5.3.4   Specimen B4

The shear cracking in the post-tensioned control beam formed slightly different to the beams without post-tensioning. The first shear crack formed at 180 kN, starting at approximately 250 mm in from the support near the bottom edge. The crack then propagated towards the applied load, increasing in width as the load was increased. Just before the maximum load of 354 kN, the maximum crack width was 2 mm. After the maximum load of 354 kN was reached, a new crack suddenly formed directly between the applied load and the support. The sudden formation of this crack was an indication this was a shear-compression failure. Once the failure crack reached the support, a new crack formed between the support and the initial steeper crack. The maximum crack width after failure was 8 mm. The shear cracking of Specimen B4 can be seen in Figure 5.7.

Figure 5.7: Failure Crack in Specimen B4

Small flexural cracks formed in the midspan of the beam at approximately 95 kN. These began to form at a load approximately 35 kN higher than for the beams without post-tensioning, due to the bottom face of the beam being placed in compression. These again stayed as fine cracks throughout the loading, and stopped increasing in size when the shear cracks began to form around 180 kN load.

5.3.5   Comparison of Crack Patterns

The shear cracking of Specimen B1, Specimen B2, and the preloading of Specimen B3 formed in the same way. This cracking was flatter at the top and bottom of the beam, and steeper through the middle section of the beam. Specimen B2 after post-tensioning still had the same crack pattern as the other reinforced beams, as the existing cracks continued to open up after post-tensioning. The shear cracking in Specimen B4 and Specimen B3 after epoxy injection and post-tensioning were also similar. The failure cracks for these beams formed a direct line between the support and the loading point. This indicates that the epoxy repaired beam behaved similarly to the post-tensioned control beam, and had the same failure mechanism. This in

contrast to the beam strengthened only with post-tensioning, where the failure crack was the same as for the reinforced beam. Figure 5.8 shows a comparison of the two general crack patterns observed.
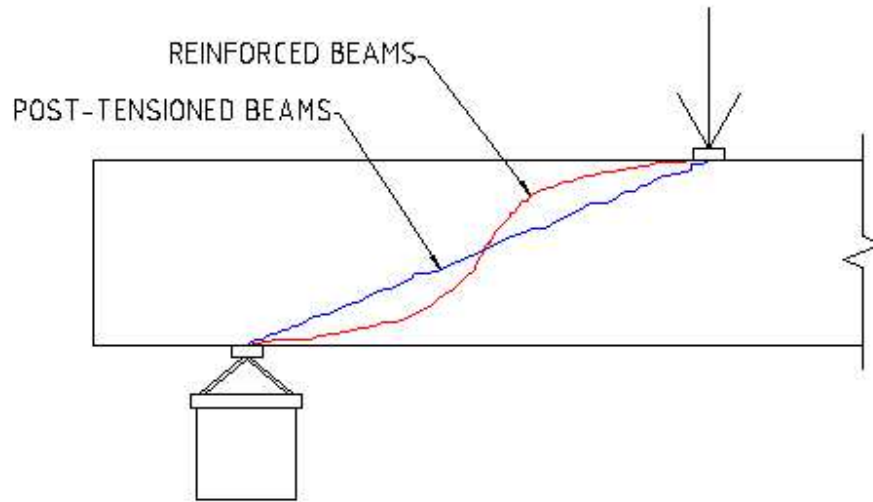
Figure 5.8: Comparison of Crack Patterns

5.4   Load – Deflections Characteristics

The load versus deflection relationship for each of the test beams is discussed in this section.

5.4.1   Specimen B1

B1 - Load vs Deflection
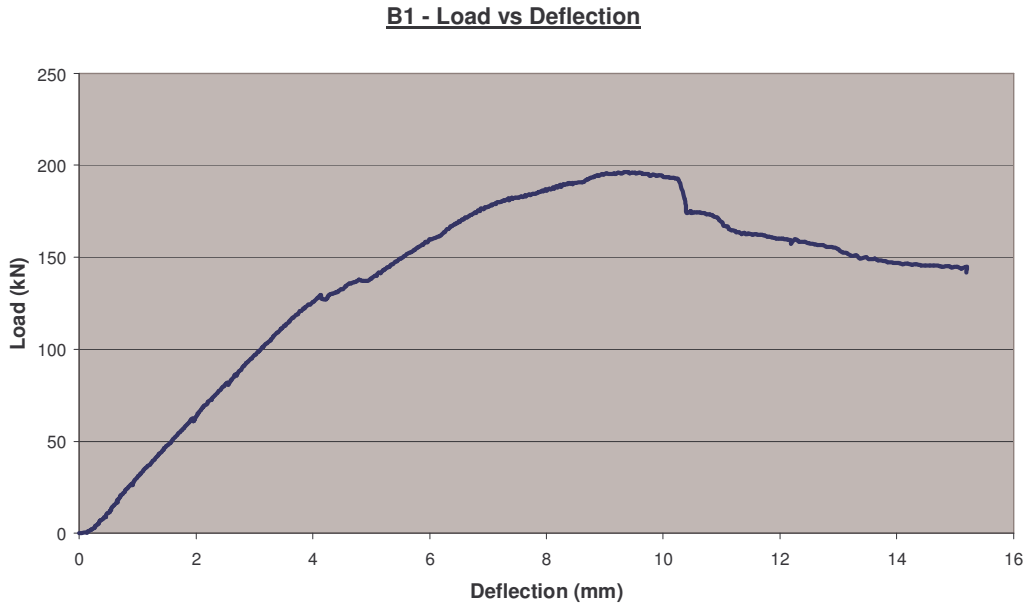
Figure 5.9: Load - Deflection Relationship for B1

The load versus deflection graph for the reinforced control beam, Specimen B1, is shown in Figure 5.9. The graph shows a linear shape up until 125 kN load, when the shear cracks began to form. The formation of these cracks caused the stiffness of the beam to reduce after this point. The maximum load recorded was 196 kN at 9.5 mm deflection.   The sharp drop in load at 10.3 mm deflection was due to a shear-compression failure occurring, causing a sudden increase in crack width. The load was continued to be applied after this point, with the crack width and deflection increasing for a reduced load. The required load was reduced due to the crack width increasing, which decreased the concrete component of the beam's shear strength.

5.4.2   Specimen B2

B2 - Load vs Deflection
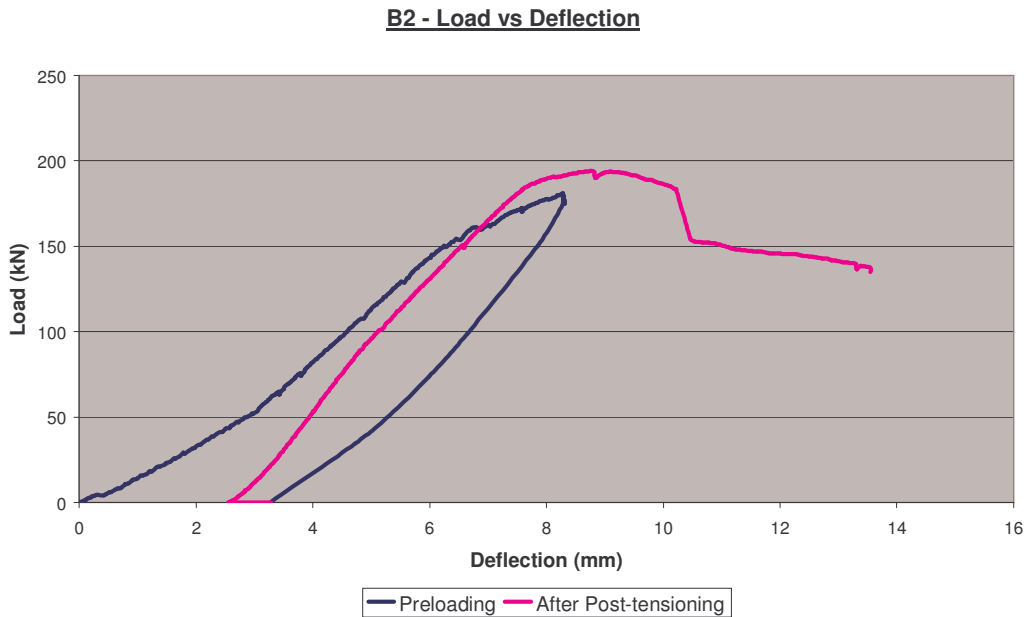
Figure 5.10: Load - Deflection Relationship for B2

The load versus deflection graph for the post-tensioned repair beam, Specimen B2, is shown in Figure 5.10. The preloading of Specimen B2 shows similar behaviour to Specimen B1, except Specimen B2 has exhibited a seating error at the start of loading. The flatter slope at the start of loading is likely due to a loading plate slowly flattening down an edge piece of concrete that was sticking up. The linear section between 50 kN and 125 kN load should have extrapolated to the origin. The preloading was taken to 181 kN, with 8.28 mm deflection. As the load was removed, the deflection reduced to 3.28 mm.

The beam was then post-tensioned, causing the deflection to reduce by a further 0.73 mm to 2.55 mm. This was due to the eccentricity of the post-tensioning causing the beam to camber upwards, thus reduce the deflection. After post-tensioning, the maximum load taken by the beam was 194 kN, compared to Specimen B1 which took a load of 196 kN. This equates to a 1% decrease in strength due to the post-tensioning. This can be explained by the angle of the shear cracks relative to the

post-tensioning force. As the cracks are on an angle of approximately 30 degrees, part of the post-tensioning force is actually causing the crack faces to slide against each other, instead of forcing them together. This reduces the concrete component of the shear strength for the beam, leaving the load to be predominantly taken by the shear ligatures. The small drop in load after the maximum load was reached was due to a crack opening up. After this point, the load was taken predominantly by the ligatures, with a major drop in load evident at 10.2 mm deflection, when a shear-compression failure occurred. This shows that post-tensioning alone will not increase a beam's shear strength if it has existing shear cracks. The loading was stopped at 13.6 mm deflection, as the beam had obviously failed.

5.4.3   Specimen B3

Figure 5.11: Load - Deflection Relationship for B3

The load versus deflection graph for the beam that had its shear cracks repaired with epoxy injection and was then post-tensioned, Specimen B3, is shown in Figure 5.11. The preloading of Specimen B3 shows similar behaviour to Specimens B1 and B2. The graph shows a linear shape up until 115 kN load, when the shear cracks began

to form. The preloading was taken to 183 kN, with 7.63 mm deflection. As the load was removed, the deflection reduced to 2.10 mm.

The beam had its shear cracks repaired with epoxy injection, and was then post-tensioned, causing the deflection to reduce by a further 0.55 mm to 1.55 mm. The very flat slope of the graph at the beginning of loading after epoxy repair and post-tensioning is again due to a seating error. The deflection has increased from 1.55 mm to 2.13 mm for a load of just 5.0 kN. The linear section between 5 kN and 220 kN load should have extrapolated to 1.55 mm deflection for zero load. The first shear cracks formed in the repaired beam at 220 kN. This is evident on the graph by the end of the linear section of load versus deflection. The slope of the graph after this point is much flatter, as the load is predominantly being taken by the ligatures. The maximum load taken by the beam was 310 kN at 13.84 mm deflection. This is a 58% increase in strength from the reinforced control beam. The sharp drop in load after the maximum is due to a sudden shear-compression failure occurring. After this occurred, almost the entire load of 162 kN was being taken by the ligatures.

5.4.4   Specimen B4
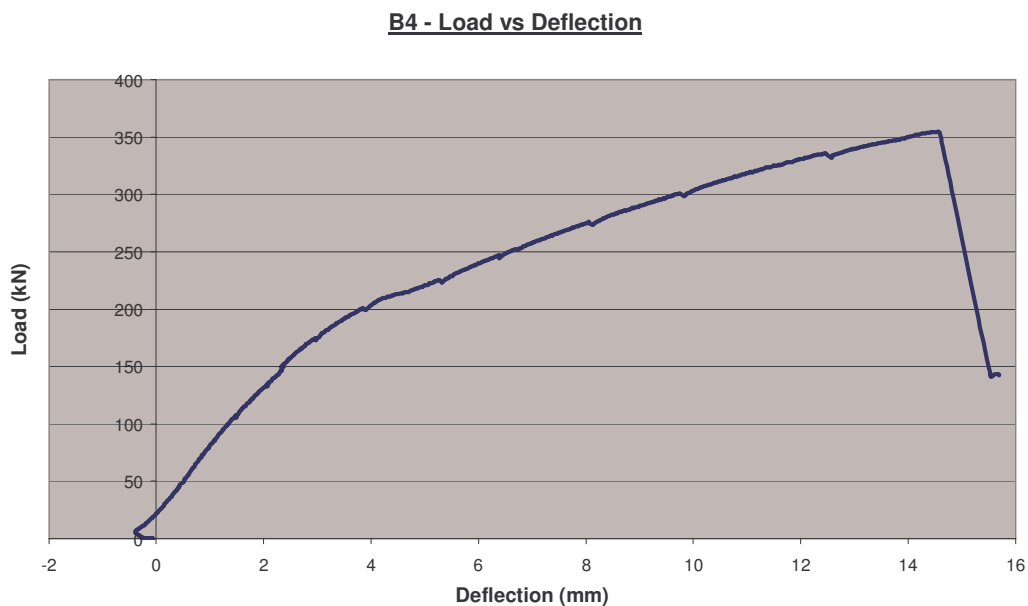
Figure 5.12: Load - Deflection Relationship for B4

The load versus deflection graph for the post-tensioned control beam, Specimen B4, is shown in Figure 5.12. The beam was post-tensioned before loading, and was then loaded until failure. The post-tensioning caused the beam to deflect upwards by 0.38 mm. The graph shows a linear shape up until 180 kN load, when the shear cracks began to form. The slope of the graph is then flatter up until the maximum load of 354 kN. This load is 81% higher than for the reinforced control beam. The sharp drop in load after the maximum is again due to a sudden shear-compression failure occurring. This behaviour is very similar to that exhibited by Specimen B3.

5.4.5   Comparison of Load – Deflection Characteristics

The beam that was repaired only with post-tensioning did not gain any strength compared to the reinforced control beam. This is in contrast to the beam that was repaired with epoxy injection and then post-tensioned, which had a 58% increase in strength. This compared to the post-tensioned control beam which had an 81% increase in strength from the reinforced control beam.

The shape of the load versus deflection graph for the post-tensioned control beam, Specimen B4, is very similar to that of the epoxy repaired beam, Specimen B3. The only significant difference is that Specimen B4 continued to be loaded to 354 kN, where Specimen B3 failed at 310 kN. The reason the repaired beam did not reach as high a failure load is that it probably received minor damages in preloading, that have caused it to fail earlier than the post-tensioned control beam. This is due to the small cracks and damages acting as initiators for the shear cracks. This shows that the beam that was epoxy injected and post-tensioned behaved very similarly to the post-tensioned control beam, except it did not gain the entire strength of the new member. The testing has also shown that epoxy injection of shear cracks combined with external post-tensioning substantially increases a beam's shear capacity.

5.5   Concrete Strain Distribution of Beams

Concrete strain gauges were used to measure the strain in the concrete at midspan and in the shear span using a strain rosette. This section will discuss the results obtained from these measurements.

5.5.1   Strain Gauge Rosette

The principal strains in the shear span for each of the test beams during loading have been shown in this section. The positioning of the strain rosettes can be seen in Figure 4.9. The principal strains have been calculated from the strains recorded in the strain rosettes on each test beam. The calculations used to find the principal strains are shown below.

The three strains recorded in the strain rosette were:

$$\varepsilon_0 = \text{horizontal strain}, \varepsilon_x$$
$$\varepsilon_{90} = \text{vertical strain}, \varepsilon_y$$
$$\varepsilon_{45} = \text{diagonal strain}$$

The shear strain, γ_{xy}, is calculated by:

$$\gamma_{xy} = 2\varepsilon_{45} - \varepsilon_0 - \varepsilon_{90}$$

Using the strains ε_0, ε_{90}, and γ_{xy}, the principal strains, ε_{min} and ε_{max}, can be found using Mohr's circle, as shown in Figure 5.13.
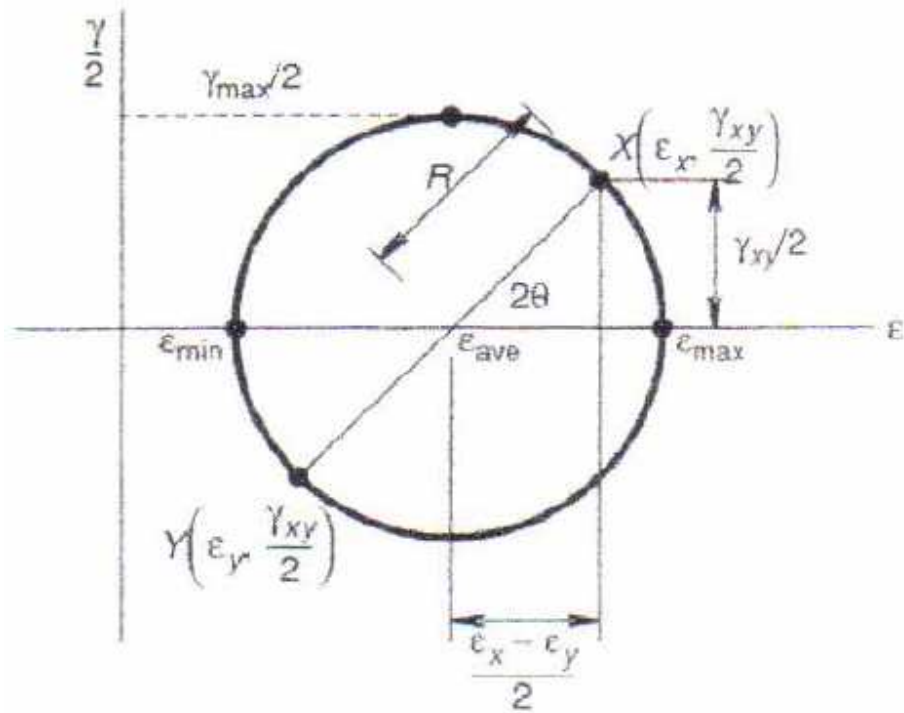
Figure 5.13: Mohr's Circle of Strain

(Source: Stress Analysis Study Book, 2003)

Where,

$$\varepsilon_{avg} = \frac{(\varepsilon_x + \varepsilon_y)}{2}$$

$$R = \sqrt{\left(\left(\frac{(\varepsilon_x - \varepsilon_y)}{2}\right)^2 + \left(\frac{\gamma_{xy}}{2}\right)^2\right)}$$

$$\varepsilon_{max} = \varepsilon_{avg} + R$$

$$\varepsilon_{min} = \varepsilon_{avg} - R$$

5.5.1.1   Specimen B1

Figure 5.14 shows the principal strains of the concrete in the shear spans during loading of Specimen B1. It can be seen that that the maximum principal strain in strain rosette 1 (SR1) was 3490 micro strain at 129 kN load. At this point, the minimum principal strain was -3430 micro strain, with the negative sign indicating it was in compression. The graph for SR1 ceased at this point as one of the strain gauges broke, due to a shear crack propagating through it. The maximum principal strain in SR2 was 640 micro strain at 120 kN load. The strain did not get as high as in SR1, as the shear crack in this end formed slightly away from the rosette. After the crack formed near SR2, the strain began to reduce due to the ligatures taking the load. At the maximum load of 196 kN, the principal strains in SR2 were 220 and -90 micro strain. The highest magnitude recorded in the minimum principal strain of SR2 was -990 micro strain at 160 kN load. The strains in SR2 continued to increase after the maximum load was reached up to this point, as a compression strut had formed between the applied load and the support. The failure crack for this beam formed on the side of SR2.

B1 - Load vs Principal Strains
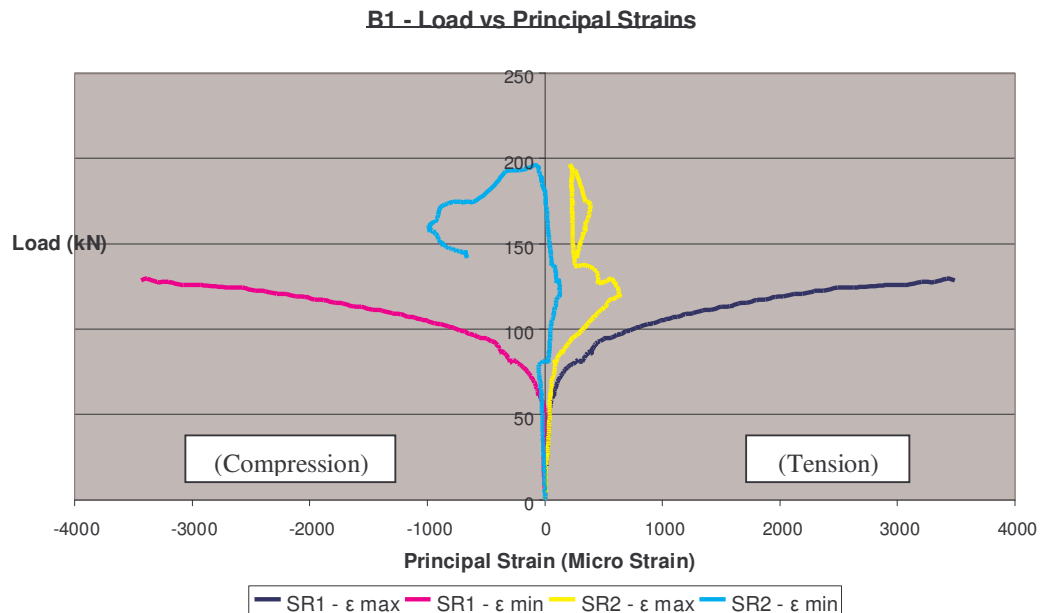
Figure 5.14: Principal Strains for Beam 1

5.5.1.2   Specimen B2

Figure 5.15 shows the principal strains of the concrete in the shear spans during preloading of Specimen B2. The shear cracks in both ends of this beam formed slightly away from either rosette, so the strains recorded were quite small. The horizontal reduction in the maximum principal strain in SR1 at 117 kN load, indicates that a shear crack formed near the rosette at this time. The formation of a crack would reduce the stress on the concrete around it, as the load is then partially taken by the ligatures. The highest magnitude recorded in the minimum principal strains of SR1 and SR2 were -260 and -240 micro strain respectively, at the maximum preload of 181 kN.

B2 - Load v Principal Strains (Preloading)
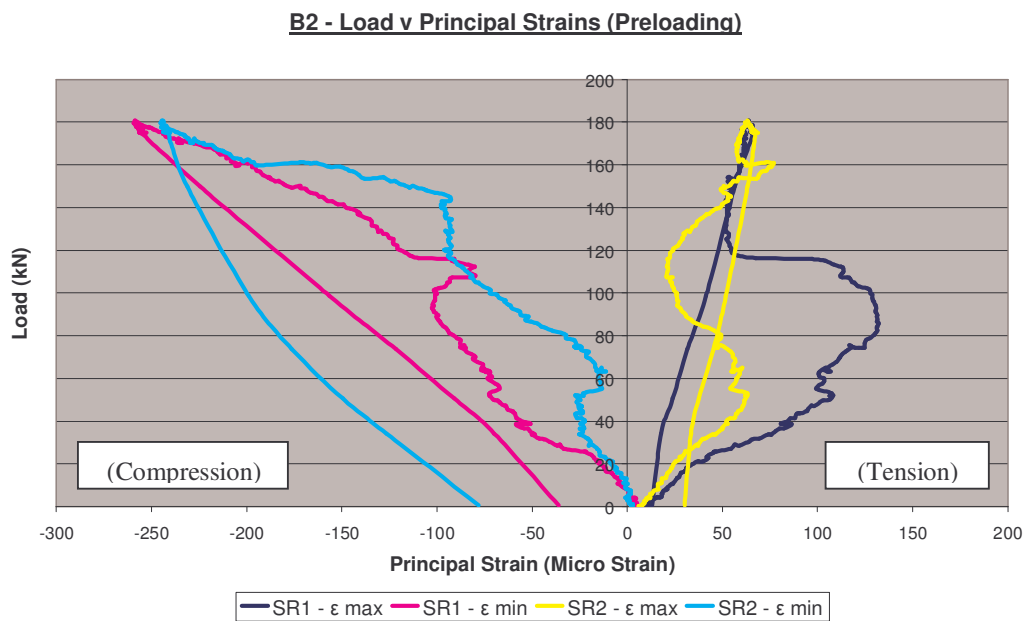
Figure 5.15: Principal Strains for Beam 2 (Preloading)

Figure 5.16 shows the principal strains of the concrete in the shear spans during loading of Specimen B2 after it was post-tensioned. The failure crack for this beam formed on the side of SR1. The cracks from the preloading continued to open up, with no new cracks forming, so again both rosettes did not have cracks through them. For this reason, the maximum principal strains were small. The sharp drop in

minimum and maximum principal strains in SR1 at 183 kN load was due to a shear compression failure occurring. This also translates to a sharp drop on the load vs deflection graph for this beam, as shown in Figure 5.10. The highest magnitude recorded in the minimum principal strain of SR1 was -430 micro strain at 145 kN load.

B2 - Load v Principal Strains (After Post-tensioning)
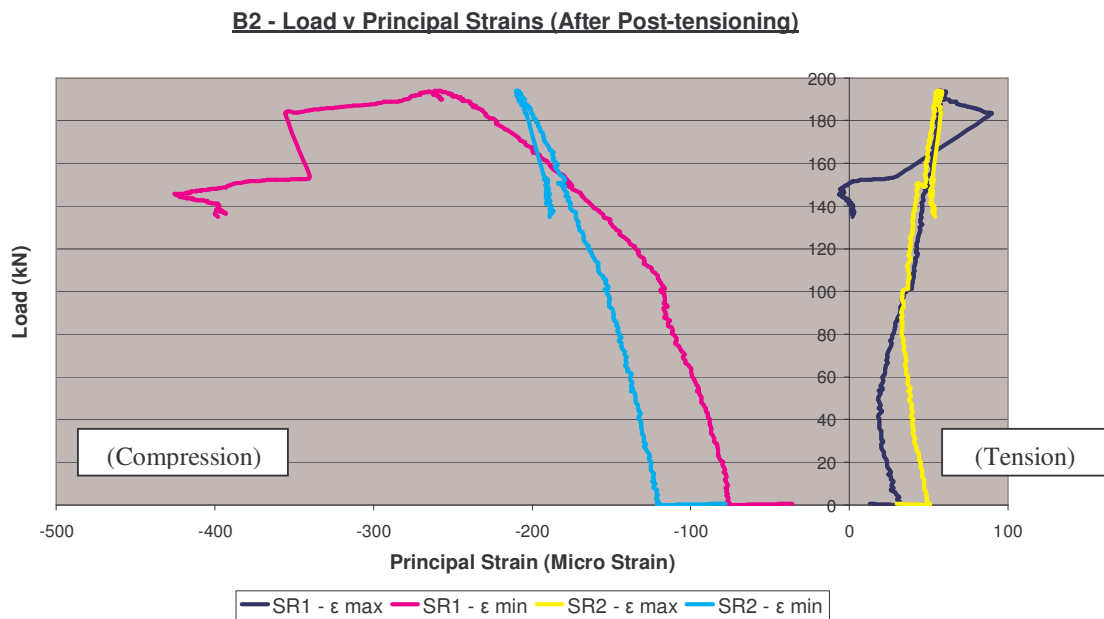
Figure 5.16: Principal Strains for Beam 2 (After Post-tensioning)

5.5.1.3   *Specimen B3*

Figure 5.17 shows the principal strains of the concrete in the shear spans during preloading of Specimen B3. A shear crack formed through SR2, but the shear crack on the side of SR1 formed slightly away from the rosette, and therefore SR1 had very small strains compared to SR2. The maximum principal strain in SR2 at 140 kN load, just before one of the strain gauges broke due to a crack propagating through it, was 4240 micro strain. The horizontal increase in strain on the graph for SR2 at 117 kN load, indicates that a shear crack was initiating very close to the rosette. It then propagated through the rosette, causing the principal strains to increase rapidly.

B3 - Load v Principal Strains (Preloading)
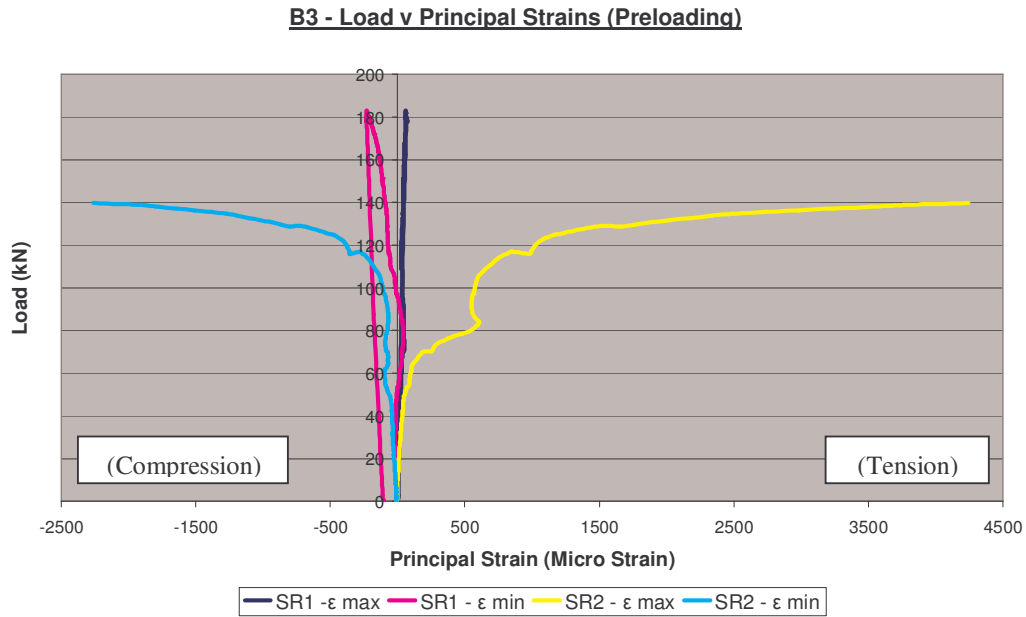
Figure 5.17: Principal Strains for Beam 3 (Preloading)

Figure 5.18 shows the principal strains of the concrete in the shear spans during loading of Specimen B3 after epoxy injection of the cracks and post-tensioning. As the strain gauges in SR2 were broken during the preloading, this rosette position was not used for the loading after epoxy injection and post-tensioning. It was decided this rosette would be replaced by one which was approximately 200 mm further towards the middle, on the side of SR1, as can be seen in Figure 5.6. This position was chosen as the post-tensioned control beam had exhibited initial shear cracking in this area. This strain rosette was called SR3, and was used to find the difference between the two rosette positions for the post-tensioned beam.

It can be seen that SR3 exhibited very little strain up until 254 kN load. After this point, the maximum principal strain in SR3 increased rapidly to 4130 micro strain, at 263 kN load, before one of the strain gauges broke. This was due to a crack propagating through the rosette, as expected would occur. The shear cracks near SR1 initiated at approximately 220 kN load, and began to open significantly at 300 kN load. This translates to the near horizontal increase of the minimum principal

strain of SR1 at 300 kN load. The minimum principal strain was increasing rapidly at this time, due to a compression strut forming between the support and the applied load. The maximum principal strain of SR1 was not increasing at the same rate at this time, as the crack was opening up, and the tensile load was being predominantly taken by the ligatures. At the point before ultimate failure, the principal strains in SR1 were 710 and -1170 micro strain. The beam failed due to shear compression failure, with the main crack located just above SR1.

B3 - Load v Principal Strains (After Epoxy Repair and Post-tensioning)
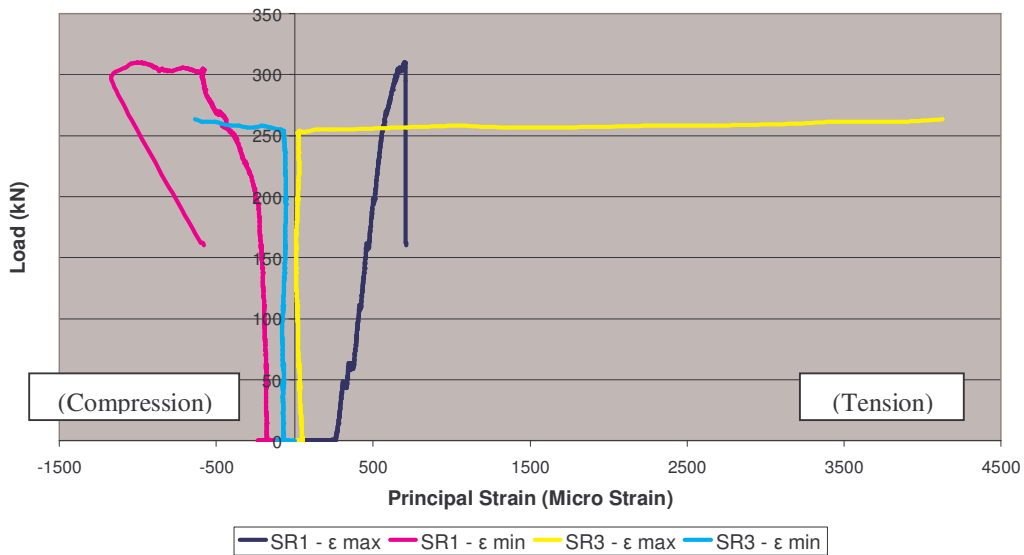
Figure 5.18: Principal Strains for Beam 3 (After Epoxy Repair and Post-tensioning)

5.5.1.4   Specimen B4

Figure 5.19 shows the principal strains of the concrete in the shear spans during loading of Specimen B4. The failure crack for this beam formed on the side of SR1, but neither rosette had a crack form through it. The principal strains in SR1 just before failure were 110 and -630 micro strain. This beam exhibited a sudden shear compression failure, with the main crack running above SR1. The principal strains along the crack line would most likely have been significantly higher than those measured in SR1. This is inferred from the principal strains in Specimen B3 just

before failure being 710 and -1170 micro strain, with a similar failure mode exhibited.

B4 - Load v Principal Strains
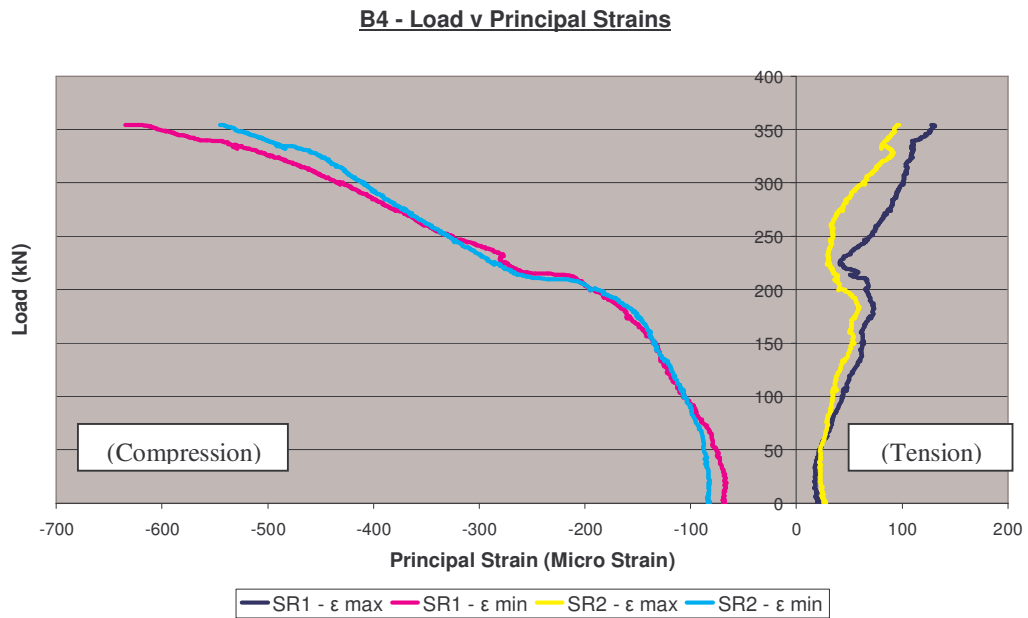
Figure 5.19: Principal Strains for Beam 4

5.5.2   Mid-span Concrete Strain

The midspan concrete strains for each of the test beams during loading have been shown in this section. The positioning of the four strain gauges in the midspan is shown in Figure 5.20.
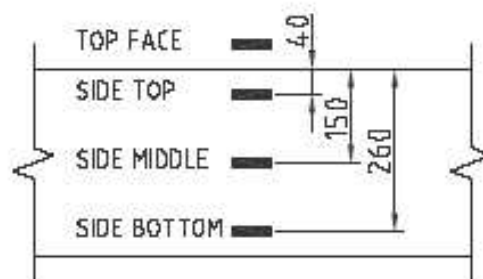
Figure 5.20: Positioning of Midspan Concrete Strain Gauges

5.5.2.1   Specimen B1

Figure 5.21 shows the midspan concrete strains of Specimen B1 during loading. The maximum compressive strain on the top face was 1100 micro strain at the maximum load of 196 kN. There is a linear relationship from when loading began to when the maximum load was achieved, for both the top face gauge and the side top gauge. This is because the top section was in compression for the entire loading. The side middle gauge and the side bottom gauge have shown unexpected results. Both gauges have started as expected, with the bottom in tension and the middle tending from neutral to tension. At 19 kN load, the bottom gauge has switched from being in tension to compression. This is in contrast to the tensile reinforcement strains which have increased in tension throughout the loading. The middle gauge has increased in tension until 42 kN load, before reducing and then switching to compression. It is believed these two gauges were faulty, and the results are not reliable.
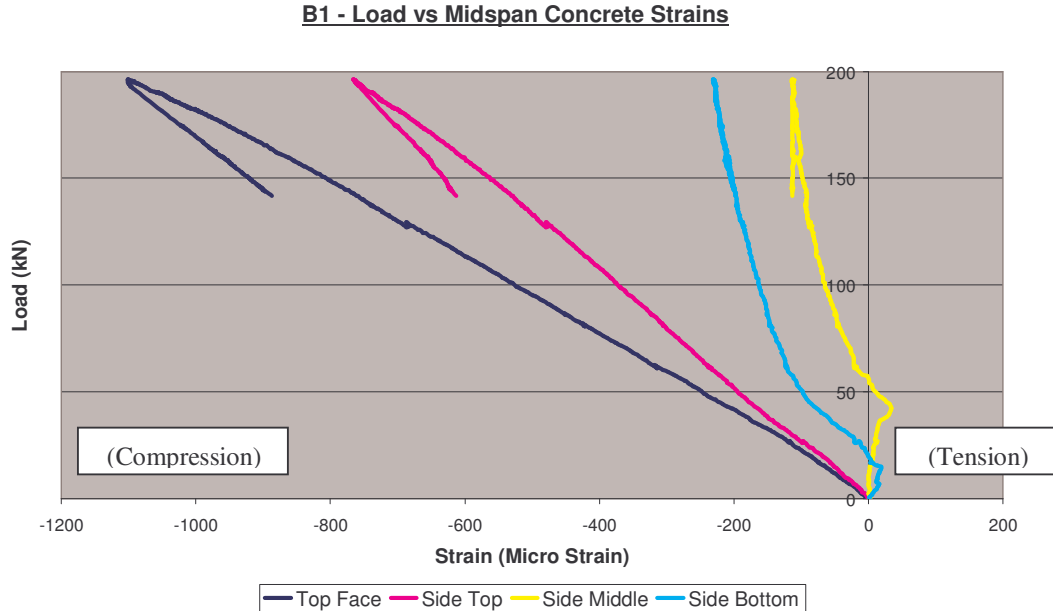
Figure 5.21: Midspan Concrete Strains for Beam 1

5.5.2.2   Specimen B2

Figure 5.22 shows the midspan concrete strains of Specimen B2 during loading. The maximum tensile strain in the bottom gauge before breaking due to a flexural crack was 3450 micro strain at a load of 86 kN. The strain profile for the gauge on the top face of the beam had no change after post-tensioning, due to the eccentricity of the force. The compression exerted on the beam was neutralised by the tensile force from the induced moment. The side top gauge had slightly higher compression after the post-tensioning, as this level had the same compressive force, but less tensile force from the induced moment. The side middle gauge had significantly less tension after post-tensioning than in the preloading, due to the compressive force exerted on the beam.

Figure 5.22: Midspan Concrete Strains for Beam 2

5.5.2.3   Specimen B3

Figure 5.23 shows the midspan concrete strains of Specimen B3 during loading. The maximum tensile strain in the bottom gauge before breaking due to a flexural crack was 3580 micro strain at a load of 95 kN. The changes in strain due to the

application of post-tensioning, as previously mentioned, were again evident in this beam. The strains in the top gauges reached higher compression strains than the in the previous beams, as a 58% higher load was achieved. The maximum compressive strain reached in the top face of the beam was 2570 micro strain. This is still well short of the nominal crushing strain of concrete, which is 3000 micro strain.

B3 - Load vs Midspan Concrete Strains
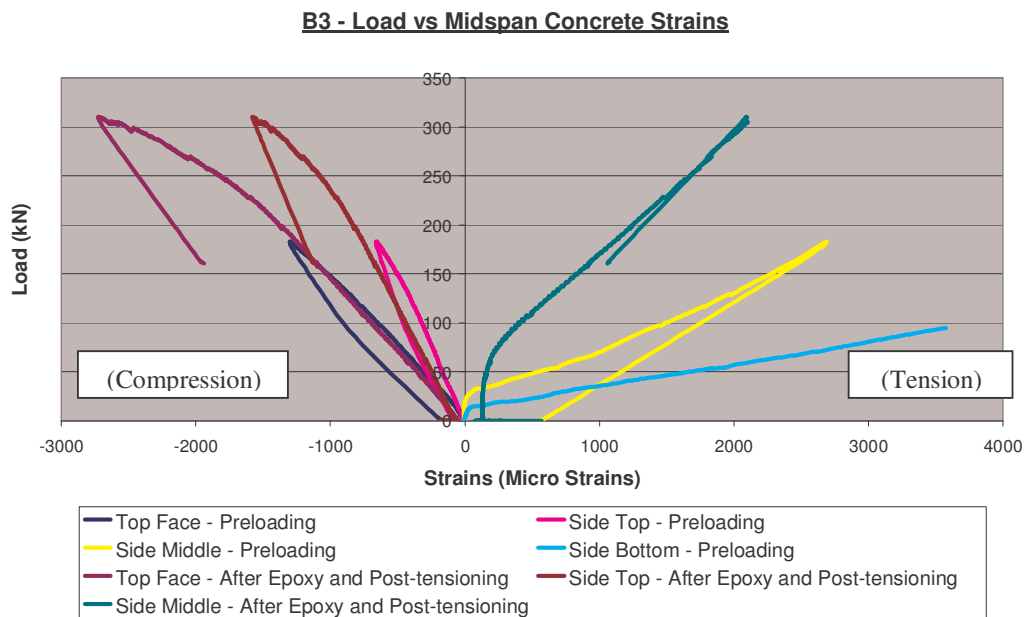
Figure 5.23: Midspan Concrete Strains for Beam 3

5.5.2.4   Specimen B4

Figure 5.24 shows the midspan concrete strains of Specimen B4 during loading. At the beginning of loading, the middle and bottom gauges had compressive strains due to the post-tensioning. The compressive strain in the bottom gauge was 170 micro strain, and in the middle gauge there was 80 micro strain. The strains in the top gauges at this time were negligible. The maximum tensile strain in the bottom gauge before breaking was 4040 micro strain at a load of 246 kN. The flexural cracks in this beam began at a much higher load than for the other reinforced beams, due to the compressive force from the post-tensioning. A higher moment was

required to induce a tensile cracking stress at the bottom of the beam, which had overcome the initial compressive stress. The maximum compressive strain reached in the top face of the beam was 2980 micro strain, which is approaching the nominal crushing strain of concrete. This beam had the highest concrete compressive strain, as it took the highest load.

B4 - Load vs Midspan Concrete Strains
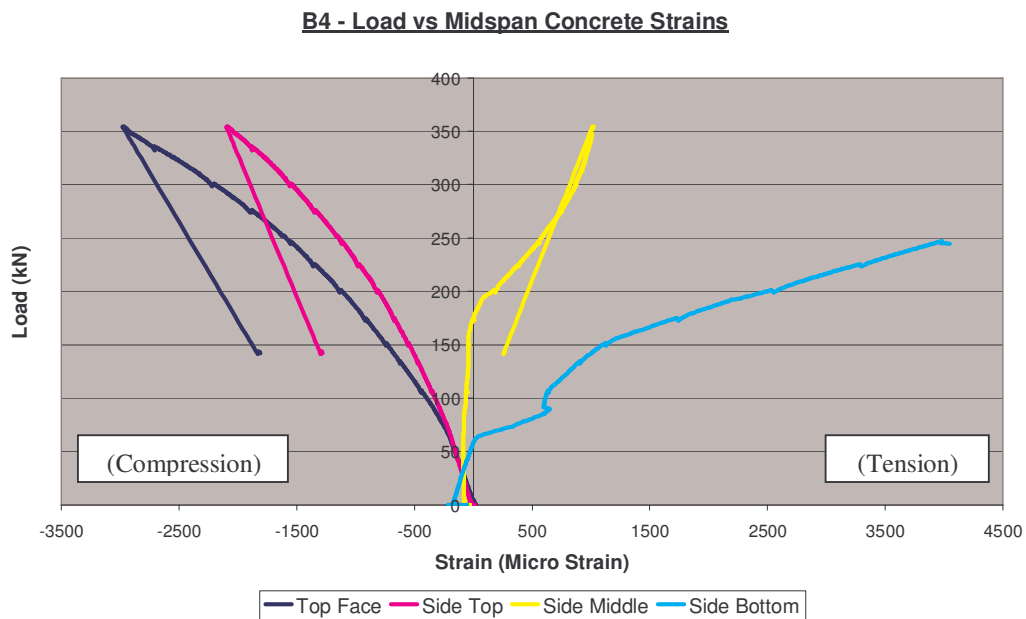
Figure 5.24: Midspan Concrete Strains for Beam 4

5.6   Steel Strain Distribution of Beams

Steel strain gauges were used to measure the strain in the midspan tensile reinforcement, and in the ligatures in the shear span. This section will discuss the results obtained from these measurements.

5.6.1   Tensile Reinforcement Strains

The strain in the tensile reinforcement for each of the beams is shown in Figure 5.25. It can be seen from the graph that the tensile steel remained in the elastic range for all of the testing. This was due to the beams being over-designed for flexural

capacity, to ensure shear failures. The maximum strain recorded in the tensile steel was 2550 micro strain, which was in Specimen B4 just before failure. The shape of the graphs for B1 and the preloading of B2 and B3 were very similar.   The maximum strain recorded in the preloading of B2 and B3 was approximately 1620 micro strain. As each of the beams was then post-tensioned, the tensile steel was forced into compression, as expected. The shape of the graph for Specimen B3 after epoxy repair and post-tensioning was very similar to that of Specimen B4, except it did not gain as high a strain, as it failed due to a smaller load.

Load vs Tensile Reinforcement Strain
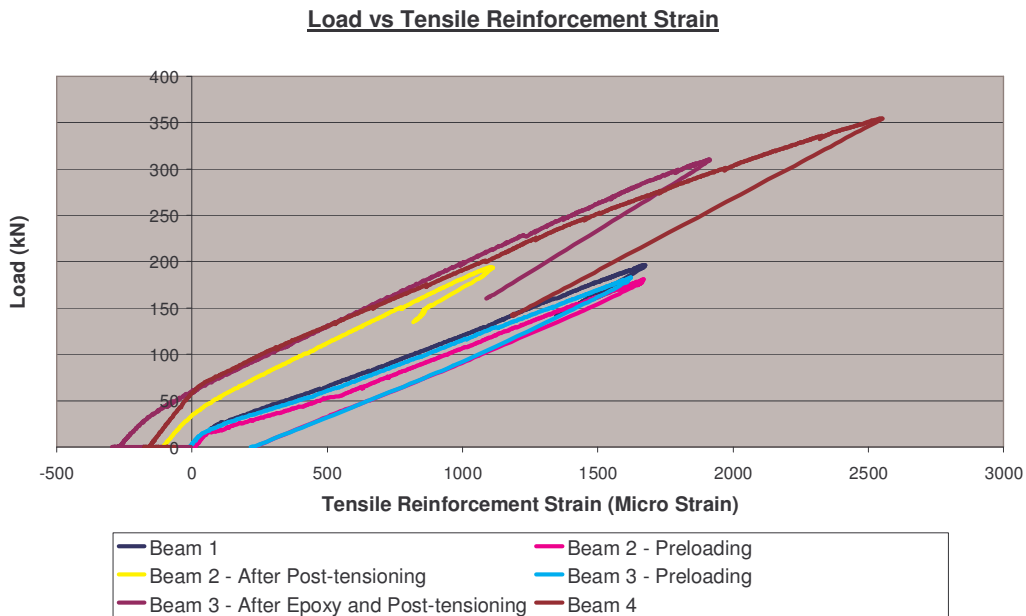
Figure 5.25: Load vs Tensile Reinforcement Strain of the Four Beams

The tensile reinforcement strain gauges were at the same level as the side bottom midspan concrete strain gauges, but the steel gauges recorded lower strains than the concrete gauges. The maximum tensile reinforcement strains were between 1650 and 2550 micro strain, while the maximum strains in the side bottom concrete strain gauges reached approximately 3500 micro strain by half the ultimate load, before breaking. The concrete strain gauges reached higher strains than the steel gauges due to localised increases in strain, normally due to cracking. If a crack passed through a concrete strain gauge, the gauge area took the entire increase in strain, but

the tensile reinforcement redistributed the strain over a large length. This was due to the tensile reinforcement slightly debonding from the concrete, thus allowing the reinforcement to redistribute the strain over a larger area. This is why the side bottom concrete strains and the tensile reinforcement strains did not match, even though they were positioned at the same level.

5.6.2   Shear Reinforcement Strains

The strain developed in the shear ligatures during loading of each beam is discussed in this section. The positioning of the shear ligatures can be seen in Figure 4.4.

5.6.2.1   Specimen B1

Figure 5.26 shows the strain in the shear ligatures during loading of Specimen B1. The failure crack for this beam was on the side of ligatures 3 and 4. It can be seen that the strain in ligatures 1 and 4 began to increase at 125 kN load. This is when the shear cracks began to form through the ligatures, therefore leaving the load to be taken predominantly by the ligatures. The flat sections of the graph indicate when major cracks have opened up, and the load carried by the ligature has increased. The maximum strain recorded in ligature 4 was 4420 micro strain at the maximum load of 196 kN. The large increase in strain up to this point was due to the failure crack opening widely at this point, causing the strain in this ligature to increase dramatically. The graph of ligature 3 has stopped at 1970 micro strain, at a load of 192 kN. This point translates to when the failure crack opened significantly, and there was a sharp drop in load carried. It is believed the readings from the gauge stopped at this point due to breaking when the ligature yielded.

B1 - Load vs Shear Ligature Strain
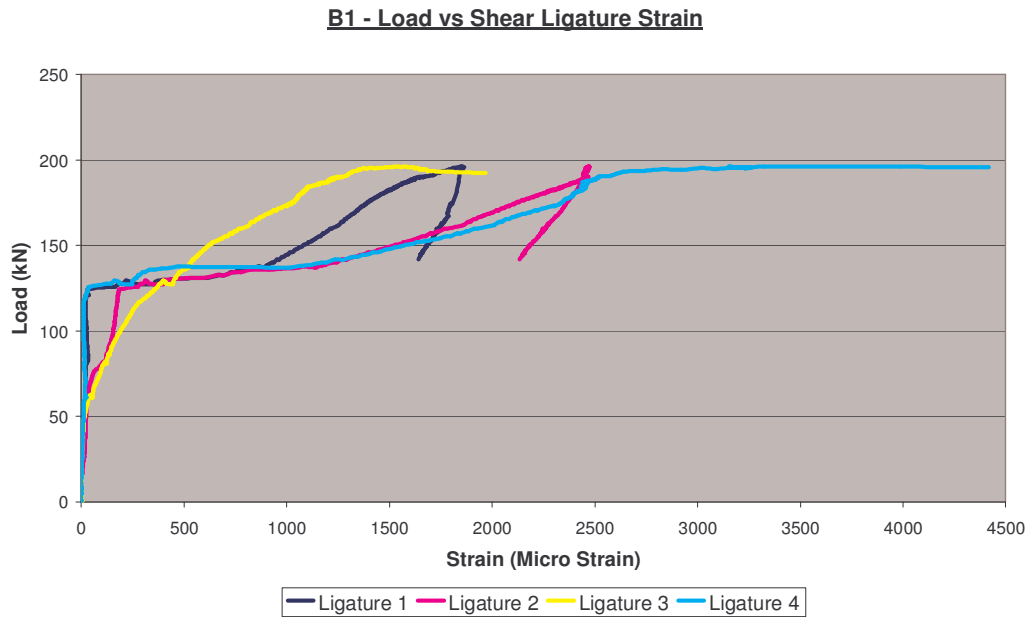
Figure 5.26: Strain Measured in Shear Ligatures in Beam 1

5.6.2.2   *Specimen B2*

Figure 5.27 shows the strain in the shear ligatures during the preloading of Specimen B2. The maximum strain in ligature 1 was 2820 micro strain, while in ligatures 2, 3 and 4 it was approximately 1700 micro strain. This indicates that a major crack has formed through ligature 1, and the ligature has yielded. This was confirmed by the visual crack inspection, where the largest crack was seen on the side of ligatures 1 and 2. It can be noted that a significant crack opened through ligature 4 at 161 kN load, as a horizontal increase of 1000 micro strain can be seen at this load.

B2 (Preloading) - Load vs Shear Ligature Strain
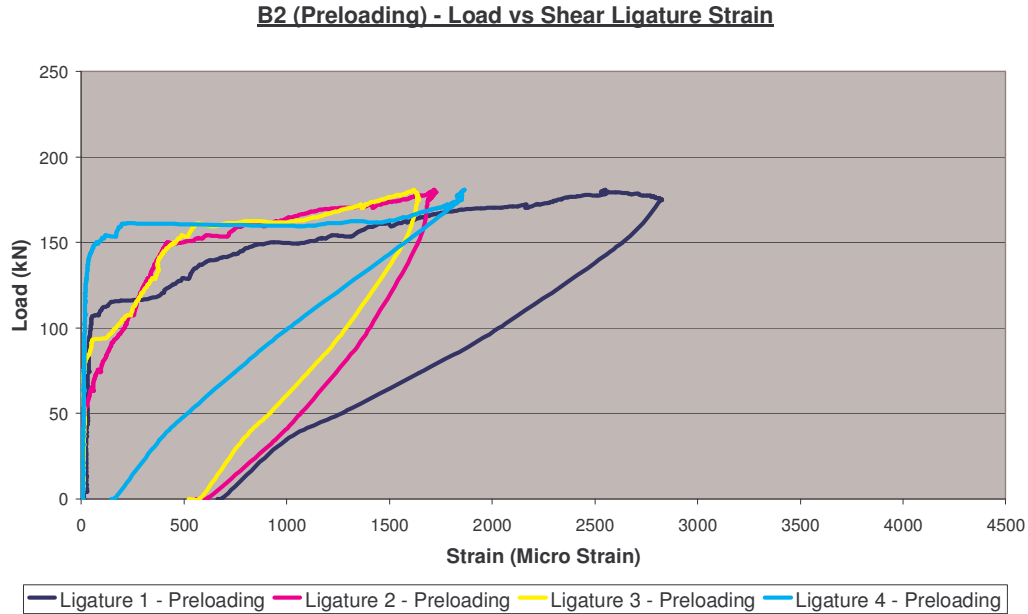
Figure 5.27: Strain Measured in Shear Ligatures in Beam 2 (Preloading)

Figure 5.28 shows the strain in the shear ligatures of Specimen B2 after being post-tensioned. The failure crack for this beam was on the side of ligatures 1 and 2. The ligatures began to take the load when the initial cracks began to reopen at a load of 85 kN. From this point up to a load of 185 kN, the graph for all the ligatures are almost linear, as they are in the elastic range. The graph for ligature 2 then flattens out as it began to yield. Ligature 1 also yielded after this point, with the maximum strain recorded as 2980 micro strain. After the maximum load was reached, ligature 2 continued to yield to 2410 micro strain before it broke at 154 kN load. This translates to a sharp drop in load as can be seen in the load-deflection graph, Figure 5.10.

B2 (After Post-tensioning) - Load vs Shear Ligature Strain
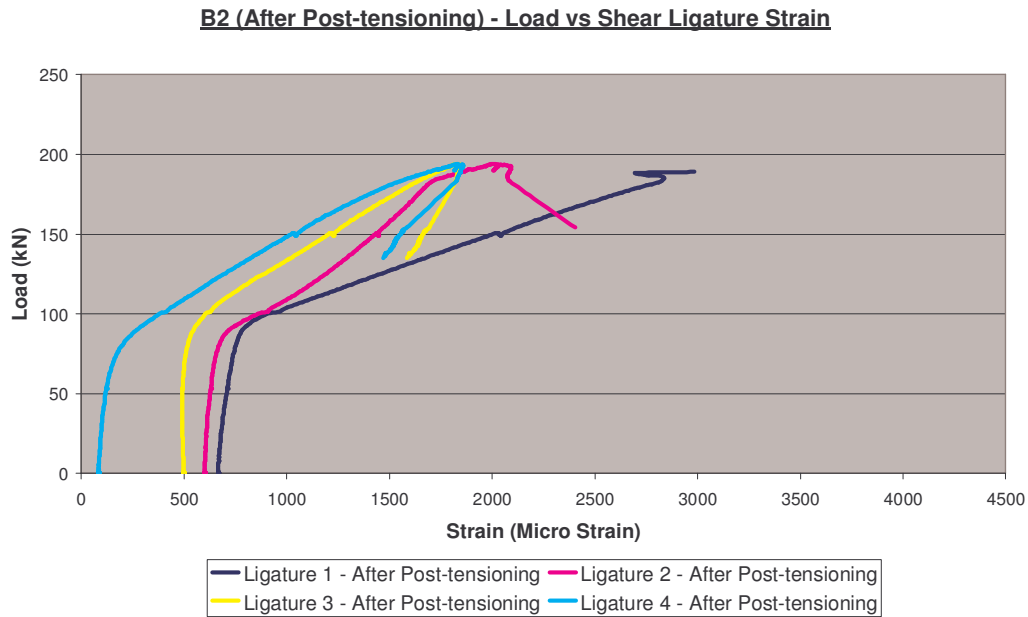
Figure 5.28: Strain Measured in Shear Ligatures in Beam 2 (After Post-tensioning)

5.6.2.3   Specimen B3

Figure 5.29 shows the strain in the shear ligatures during the preloading of Specimen B3. The shape of the graph is similar to that for the preloading of Specimen B2. The maximum strain in ligature 3 was 1890 micro strain, 1370 micro strain in ligature 2, and approximately 1200 micro strain in ligatures 1 and 4. These strains indicate that none of the ligatures had yielded at this point. Having all the strains at approximately the same level confirmed the visual crack inspection, where both sides cracking appeared equal.

B3 (Preloading) - Load vs Shear Ligature Strain
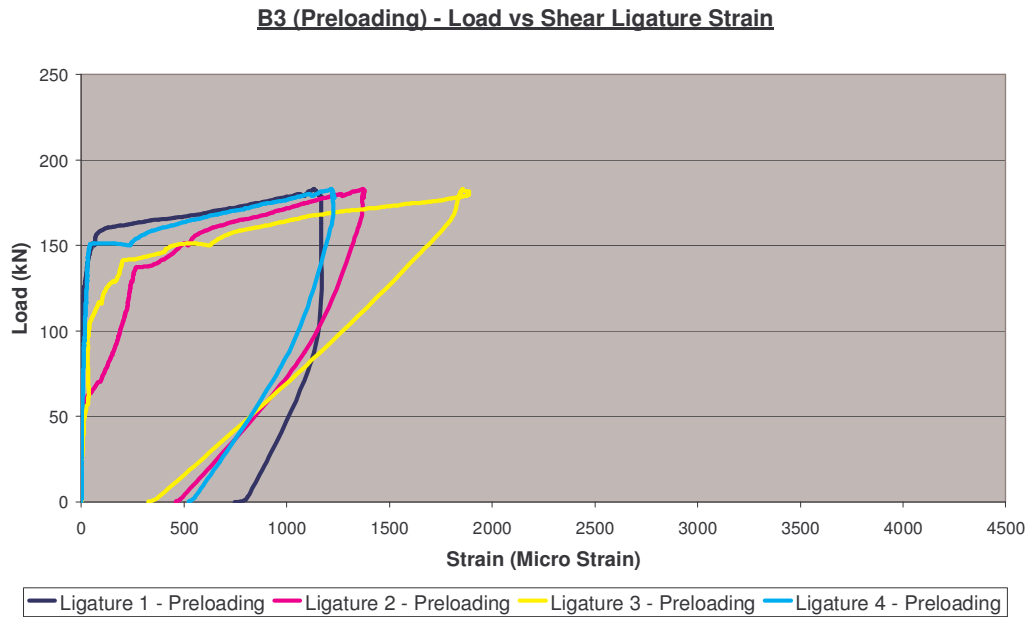
Figure 5.29: Strain Measured in Shear Ligatures in Beam 3 (Preloading)

Figure 5.30 shows the strain in the shear ligatures of Specimen B3, after epoxy repair and post-tensioning. It can be seen from the graphs for ligatures 2 and 3, the cracks through these ligatures started at a load of 270 kN. To show detail of the graph, it has only been shown up to 4500 micro strain, but the maximum strain for three of the ligatures were much higher than this. The maximum strain for ligature 1 was 5300 micro strain, ligature 2 was 16800 micro strain, and ligature 3 was 5900 micro strain. These ligatures each began to yield at 2200 micro strain, which is indicated by the almost horizontal graphs for each of the ligatures after this point. The failure crack for this beam was on the side of ligatures 1 and 2.

B3 (After Epoxy and Post-tensioning) - Load vs Shear Ligature Strain
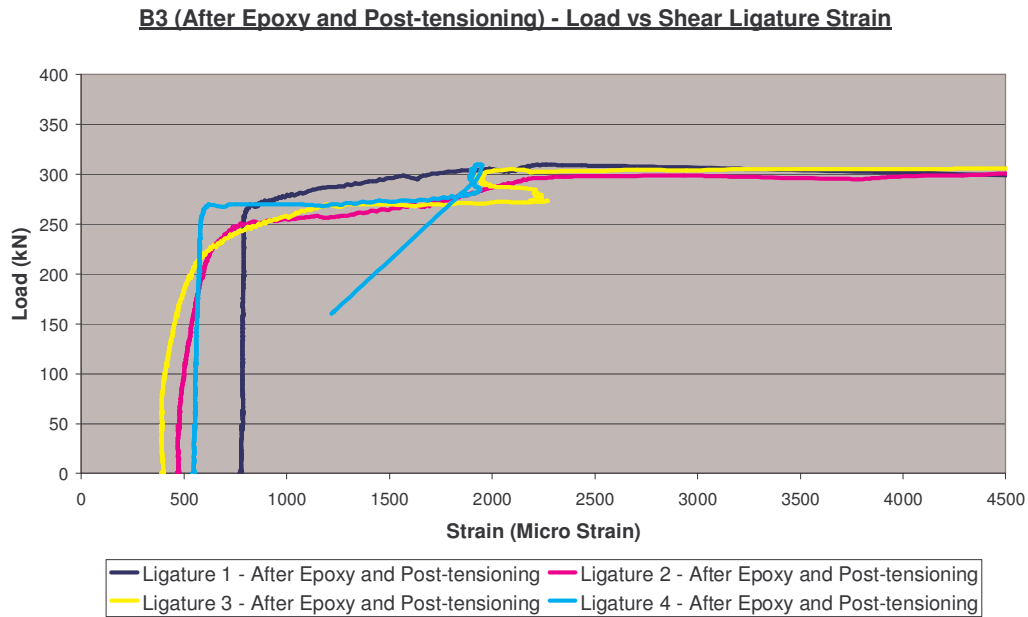
Figure 5.30: Strain Measured in Shear Ligatures in Beam 3 (After Epoxy and Post-tensioning)

5.6.2.4   Specimen B4

Figure 5.31 shows the strain in the shear ligatures during loading of Specimen B4. The failure crack for this beam was on the side of ligatures 1 and 2. The first shear cracks formed in this beam at approximately 180 kN. These initial cracks formed approximately 250 mm in from the supports, so they crossed the middle ligatures (2 and 3) more so than the outer ligatures (1 and 4). This is why the graphs for ligatures 2 and 3 are much flatter than for ligatures 1 and 4. When the sudden shear-compression failure occurred, the gauges for ligatures 1 and 2 ceased reading. The maximum strain in ligature 1 at this point was 1220 micro strain, which indicates it had not yielded.

B4 - Load vs Shear Ligature Strain
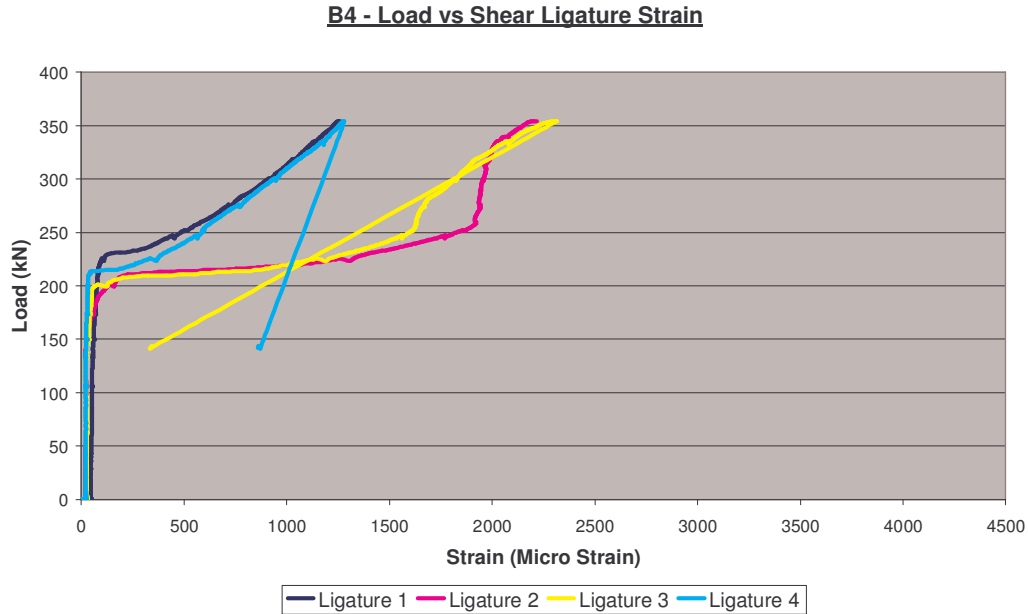
Figure 5.31: Strain Measured in Shear Ligatures in Beam 4

5.7   Increase in External Post-tension Force

As the beams were loaded and began to deflect, the tension side of the beam increased in length. This caused the post-tensioning rods to also increase in length, which therefore increased the force in the rods. Figure 5.32 shows the increase in post-tension force as the beams have been loaded. Note that the deflection shown is the deflection from when the post-tensioned beam has begun loading.

Increase in Post-tension Force vs Deflection
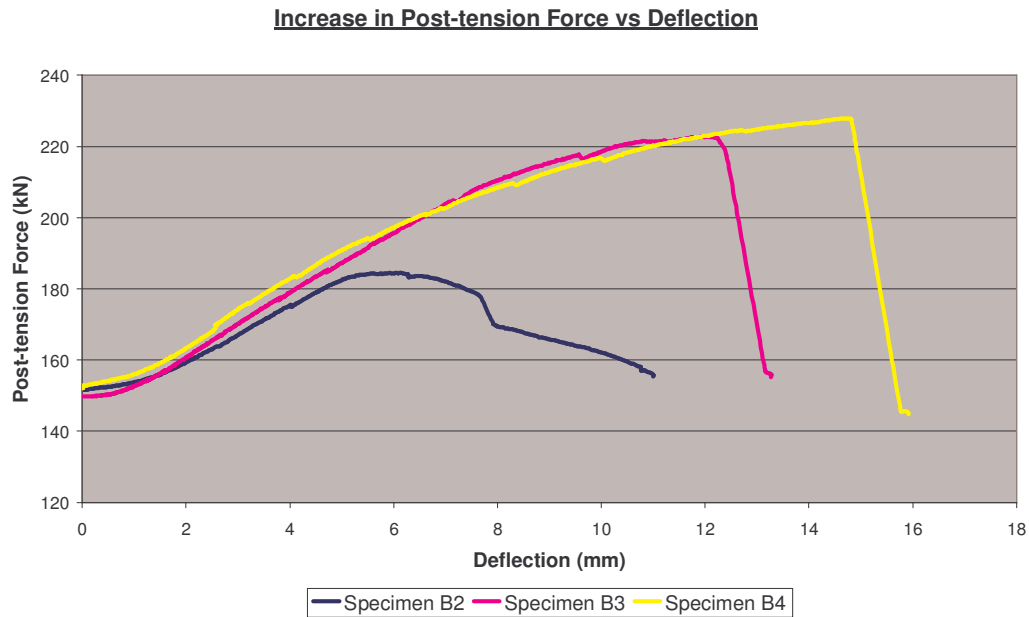
Figure 5.32: Increase in Post-tension Force as the Beams are Loaded

The graph shows that the post-tensioned force in Specimens B3 and B4 has increased dramatically more than Specimen B2. This is due to the sliding action that has occurred in B2. This has meant that the tension side of the beam has not increased in length as much as for B3 and B4, as the deflection has occurred due to the crack width increasing, not the beam bending as a whole. The post-tension force in B2 has gradually decreased after the maximum load was reached at 5.5 mm deflection, with a sharp drop at 7.7 mm deflection. The sharp drop relates to when a crack has opened up from the loading, and then allowed the post-tensioning rods to decrease in length, by partially closing the crack. The post-tension force has increased in Specimens B3 and B4 up until failure, as these two beams were bending as a whole, and therefore increasing the rods' length. Specimen B4 had a larger increase than B3, as it took a higher load and sustained a larger deflection. The major drops in post-tension force for B3 and B4 are due to the shear-compression failures that occurred, which caused major cracking. The percentage increase in post-tensioning force for each of the beams is shown in Table 5.3. The percentage increase of post-tensioning force, combined with the shape of the graph, indicates

that the epoxy repaired beam, Specimen B3, is behaving almost as a new condition member.

Table 5.3: Percentage Increase in Post-tensioning Force

Specimen	Initial Force (kN)	Maximum Force (kN)	Percentage Increase (%)
B2	152	184	21.1
B3	150	223	48.7
B4	152	228	50.0

Table 5.4 shows the maximum stress in the post-tensioning rods recorded during loading, compared to the predicted stress using AS3600. The percentage difference between the two has also been shown. It can be seen that the actual maximum stress for each of the beams is lower than the predicted. Part of this difference is due to the predicted stress being based on the ultimate moment capacity, which was not reached for any of the beams, as each beam failed in shear. The increase in Specimen B2 was significantly less than the predicted due to the sliding affect that occurred, as previously mentioned. The predicted stress in Table 5.4 is found from Clause 8.1.6 of AS3600:

$$\sigma_{pu} = \sigma_{p.ef} + 70 + \left(\frac{f'_c \cdot b_{ef} \cdot d_p}{100.A_{pt}} \right) \leq \sigma_{p.ef} + 400$$

Table 5.4: Comparison of Predicted and Actual Stress in Post-tensioning Rods

Specimen	Predicted Stress (MPa)	Actual Stress (MPa)	Percentage Difference (%)
B2	220.3	173.3	21.3
B3	220.3	210.0	4.7
B4	220.3	214.7	2.5

5.8   Section Capacities Based on Actual Material Properties

The section capacities of the test beams were calculated in Chapter 3 using theoretical material properties. Material tests conducted have shown material strengths different to the expected. To accurately compare the practical test results

with AS3600 prediction equations, the section capacities need to be recalculated using the observed material properties.

The following section will show the calculations of the shear capacities of the beams, using actual material properties. The flexural capacity of the beams will not be recalculated, as each the test beams failed in shear.

5.8.1 Before Post-tensioning

Section Properties
$$f'_c = 40MPa$$

Reinforcing Properties
$$f_{sy.f} = 365MPa$$

Shear strength of the concrete:

$$V_{uc} = 1.48 \times 1 \times 1 \times 150 \times 257 \times \left(\frac{900 \times 40}{150 \times 257} \right)^{\frac{1}{3}}$$
$$= 55.76kN$$

Shear strength of the reinforcement:

$$V_{us} = \left(\frac{A_{sv} \cdot f_{sy.f} \cdot d_o}{s} \right) \cot \theta_v$$

Where,

$$\theta_v = 30^o + 15^o \left(\frac{A_{sv} - A_{sv.min}}{A_{sv.max} - A_{sv.min}} \right)$$

Where,

$$A_{sv} = 56.5mm^2$$

$$A_{sv.\,min} = \frac{0.35b_v \cdot s}{f_{sy.f}}$$

$$= \frac{0.35 \times 150 \times 250}{365}$$

$$= 36.0mm^2$$

$$A_{sv.\,max} = \frac{b_v \cdot s\left(0.2f'_c - \dfrac{V_{uc}}{b_v \cdot d_{st}}\right)}{f_{sy.f}}$$

$$= \frac{150 \times 250 \times \left(0.2 \times 40 - \dfrac{55760}{150 \times 257}\right)}{365}$$

$$= 673.6mm^2$$

Therefore,

$$\theta_v = 30^o + 15^o\left(\frac{56.5 - 36.0}{673.6 - 36.0}\right)$$

$$= 30.48^o$$

Therefore, the ultimate shear strength of the shear reinforcement, V_{us}, is:

$$V_{us} = \left(\frac{56.5 \times 365 \times 257}{250}\right)\cot(30.48)$$

$$= 36.04kN$$

Calculating the reinforced concrete beam's ultimate shear capacity:

$$V_u = V_{uc} + V_{us}$$

$$= 55.76 + 36.04$$

$$= 91.80kN$$

As four point loading is used, the ultimate shear capacity load, $P_{u.s}$, is calculated as:

$$P_{u.s} = 2 \times 91.80$$

$$= 183.60kN$$

5.8.2   After Post-tensioning

Shear strength of the concrete:

$$V_{uc} = 1.477 \times 1 \times 1 \times 150 \times 257 \times \left(\frac{(900 + 1061.9) \times 40}{150 \times 257} \right)^{\frac{1}{3}} + 20 \times 10^3 + 0$$

$$= 92.16 kN$$

Shear strength of the reinforcement, as previously found:

$$V_{us} = 36.04 kN$$

Calculating the post-tensioned beam's ultimate shear capacity:

$$V_u = V_{uc} + V_{us}$$

$$= 92.16 + 36.04$$

$$= 128.20 kN$$

As four point loading is used, the ultimate shear capacity load, $P_{u.s}$, is calculated as:

$$P_{u.s} = 2 \times 128.20$$

$$= 256.40 kN$$

5.9   Comparison of Practical Results with AS3600 Predictions

This section compares the capacities of the beams found from the experimental testing with the recalculated theoretical section capacities found in section 5.8. This will indicate the accuracy of the prediction equations for this testing. The comparison for the four specimens is shown in Table 5.5.

Table 5.5: Comparison of Theoretical and Experimental Failure Loads

Specimen No.	Recalculated Theoretical Capacity, P_u (kN)	Experimental Capacity, P_{ue} (kN)	Percentage Difference
B1	184	196	7%
B2	256	194	-24%
B3	256	310	21%
B4	256	354	38%

It can be seen from the table that there were significant differences between the applied load in testing, and the theoretical capacity from AS3600. For Specimen B1, the reinforced control beam, AS3600 slightly under predicted the failure load. This 7% difference is acceptable, as this testing was done in laboratory conditions with a high level of control. AS3600 predictions are designed for use in practical applications, where less control is likely, so this small difference is acceptable. Specimen B2 had an actual capacity 24% less than the theoretical prediction for the post-tensioned beam. This was expected, as the AS3600 predictions are based on a new condition post-tensioned member. As this beam had initial shear cracking before post-tensioning, the ultimate capacity was reduced.

The beam that was epoxy repaired and post-tensioned, Specimen B3, showed an actual capacity 21% higher than the predicted. The post-tensioned control beam, Specimen B4, had an actual capacity 38% higher than the predicted. These two beams may have had higher capacities than predicted for a number of reasons. The first reason is due to the tests being conducted in a controlled environment, as previously mentioned. The other reason is that the post-tensioning rods were unusually large for the tensioning force used. This means the beams acted very stiffly while being loaded, so it therefore did not allow the shear cracks to form as early. Overall, AS3600 appears conservative for its ultimate capacity predictions of post-tensioned beams.

5.10 Adjustments to AS3600 Predictions

To try to predict the shear capacity of the post-tensioned beams more accurately, adjustments to the prediction equations will be looked at. This is due to the AS3600 predictions appearing conservative for a new condition post-tensioned beam, and providing an over estimate of the shear strength for a beam with existing shear cracks, strengthened only with post-tensioning. The V_{us} component of the shear strength will be kept the same, but the V_{uc} component will be adjusted in a number of ways, as the method for predicting this is unclear. Warner et al (1998, p340)

argue that the equations used to calculate V_{uc} have no rational justification, but are used due to the relatively simple design procedure. This infers changes to the equations could be made to more accurately predict the concrete component of the member's shear strength. Four methods will be examined for better predicting the shear capacity of post-tensioned beams. The first method to be looked at involves modelling the specimen as a reinforced beam with an axial compressive force (using initial post-tension force). This compressive force will increase the β_2 multiplying factor for V_{uc}. The second method also involves taking the specimen as a reinforced beam, but using the ultimate post-tension force recorded for the compressive force. The third method involves using the standard equation for V_{uc} of a post-tensioned beam, but not excluding the post-tension force from the β_2 factor (using the initial post-tension force). The fourth method is the same as the third, but the compressive force is taken as the ultimate post-tension force. The adjusted methods will be compared to the experimental results, to find the most accurate predictions.

5.10.1 Method 1 (Reinforced Beam, β_2 Using Initial Post-tension Force)

This method involves taking the specimen as a reinforced beam with an axial compressive force, taken as the initial post-tension force. This predicted capacity would be the same for the three post-tensioned beams, as each began with 150 kN initial post-tension force.

The V_{uc} component of the capacity of the beams would then be predicted by:

$$V_{uc} = \beta_1 \cdot \beta_2 \cdot \beta_3 \cdot b_v \cdot d_o \left(\frac{A_{st}.f'_c}{b_v \cdot d_o} \right)^{\frac{1}{3}}$$

Where,

    $\beta_1,\ \beta_3,\ b_v,\ d_o,\ f'_c$, and A_{st} are the same as for Specimen B1

$$\beta_2 = 1 + \left(\frac{N*}{14A_g} \right)$$

$$= 1 + \left(\frac{150000}{14 \times (300 \times 150)} \right)$$

$$= 1.24$$

Therefore,

$$V_{uc} = 1.48 \times 1.24 \times 1 \times 150 \times 257 \times \left(\frac{900 \times 40}{150 \times 257} \right)^{\frac{1}{3}}$$

$$= 69.15kN$$

Calculating the ultimate shear capacity:

$$V_u = V_{uc} + V_{us}$$

$$= 69.15 + 36.04$$

$$= 105.19kN$$

Therefore, the ultimate shear capacity load is:

$$P_{u.s} = 2 \times 105.19$$

$$= 210.38kN$$

This is an under estimate for Specimens B3 and B4, but still an over estimate for Specimen B2.

5.10.2 Method 2 (Reinforced, β_2 Using Max. Post-tension Force)

This method involves taking the specimen as a reinforced beam with an axial compressive force, taken as the ultimate post-tension force recorded. The predicted capacities would be different for each of the three post-tensioned beams, as each recorded a different maximum post-tension force.

5.10.2.1 Specimen B2

$$N^* = 184kN$$

$$\beta_2 = 1 + \left(\frac{184000}{14 \times (300 \times 150)} \right)$$

$$= 1.29$$

$$V_{uc} = 1.48 \times 1.29 \times 1 \times 150 \times 257 \times \left(\frac{900 \times 40}{150 \times 257} \right)^{\frac{1}{3}}$$

$$= 71.94kN$$

Calculating the ultimate shear capacity:

$$V_u = V_{uc} + V_{us}$$

$$= 71.94 + 36.04$$

$$= 107.98kN$$

Therefore, the ultimate shear capacity load is:

$$P_{u.s} = 2 \times 107.98$$

$$= 215.96kN$$

5.10.2.2 Specimen B3

$$N^* = 223kN$$

$$\beta_2 = 1 + \left(\frac{223000}{14 \times (300 \times 150)} \right)$$

$$= 1.35$$

$$V_{uc} = 1.48 \times 1.35 \times 1 \times 150 \times 257 \times \left(\frac{900 \times 40}{150 \times 257} \right)^{\frac{1}{3}}$$

$$= 75.29kN$$

Calculating the ultimate shear capacity:

$$V_u = V_{uc} + V_{us}$$

$$= 75.29 + 36.04$$

$$= 111.33kN$$

Therefore, the ultimate shear capacity load is:

$$P_{u.s} = 2 \times 111.33$$
$$= 222.66 kN$$

5.10.2.3 Specimen B4

$$N^* = 228 kN$$

$$\beta_2 = 1 + \left(\frac{228000}{14 \times (300 \times 150)} \right)$$
$$= 1.36$$

$$V_{uc} = 1.48 \times 1.36 \times 1 \times 150 \times 257 \times \left(\frac{900 \times 40}{150 \times 257} \right)^{\frac{1}{3}}$$
$$= 75.84 kN$$

Calculating the ultimate shear capacity:

$$V_u = V_{uc} + V_{us}$$
$$= 75.84 + 36.04$$
$$= 111.88 kN$$

Therefore, the ultimate shear capacity load is:

$$P_{u.s} = 2 \times 111.88$$
$$= 223.76 kN$$

This method provides an under estimate for Specimens B3 and B4, but an over estimate for Specimen B2.

5.10.3 Method 3 (Post-tensioned, β_2 Including Initial Post-tension Force)

This method involves calculating the capacity of the beams with the normal equations for a post-tensioned beam, but not excluding the post-tension force from the β_2 factor. This method uses the initial post-tension force for N* in the equation

for β_2. The predicted capacity would be the same for the three post-tensioned beams, as each began with 150 kN initial post-tension force.

The V_{uc} component of the capacity of the beams would then be predicted by:

$$V_{uc} = \beta_1 \cdot \beta_2 \cdot \beta_3 \cdot b_v \cdot d_o \left(\frac{(A_{st} + A_{pt})f'_c}{b_v \cdot d_o} \right)^{\frac{1}{3}} + V_o + P_v$$

Where,

β_1, β_3, b_v, d_o, f'_c, V_o, and A_{st} are the same as for the previous predictions, and A_{pt} is the same as for the initial predictions.

$$\beta_2 = 1 + \left(\frac{N*}{14A_g} \right)$$

$$= 1 + \left(\frac{150000}{14 \times (300 \times 150)} \right)$$

$$= 1.24$$

$$V_{uc} = 1.48 \times 1.24 \times 1 \times 150 \times 257 \times \left(\frac{(900 + 1061.9) \times 40}{150 \times 257} \right)^{\frac{1}{3}} + 20 \times 10^3 + 0$$

$$= 109.66 kN$$

Calculating the ultimate shear capacity:

$$V_u = V_{uc} + V_{us}$$

$$= 109.66 + 36.04$$

$$= 145.7 kN$$

Therefore, the ultimate shear capacity load is:

$$P_{u.s} = 2 \times 145.7$$

$$= 291.4 kN$$

This method provides a slight under estimate for Specimens B3 and B4, but a major over estimate for Specimen B2.

5.10.4 Method 4 (Post-tensioned, β₂ including Max. Post-tension Force)

This method is the same as Method 3, except the compressive force is taken as the maximum post-tension force recorded, when calculating the β_2 factor. The β_2 factors used in this method are the same as those calculated in section 5.10.2. The predicted capacities would be different for each of the three post-tensioned beams, as each recorded a different maximum post-tension force.

5.10.4.1 Specimen B2

$$\beta_2 = 1.29$$

$$V_{uc} = 1.48 \times 1.29 \times 1 \times 150 \times 257 \times \left\{ \left(\frac{(900 + 1061.9) \times 40}{150 \times 257} \right)^{\frac{1}{3}} + 20 \times 10^3 + 0 \right.$$

$$= 113.28 kN$$

Calculating the ultimate shear capacity:

$$V_u = V_{uc} + V_{us}$$
$$= 113.28 + 36.04$$
$$= 149.32 kN$$

Therefore, the ultimate shear capacity load is:

$$P_{u.s} = 2 \times 149.32$$
$$= 298.64 kN$$

5.10.4.2 Specimen B3

$$\beta_2 = 1.35$$

$$V_{uc} = 1.48 \times 1.35 \times 1 \times 150 \times 257 \times \left\{ \left(\frac{(900 + 1061.9) \times 40}{150 \times 257} \right)^{\frac{1}{3}} + 20 \times 10^3 + 0 \right.$$

$$= 117.62 kN$$

Calculating the ultimate shear capacity:

$$V_u = V_{uc} + V_{us}$$
$$= 117.62 + 36.04$$
$$= 153.66kN$$

Therefore, the ultimate shear capacity load is:

$$P_{u.s} = 2 \times 153.66$$
$$= 307.32kN$$

5.10.4.3 Specimen B4

$$\beta_2 = 1.36$$

$$V_{uc} = 1.48 \times 1.36 \times 1 \times 150 \times 257 \times \left(\frac{(900 + 1061.9) \times 40}{150 \times 257} \right)^{\frac{1}{3}} + 20 \times 10^3 + 0$$

$$= 118.49kN$$

Calculating the ultimate shear capacity:

$$V_u = V_{uc} + V_{us}$$
$$= 118.49 + 36.04$$
$$= 154.53kN$$

Therefore, the ultimate shear capacity load is:

$$P_{u.s} = 2 \times 154.53$$
$$= 309.06kN$$

This method provides a significant over estimate for Specimen B2, an accurate prediction for Specimen B3, and a slight under estimate for Specimens B4.

5.10.5 Comparison of Adjusted Prediction Methods

Table 5.6 shows a summary of the capacities found for each post-tensioned beam by the four adjusted predictions methods.

Table 5.6: Comparison of Modified Theoretical Capacities

Specimen No.	Experimental Capacity, P_{ue} (kN)	Modified Theoretical Capacity, P_u (kN)			
		Method 1	Method 2	Method 3	Method 4
B2	194	210	216	291	299
B3	310	210	223	291	307
B4	354	210	224	291	309

Using Method 1 for Specimen B2 has found the capacity closest to the experimental result, but the capacity has still been predicted too high. The most accurate way to predict the capacity of a beam with existing shear cracks which has had post-tensioning applied, may be to ignore the post-tensioning contribution. The experimental capacity of Specimen B2 (194 kN) was close to the AS3600 prediction for the reinforced beam (184 kN). This is suggested, as Specimen B2 had no increase in strength from a reinforced beam, when the post-tensioning was applied.

Method 4 has provided a good estimate of the capacity of the beam that was repaired with epoxy injection and post-tensioning, Specimen B3. The calculated capacity of the beam using this method was 307 kN, which is very close to the experimental capacity of 310 kN. Method 4 has also provided the closest estimate of the capacity of Specimen B4, but was still slightly conservative.

5.11 Summary of Practical Results

Table 5.7 shows a summary of the experimental shear capacities of the four beams. The percentage increase in capacity of the post-tensioned beams compared to the reinforced control beam has also been shown. The percentage of possible increase shown is a comparison of the increase in strength of the repaired beams compared to the post-tensioned control beam. It can be seen that Specimen B3 had a 58% increase in capacity, which equates to 72% of the possible increase.

Table 5.7: Strength Increase of Post-tensioned Beams

Specimen No.	Shear Capacity, P_{ue} (kN)	Percentage Increase	Percentage of Possible Increase
B1	196	n/a	n/a
B2	194	-1%	0%
B3	310	58%	72%
B4	354	81%	100%

5.12 Conclusions

It has been found from this research that applying post-tensioning alone to a shear cracked member will not increase the member's capacity. The member in this testing repaired only with post-tensioning actually had a 1% decrease in ultimate capacity. This research has indicated that combining epoxy injection of cracks with external post-tensioning will increase the shear capacity of a concrete girder. The rehabilitation method in this experimental testing showed a 58% increase in ultimate shear capacity.

The AS3600 prediction equations for ultimate shear capacity of a reinforced concrete beam have been accurate for this testing. This research has shown discrepancies in the prediction equations for the shear strength of post-tensioned beams. As expected, the prediction equations over estimated the shear capacity of the beam that was repaired only with post-tensioning. This was due to the AS3600 prediction equations being based on new condition members. For this type of repaired member, the most accurate way to predict the shear capacity may be to ignore the post-tensioning contribution. The shear capacity of the beam would then be predicted using the equations for the reinforced beam.

The AS3600 prediction equations under estimated the capacity of Specimens B3 and B4. It was found that by not excluding the post-tensioning compressive force from the β_2 factor in the equations for the post-tensioned beam, the capacity was predicted more accurately. By using the ultimate compressive force measured in the post-tensioning rods, the predicted capacities closely matched the experimental results. For the epoxy repaired beam, Specimen B3, the adjustment to the equation made the

prediction almost perfectly match the experimental result. For the post-tensioned control beam, Specimen B4, the adjustment to the equation still left the experimental capacity 15% higher than the predicted. This difference was accepted due to the conservative nature of shear capacity predictions, and the controlled nature of the experimental testing.

CHAPTER 6

CONCLUSIONS AND RECOMMENDATIONS

6.1   Summary

This research project has investigated the shear strengthening of concrete girders with external post-tensioning combined with epoxy injection of existing cracks. The research was based on the experimental testing of four model beams. This section will outline the achievement of specified objectives, conclusions reached from the investigation, and possible areas for further research.

6.2   Achievement of Objectives

This section gives an overview of the achieved objectives that were set at the start of the project.

1.   *Research and review background information on the shear strengthening of concrete girders using epoxy injection and external post-tensioning.*

As limited literature was available on the shear strengthening of concrete members with epoxy injection combined with external post-tensioning, both aspects were also reviewed individually. These were covered in Chapter 2

2.   *Design model test beams for experimental investigations, taking into account previous test results.*

The model test beams were designed to fail in shear over flexure, and this was the case in testing. Problems associated with previous testing of model beams at USQ were addressed, so they would be avoided in this research. The problems included

varying concrete strengths, inadequate cover, and slipping of reinforcement. The process used in the design of the test beams was shown in Chapter 3.

3.   *Prepare model beams, and arrange testing devices.*

The model beams were successfully constructed and set up for testing. The steps involved in the construction of the specimens, and the test set up used were discussed in Chapter 4.

4.   *Conduct tests on the model beams, and record observed results.*

The four model beams were successfully tested, with observations and test data recorded. Three of the beams had post-tensioning applied, and one of the beams had its shear cracks repaired with epoxy injection. The testing of the model beams was discussed in Chapter 4, and the observed results were discussed in Chapter 5.

5.   *Evaluate and analyse the test results of the different model beams.*

The results from the testing of the four model beams have been discussed in Chapter 5. These results have been analysed to see the effect of the epoxy injection, and the external post-tensioning on the shear strengthening of the model test beams.

6.   *Arrive at a conclusion for the project, which will better explain the shear behaviour of rehabilitated girders using epoxy injection and external post-tensioning.*

Conclusions have been reached on the shear strengthening of concrete girders with epoxy injection of cracks and external post-tensioning. These have been discussed in Chapter 5. The conclusions reached have been that combining epoxy injection of cracks with external post-tensioning is an effective way to shear strengthen concrete

girders. It has also been shown that post-tensioning alone will not increase a member's shear capacity, if it has existing shear cracks.

All the objectives have been achieved, therefore the research project has been successfully completed.

6.3   Conclusions

The results from this research were positive with respect to the rehabilitation technique tested. The practical results from the testing showed some marked variation to the AS3600 prediction equations. These two aspects of the research will be summarised in the following sections.

6.3.1   Rehabilitation Technique

The results of the experimental investigation have shown that by repairing existing shear cracks with epoxy injection, concrete girders can then be shear strengthened by external post-tensioning. The strengthened member has increased stiffness and ultimate capacity. The beam that had its existing shear cracks repaired by epoxy injection, and was then post-tensioned, had a 58% higher ultimate capacity. This repaired beam gained 72% of the difference between the capacity of the reinforced beam and that of a new member that was post-tensioned.

The testing also highlighted the importance of structurally repairing the shear cracks to gain any benefit from the post-tensioning. The beam that was just post-tensioned, without any repair to the existing cracks, had a 1% lower ultimate capacity than the reinforced beam. As discussed in Chapter 5, this was due to the crack surfaces sliding against each other, instead of bonding together. The effectiveness of using post-tensioning alone to strengthen girders with existing shear cracks will be highly variable, with high dependence on crack angle and width. These are the factors that would influence the bond gained between crack surfaces due to post-tensioning alone. This is where the benefit of the epoxy injection was gained, by eliminating

this variability. Once the existing cracks were structurally repaired by the epoxy injection, the beam behaved similarly to a new post-tensioned member.

Both the epoxy repaired beam and the post-tensioned control beam had ultimate capacities well above the predicted. The repaired beam had an ultimate capacity slightly lower than the post-tensioned control beam. This is likely to have been due to the minor damage caused by preloading, which may have initiated shear cracks earlier than for a new condition member.

6.3.2   Shear Capacity Based on AS3600

The equations used to predict the ultimate capacity of the reinforced beam in this testing proved to be quite accurate. The prediction equations for the ultimate capacity of the post-tensioned beams were less accurate for this testing.

The prediction equations showed an over estimate for the capacity of the beam that was repaired only with post-tensioning. As discussed in Chapter 5, this was due to the ineffectiveness of the post-tensioning on the shear cracked member. The AS3600 prediction equations are designed for post-tensioning applied to new condition members. For these reasons, it is recommended that the capacity of a beam with existing shear cracks, which has had post-tensioning applied, be predicted using only the equations for the reinforced beam, ignoring any contribution from the post-tensioning.

The prediction equations showed a significant under estimate for the capacity of the post-tensioned control beam and the beam that was epoxy repaired and post-tensioned. This research looked at not excluding the post-tension compressive force, from the β_2 factor in the prediction equations for the post-tensioned beam. By using the ultimate compressive force measured in the post-tensioning rods, the predicted capacities matched the experimental results more accurately. The modified theoretical capacities matched the experimental capacity almost perfectly for the

epoxy repaired beam, and provided a conservative estimate for the post-tensioned control beam. More extensive testing is required, but the adjusted equations do appear to offer a more accurate estimate of the shear capacity of new condition or epoxy repaired members. Extensive testing should be completed before using these equations for final designs of rehabilitated members.

6.4   Recommendations

As the need for repair and strengthening techniques of concrete girders becomes more sought after, cost effective solutions are required. For concrete girders with existing shear cracks, epoxy injection of cracks combined with external post-tensioning is a viable option. This rehabilitation method increases a member's stiffness and ultimate capacity, and reduces the risk of reinforcement corrosion.

Recommendations for further studies include:

- Conducting more extensive testing on members shear strengthened with epoxy injection of cracks and external post-tensioning, to establish a way to accurately predict the ultimate shear capacity of a repaired member, and correlate this to AS3600 prediction equations.

- Investigating the use of deviators for the post-tensioning when strengthening a shear cracked member. By setting the profile of the tendons perpendicular to the existing shear cracks, the need for epoxy injection to rebond the crack surface may be avoided. The strength increase for this method with, and without, epoxy injection of cracks could be studied.

- Other rehabilitation methods for strengthening shear cracked members, such as vertical clamping or post-tensioning over the region with shear cracks

- Modelling of shear cracks using computer software, to accurately model the behaviour of a girder with shear cracks, or one previously repaired with epoxy injection.

REFERENCES

Alam, M. 2004, 'Effect of Epoxy repairing on Girders Shear Strengthened with External post Tensioning', *Undergraduate Dissertation*, October, University of Southern Queensland (USQ), Australia

Chung, H. W. 1975, 'Epoxy-Repaired Reinforced Concrete Beams.' *ACI Structural Journal*, May, vol. 72, No. 5, pp. 233-234

Chung, H. W., & Lui, L. M. 1977, 'Epoxy-Repaired Concrete Joints.' *ACI Structural Journal*, vol. 74, No. 6, pp. 264-267

Epoxysystems, 2001, 'Epoxy Manufacture and Supply, organization.' *Epoxy Manufacturing Incorporation*, viewed 29th April 2005, <http://www.epoxy.com>

French, C.W., Thorp, G.A., & Tsai, W.J. 1990, 'Epoxy Repair for Moderate Earthquake Damage.' *ACI Structural Journal*, July-August, vol. 87, No. 4, pp. 416-424

Haraji, M. H. 1993, 'Strengthening of Concrete Beams by External Prestressing.' *PCI Journal*, vol. 38, No. 6, pp 76-88

Jobling, L. 2004, 'Shear Strengthening of Headstocks using Prestressed Fibre Strips', *Undergraduate Dissertation*, October, University of Southern Queensland (USQ), Australia

Klaiber, F. W., Dunker, K. F., & Saunders, W. W. 1989, 'Strengthening of Existing Bridges (simple and continuous span) by Post-tensioning.' *ACI SP*, Pros. Int. Symp. A. E Naaman and J. E Breen, Eds. American Concrete Institute (ACI) Detroit, vol. 120, No. 10, pp. 207-228

MEC2402 – Stress Analysis Study Book, 2003, *Distance Education Centre*, USQ, Toowoomba, Australia

Pisani, M. A. 1999, 'Strengthening by means of External Prestressing.' *Journal of Bridge Engineering*, May, vol. 4, No. 2, pp. 131-135

Standards Australia. 2003, 'Australian Standards for Civil Engineering Students, Part 2: Structural Engineering'. Standards Australia International, Sydney.

Tan, K. H., & Naaman, A. E. 1993, ' Strut-and-Tie Model for Externally Prestresses Concrete.' *ACI Structural Journal*, vol. 90, No. 6, November-December, pp. 683-691

Tan, K. H., & Ng, C. K.1998, 'Effect of Shear in Externally Prestressed Beams.' *ACI Structural Journal*, vol. 95, No. 2, March-April, pp 116-128

Tan, K. H., & Ng, C. K.1997, 'Effect of Deviators and Tendon Configuration on Behavior of Externally Prestressed Beams.' *ACI Structural Journal*, vol. 94, No. 1, pp. 13-22

Warner, R. F., Rangan, B. V., Hall, A.S., & Faulkes, K. A. 1998, 'Concrete Structures.' Addison Wesley Longman Australia Pty Ltd, Melbourne

Woods, E. 2004, 'Shear Strengthening and Model Testing of Concrete Bridge Headstocks', *Undergraduate Dissertation*, October, University of Southern Queensland (USQ), Australia

BIBLIOGRAPHY

Burns, N. H., Helwig, T., & Tsujimoto. 1991, 'Effective Prestress Force in Continuous Post-tensioned Beams with Unbonded Tendons.' *ACI Structural Journal*, January-February, vol. 88, No. 1, pp. 84-90

CIV3506-Concrete Structures Study Book, 2004, *Distance Education Centre*, USQ, Toowoomba, Australia

David, P.B. 2004, 'Historical Perspective on Prestressed Concrete.' *PCI Journal*, January-February, vol. 49, No. 1, pp. 14-30

Haraji, M. H., & Hijazi, S.A. 1991, 'Evaluation of the Ultimate Steel Stress in Partially Prestressed Concrete Members.' *PCI Journal*, vol. 36, No. 1, pp. 62-82

Rabbat, B. G., & Sowlat, K. 1987, 'Testing of Segmental Concrete Girders with External Tendons.' *PCI Journal*, vol. 32, No. 2, pp 86-107

Towards Sustainable Engineering Practice: Engineering Frameworks for Sustainability, Institution of Engineers, Australia, Canberra, 1997

Virlogeux, M. 1982, 'External Prestressing.' IABSE Proceedings, International Association for Bridge and Structural Engineering, Zurich, Switzerland

APPENDIX A

Project Specification

University of Southern Queensland (USQ)

Faculty of Engineering and Surveying

ENG 4111/4112 Research Project
PROJECT SPECIFICATION

FOR: **Steven Luther**

TOPIC: Effect of crack widths and epoxy injection in structural
                    rehabilitation with external post-tensioning.

SUPERVISOR   Dr. Thiru Aravinthan

SPONSORSHIP: Faculty of Engineering and Surveying, USQ

PROGRAMME: <u>**Issue A, 17 March 2005**</u>

1. Research and review background information on the shear strengthening of
   concrete girders using epoxy injection and external post-tensioning.

2. Design model beams for experimental investigations, taking into account
   previous test results.

3. Prepare model beams, and arrange testing devices.

4. Conduct tests on the model beams, and record observed results.

5. Evaluate and analyse the test results of the different model beams.

6. Arrive at a conclusion for the project, which will better explain the shear
   behaviour of rehabilitated girders using epoxy injection and external post-
   tensioning.

AGREED: _____ (Student) _____
            (Supervisor)
            __ / __ / __   __ / __ / __

APPENDIX B

End Anchorage Plate Capacity

The capacity of the end anchorage plates will be checked in this section. The design bending moments and shear forces of the end anchorage plates will be found, and compared to the calculated section capacities. The free body diagram, bending moment diagram, and shear force diagram of the end plates are shown below.
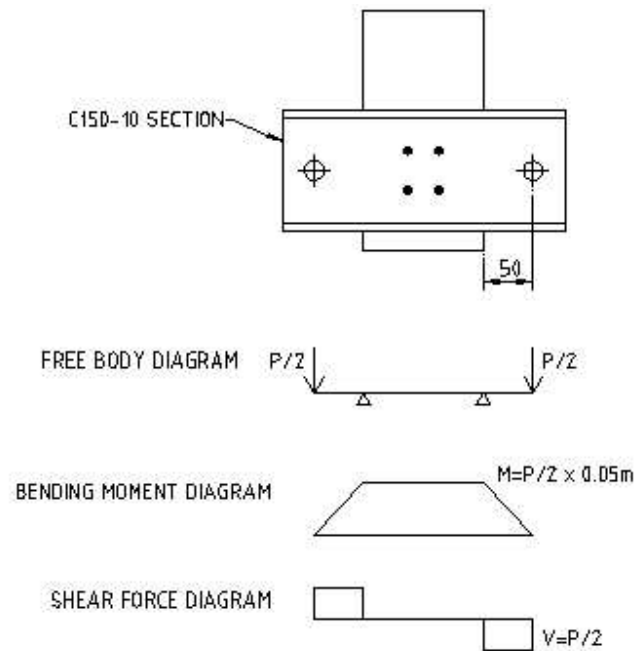
To have adequate capacity:

$$M^* \le \phi M_s$$
and
$$V^* \le \phi V_v$$

From table 3.4 of AS4100:

$$\varphi = 0.9$$

Using A_{pt} and σ_{pu} as found in section 3.4.2, the design post-tension force, P is:

$$P = A_{pt} \times \sigma_{pu}$$
$$= 1061.9 \times 220.3$$
$$= 234kN$$

Therefore, the design bending moment, $M*$ is:

$$M* = \frac{P \times 0.05}{2}$$
$$= \frac{234 \times 0.05}{2}$$
$$= 5.85 kN.m$$

The design shear force, $V*$ is:

$$V* = \frac{P}{2}$$
$$= \frac{234}{2}$$
$$= 117 kN$$

The section moment capacity, M_s is:

$$M_s = f_y.Z_e$$

Where,

$$f_y = \text{yield stress}$$
$$= 250 MPa$$
$$Z_e = \text{effective section modulus}$$
$$= 51.6 \times 10^3 \text{ mm}^4$$

Therefore,

$$M_s = 250 \times 51.6 \times 10^3$$
$$= 12.9 \times 10^6 N.mm$$
$$= 12.9 kN.m$$

$$\varphi M_s = 0.9 \times 12.9$$
$$= 11.6 kN.m$$

From clause 5.11.4 of AS4100, the nominal shear capacity of a web, V_v is:

$$V_v = 0.6.f_y.A_w$$

Where,

A_w = gross cross - sectional area of the web

$$= 1425 \, mm^2$$

Therefore,

$$V_v = 0.6 \times 250 \times 1425$$
$$= 214 \times 10^3 \, N$$
$$= 214 kN$$

$$\varphi V_v = 0.9 \times 214$$
$$= 193 kN$$

Checking the bending capacity of the section:

$$M* \le \phi M_s$$
$$5.85 \le 11.6$$

Therefore, the section has adequate bending capacity.

Checking the shear capacity of the section:

$$V* \le \phi V_v$$
$$117 \le 193$$

Therefore, the section has adequate shear capacity.

APPENDIX C

Strain Gauge Data

1. **Steel Strain Gauge Data Sheet**

2. **Concrete Strain Gauge Data Sheet**

3. **CN Adhesive Data Sheet**

4. **PS Adhesive Data Sheet**

TML STRAIN GAUGE TEST DATA

GAUGE TYPE   : FLA-2-11   TESTED ON   : SS 400

LOT NO.   : A513411   COEFFICIENT OF
                                       THERMAL EXPANSION : 11.8 $\times 10^{-6}$/°C

GAUGE FACTOR   : 2.11   ±1%   TEMPERATURE
                                       COEFFICIENT OF G.F. : +0.1±0.05 %/10°C

ADHESIVE   : P-2   DATA NO.   : A0480

THERMAL OUTPUT (ε app : APPARENT STRAIN)

$\varepsilon\ app = -2.33 \times 10^{1} + 1.57 \times T^{1} - 1.21 \times 10^{-2} \times T^{2} - 4.97 \times 10^{-4} \times T^{3} + 4.55 \times 10^{-6} \times T^{4}$ (μm/m)

TOLERANCE : ±0.85 [(μm/m)/°C] , T : TEMPERATURE

ひずみゲージ取扱いの注意事項

- ●上記の特性データは、リード線の取付けによる影響を含んでおりません。裏面記載のリード線の測定値への影響に従って補正してください。
- ●ゲージの使用温度は、接着剤の耐熱温度などにより変わります。
- ●絶縁抵抗などの点検は、印加電圧を50V以下にしてください。
- ●ゲージリード線に無理な力を加えないでください。
- ●ゲージ裏面に接着剤を塗布して接着してください。
- ●ひずみゲージの裏面は脱脂洗浄してありますので、汚さないように取扱いください。
- ●ゲージの包装を開封後は、乾燥した場所で保管してください。
- ●ご使用に際してご不明な点などがございましたら、当社までお問い合わせください。

CAUTIONS ON HANDLING STRAIN GAUGES

- ● The above characteristic data do not include influence due to lead wires. Correct the data in accordance with the influence of lead wires on measured values described overleaf.
- ● The service temperature of strain gauge depends on the operating temperature of adhesive, etc.
- ● Check of insulation resistance, etc. should be made at a voltage of less than 50V.
- ● Do not apply an excessive force to the gauge leads.
- ● Apply an adhesive to the back of a strain gauge and stick the gauge to a specimen.
- ● As the back of strain gauge has been degreased and washed, do not contaminate it.
- ● After unpacking, store strain gauges in a dry place.
- ● If you have any questions on strain gauges or installation, contact TML or your local agent.

Made in Japan

TML 株式會社 東京測器研究所

〒 140-8560 東京都品川区南大井 6 - 8 - 2
TEL 03 - 3763 - 5611
FAX 03 - 3763 - 6128

Tokyo Sokki Kenkyujo Co., Ltd.

8 - 2, Minami - Ohi 6 - Chome
Shinagawa - ku, Tokyo 140-8560

TML STRAIN GAUGE TEST DATA

GAUGE TYPE	: PFL-30-11	TESTED ON	: SS 400
LOT NO.	: A701615	COEFFICIENT OF THERMAL EXPANSION	: 11.8 $\times 10^{-6}$/°C
GAUGE FACTOR	: 2.13 ±1%	TEMPERATURE COEFFICIENT OF G.F.	: +0.15±0.05 %/10°C
ADHESIVE	: P-2	DATA NO.	: D0030

THERMAL OUTPUT (ε app : APPARENT STRAIN)

$\varepsilon \text{ app} = -1.62 \times 10^1 + 1.63 \times T^1 - 4.55 \times 10^{-2} \times T^2 + 2.27 \times 10^{-4} \times T^3 + 3.52 \times 10^{-8} \times T^4$ (μ m/m)

TOLERANCE : ±0.85 [(μ m/m)/°C] , T : TEMPERATURE

ひずみゲージ取扱いの注意事項

● 上記の特性データは、リード線の取付けによる影響を含んでおりません。裏面記載のリード線の測定値への影響に従って補正してください。

● ゲージの使用温度は、接着剤の耐熱温度などにより変わります。

● 絶縁抵抗などの点検は、印加電圧を50V以下にしてください。

● ゲージリード線に無理な力を加えないでください。

● ゲージ裏面に接着剤を塗布して接着してください。

● ひずみゲージの裏面は脱脂洗浄してありますので、汚さないように取扱いしてください。

● ゲージの包装を開封後は、乾燥した場所で保管してください。

● ご使用に際してご不明な点などがございましたら、当社までお問い合わせください。

CAUTIONS ON HANDLING STRAIN GAUGES

● The above characteristic data do not include influence due to lead wires. Correct the data in accordance with the influence of lead wires on measured values described overleaf.

● The service temperature of strain gauge depends on the operating temperature of adhesive, etc.

● Check of insulation resistance, etc. should be made at a voltage of less than 50V.

● Do not apply an excessive force to the gauge leads.

● Apply an adhesive to the back of a strain gauge and stick the gauge to a specimen.

● As the back of strain gauge has been degreased and washed, do not contaminate it.

● After unpacking, store strain gauges in a dry place.

● If you have any questions on strain gauges or installation, contact TML or your local agent.

Made in Japan

<TML> 株式會社 東京測器研究所

〒 140-8560 東京都品川区南大井 6 - 8 - 2
TEL 03 - 3763 - 5611
FAX 03 - 3763 - 6128

Tokyo Sokki Kenkyujo Co., Ltd.

8 - 2, Minami - Ohi 6 - Chome
Shinagawa - ku, Tokyo 140-8560

OPERATION MANUAL OF TML STRAIN GAUGE ADHESIVE TYPE CN

The **CN** adhesive is a single component cement for strain gauges, and time required for bonding gauges is extremely short and handling is very easy. There are two types: **CN** (with green cap) for general purpose and **CN-E** (with white cap) featuring high viscosity.

1 UNPACKING

(1) Take off the adhesive cap and drill a minute hole on the top of nozzle with the supplied pin. (Fig. 1)

(2) Pull out the pin. Then, take care of the adhesive liquid which may jump out.

(3) Wipe off the adhesive attached to the nozzle with cloth, etc. and surely tighten the cap.

(4) If necessary, use the supplied upset-protect stand.

Fig.1
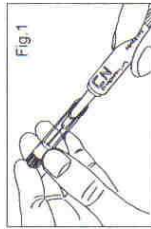
2 SURFACE PREPARATION

(1) Remove grease, scale, dust, paint, etc. from the bonding area to present a metal burnish (foundation).

(2) Grind an area somewhat larger than the bonding area uniformly and finely with abrasive paper. Finish should be achieved with #120 ~ 180 abrasive paper for steel and #240 ~ 320 for aluminium. (Fig. 2)

(3) Clean the ground area with industrial tissue paper or cloth soaked in a small quantity of chemical solvents such as acetone. Cleaning should be made till the tissue or cloth is kept contamination free. (Fig. 3)

(4) After surface preparation, stick strain gauges before the prepared surface makes oxidizing membrane or is not contaminated.

Fig.2

Fig.3
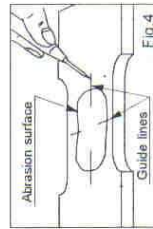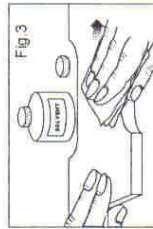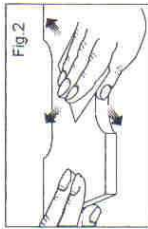
3 GENERAL BONDING PROCEDURES

(1) Position strain gauges on the bonding area and mark a guide line with a scriber or 4H pencil. (Fig. 4)

(2) Take out a strain gauge from the plastic binder. Then, you need not wipe the bonding surface with a solvent because the gauge is supplied in the thoroughly washed state.

(3) Drop a necessary amount of the adhesive on the back of the gauge base. The amount of adhesive is usually one drop but you may increase the number of drops according to the size of gauge. (Fig. 5)

(4) Spread the adhesive on the back of gauge thin and uniformly using the adhesive nozzle.

Abrasion surface
Guide lines
Fig.4

Fig.5

TML manu CN004E

(5) Place the gauge to the guide mark, put a polyethylene sheet and press down the gauge constantly by thumb or a gauge pressure application device. This work should be done quickly as curing is completed very fast. (Fig 6)

(6) The curing time is different depending on gauges, test pieces, temperature, humidity or pressing force. The curing time under normal conditions is 20 ~ 60 seconds for **CN** and 40 ~ 120 seconds for **CN-E**.

(7) Measurement gets ready about 15 minutes after hardening. For precise measurement or experiments involving temperature rise, however, leave for a few to 24 hours.

Fig 6

4 STORAGE AND HANDLING

(1) After use, wipe adhesive out of container and nozzle with cloth, etc. and replace the cap.

(2) After use, put back in the aluminum bag and store in a dry, cool and dark place.

(3) After handling, wash hands well.

(4) As curing speed gets slow in winter, it is recommended to warm the bonding surface or use a CN accelerator.

(5) For bonding on polyethylene (PE), polypropylene (PP), 4F ethylene (PTFE), etc., an exclusive surface treatment agent is required. If there is any question, consult TML or your nearest TML agent. A material safety data sheet is available on request.

Contents	
Components	Synthetic resin (100 %)　Cyanoacrylate
Operating temperature	− 30 ~ + 120 °C
Shelf life	6 months in a cool, dry and dark place such as refrigerator (5 ~ 10 °C, freezer prohibited)

2g × 5

⚠ CAUTION

1. Avoid contact with skin, eyes and clothing.
2. Should fingers be bonded, do not forcibly detach but slowly take off, rubbing in a bath.
3. Should adhesive enter eyes, flush eyes well with water and call for medical aid. Never forcibly detach nor rub eyes.
4. Do not use a textile glove in bonding work.
5. Use in a well ventilated room.
6. Handle in a place without flame.
7. Store away from children.

Made in Japan

⟨TML⟩ **Tokyo Sokki Kenkyujo Co., Ltd.**

8-2, Minami- Ohi 6- Chome
Shinagawa- Ku, Tokyo 140-8560
FAX Tokyo 03-3763-6128　　E-mail sales@tml.jp

TML manu PS003E

OPERATION MANUAL OF TML STRAIN GAUGE ADHESIVE TYPE PS

The PS adhesive is used as surface precoating agent for bonding TML strain gauge "P" and "PF" series, etc. and also as adhesive for "WFLM" series gauges. The PS is a two-component room-temperature-curing polyester adhesive and consists of drug A (main agent) in tube and drug B (hardener) in poly-ethylene bottle. The PS has excellent alkali resistance and is effective to shut off moisture and gas from a test piece. For short term loading test, you may bond gauges with CN adhesive on the PS precoated surface. High viscosity of the adhesive makes use on vertical wall or ceiling possible.

1 SURFACE PREPARATION

(1) Remove laitance, paint, dust, etc. from the bonding area to present the foundation of a test piece. As wet surface may cause a failure in hardening, take off moisture with TML surface preparation agent A.

(2) Grind an area a bit larger than the bonding area uniformly and finely with abrasive paper. Finish should be achieved with abrasive paper #80 ~ 120

(3) Clean the abraded area with industrial tissue paper or cloth soaked in a small quantity of chemical solvents such as acetone.

2 GENERAL BONDING PROCEDURES

(1) Cut the supplied gauge binder about 5mm from the folded part. (Fig. 1)

(2) Put the necessary quantity of drug A in a mixing vessel, drop the drug B by 2 ~ 4% in weight of the drug A, and mix well with a clean spatula. The mixed adhesive is effective for 10 ~ 15 minutes. 10 drops of the drug B correspond to about 3% of drug B to 10g of drug A. 35 drops of drug B are about 1g. Always drop the drug B on the drug A evenly over the surface.

(3) Plaster the mixed adhesive on an area a little wider than the gauge.

(4) Plaster the adhesive once more on the surface to finish 0.5 ~ 1mm in thickness.

(5) Put the cut binder on the adhesive layer form the end so that air bubble is not mixed. (Fig. 4)

(6) Push out the excess adhesive and air bubble by slightly pressing down the binder.

(7) The curing time depends on the material of a test piece, temperature, concentration of drug B,etc. If you use the adhesive for the first time, it is recommended to carry out adhesive-curing test by yourselves to find the proper usable time or curing time.
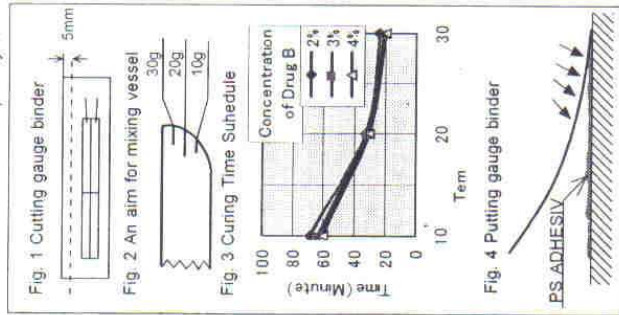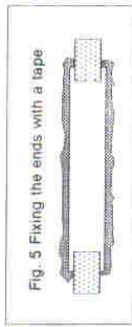
(8) The adhesive is hardened in 5 ~ 6 hours to be ready for measurement but stable measurement is achieved by leaving the bonded gauges at room temperature for a half day or one day.

(9) After the adhesive has hardened, remove the binder and install the gauge.

3 STORAGE AND HANDLING

(1) There is case that a transparent resin only separated from the filler comes out from the nozzle. In this case, dispose of the transparent resin or mix it well with the following brown liquid. The mixing does not affect the performance of bonding at all.

(2) After use, wipe adhesive out of container and nozzle with cloth, etc. and replace the cap.

(3) After use, put back in package and store in a cool, dark place without flame

(4) After handling, wash hands well.

(5) If there is any question, consult TML or your nearest TML agent. A material safety data sheet is available on request.

Contents	Drug A (main agent) = 200g	Drug B (hardener) = 10g × 2
Components	Polyester resin	Organic peroxide included
Operating temperature	$-30 \sim +100\,°C$	
Shelf life	3 months in a cool, dark place such as refrigerator ($5 \sim 10\,°C$, freezer prohibited)	

⚠ CAUTION

1. Avoid contact with skin, eyes and clothing.
2. In case of adhesion to skin and clothing, wash out well with water and soap.
3. In case of getting in eyes, flush eyes well with water and call for medical aid.
4. Use in a well ventilated area.
5. Handle in a place without flame.
6. If drug B is excessively added to drug A or a large quantity of adhesive is mixed, heat may be generated due to reaction heat in curing. Even in case of many gauge installations, mix as small a quantity as necessary.
7. Store away from children.

Made in Japan

TML Tokyo Sokki Kenkyujo Co., Ltd.

8-2, Minami- Ohi 6- Chome
Shinagawa- Ku, Tokyo 140-8560
Fax   Tokyo 03-3763-6128
E-mail   sales@tokyosokki.co.jp

Fig. 1 Cutting gauge binder

Fig. 2 An aim for mixing vessel

Fig. 3 Curing Time Suhedule

Fig. 4 Putting gauge binder

Fig. 5 Fixing the ends with a tape

APPENDIX D

Epoxy Resin Data

1. **Lokfix E Fact Sheet**
2. **Nitofill LV Fact Sheet**

FOSROC

Lokset E

Structural epoxy adhesive paste and filler

Uses

For speedy and permanent patching repairs to concrete structures; bonding of precast concrete components and all repair work to concrete cementitious substrates where strength, impermeability to water, and resistance to aggressive chemicals is essential; emergency repairs to concrete structures, sea walls, and industrial floors in chemical handling and process areas.

The thixotropic nature of Lokset E makes the product ideal for setting starter bars, dowels, holding down bolts and anchoring in general.

Advantages

- Early development of initial hardness, minimises maintenance disruption

- Pre-weighed quality controlled materials ensure consistency and reduce risk of site errors

- Two pack colour coding gives visual check on correct mixing

- Unaffected by a wide range of acids, alkalis and industrial chemicals

- 3 to 4 times stronger than typical concrete. Excellent resistance to abrasion and impact

- Natural grey colour sympathetic to aesthetic requirements

Description

Lokset E is a two-component, epoxy paste consistency, structural adhesive/filler. It cures, with minimal shrinkage, at temperatures above 5°C to a very strong, dense solid.

The mixed material is applied to a suitably prepared surface and quickly cures to form a complete impermeable repair unaffected by many forms of chemical attack.

It is supplied as a two pack colour coded material in pre-weighed quantities ready for on-site mixing and use.

Technical support

Parbury Technologies offers a comprehensive range of high quality, high performance construction products. In addition, Parbury Technologies offers technical support and on-site service to specifiers, end-users and contractors.

Properties

Data quoted is typical for this product but does not constitute a specification.

Pot life:	1.5 litre mix at 25°C – 25-35 minutes. Note: To obtain maximum pot life, spread Lokset E into a thin (less than 10 mm) layer immediately after mixing.
Initial hardness:	24 hours.
Full cure:	7 days. Below 20°C the curing time will be increased.
Minimum application temperature:	5°C.
Maximum service temperature:	50°C.
Specific gravity (mixed):	1.7 (approx.)
Chemical resistance:	
Citric Acid 10%	Excellent
Tartaric Acid 10%	Excellent
Sodium Hydroxide 50%	Excellent
Diesel Fuel/Petrol	Excellent
Sugar Solutions	Very Good
Lactic Acid 10%	Very Good
Hydrocarbons	Very Good
Phosphoric Acid 50%	Very Good
Colour:	Grey, when mixed (may yellow and/or darken when exposed to sunlight or certain chemicals.

Instructions for use

Preparation

All grease, oil, chemical contamination, dust, laitance and loose concrete must be removed by scabbling or light bush hammering to provide a sound substrate.

All concrete must be at least 14 days old prior to treatment.

Steel surfaces should be grit blasted to white metal. Surfaces which show any traces of oil must be degreased with a chemical degreaser prior to grit blasting.

FOSROC

Mixing

Thoroughly mix resin (white) and curing agent (black) until an even grey colour is obtained. Mix for minimum 3 - 5 minutes.

Application

Apply the mixed Lokset E with a notched trowel, putty knife, caulking gun, twin cartridge gun etc., depending upon the application. Bonded surfaces should be held rigidly together until the Lokset E has set.

Cleaning

All tools and equipment should be cleaned immediately after use with Fosroc Solvent 20. Hardened material can only be removed mechanically.

Estimating

Supply

Lokset E is supplied in 1.5 litre and 6 litre two component packs and a convenient 450 ml twin cartridge pack.

Quantity estimating guide

Table indicates volume of Lokset E in ml/100 mm bond.

Hole Diameter (mm)	Volume of grout for bolt diameter (mm)					
	12	16	20	25	32	40
20	25					
25	50	40	25			
32	80	70	60	40		
38		100	100	75	45	
45			150	130	100	45
50				180	150	90
62					280	225

These figures allow for a 25% wastage factor.

Storage

Lokset E has a shelf life of 12 months when stored in a dry place below 35°C in unopened containers.

Precautions

Health and safety

Prolonged and repeated skin contact with epoxy resins and curing agents may cause dermatitis in persons sensitive to these products. Gloves, barrier creams, protective clothing and eye protection should be worn when handling these products. If poisoning occurs, contact a doctor or Poisons Information Centre. If swallowed, do NOT induce vomiting - give a glass of water. If in eyes, hold eyes open, flood with water for at least 15 minutes. If skin contact occurs, remove contaminated clothing and wash skin thoroughly.

Material Safety Data Sheets (MSDS) are available to users of Parbury Technologies products on request to their nearest Parbury Technologies branch. Read MSDS, data sheet and label carefully before first use of any product.

Fire

Lokset E is non-flammable.

Additional information

Lokset E is only one product in the Parbury Technologies range of construction products. Ancillary products include concrete repair products, grouts, joint sealants, protective coatings, anchoring and flooring products, all ideally suited for industrial maintenance and construction requirements.

Manufactured and sold under license from Fosroc International Limited, England. Fosroc, the Fosroc logo and Lokset are trade marks of Fosroc International Limited, used under license.

PARBURY TECHNOLOGIES

Important note

AUS/0040/99/A

FOSROC

Nitofill LV
6/1997

Nitofill LV

Pre-packaged low viscosity epoxy crack injection system

Uses

Nitofill LV is designed for injecting cracks in concrete and masonry wherever there is a need to consolidate a structure or exclude water and air from contact with the reinforcement.

Nitofill LV is a low viscosity system and is suitable for cracks down to 0.2 mm at the surface and cracks tapering internally down to 0.01 mm.

The Nitofill LV system is ideal for small scale repairs on site and is also suitable for insitu or precast concrete elements

Advantages

System includes everything necessary to complete the crack injection.

Convenient to use, disposable cartridge pack contains both base and hardener.

Safe and clean to use.

High strength, excellent bond to concrete and masonry.

Low viscosity allows cost effective and efficient repair.

Description

Nitofill LV crack injection system incorporates a two part epoxy base and hardener contained in a dual cartridge pack.

The Nitofill LV accessory items which are packed individually and complimentary to the cartridge pack are - a cartridge gun, injection flanges, static mixers and hoses, flange adaptors and a removing tool.

Technical support

Parbury Technologies offers a comprehensive range of high performance, high quality construction products. In addition, Parbury Technologies offers a technical support service to specifiers, end-users and and contractors, as well as on site technical support.

Design criteria

Nitofill LV is suitable for injecting cracks in concrete and masonry down to 0.2 mm at the surface and internal cracks tapering down to 0.01 mm.

The system should not be used for cracks where movement is expected to continue.

Properties

The following results are typical for the hardened Nitofill LV epoxy resin.

Usable life at	10°C:	40 minutes
	20°C:	20 minutes
	30°C:	10 minutes
Viscosity at	10°C:	250-450 cps
	20°C:	150-200 cps
	30°C:	50-100 cps
Compressive strength	1 day	57MPa
(BS 6319)	3 day	66MPa
	7 day	83MPa
Tensile strength (BS 6319):	>25 MPa	
Flexural strength (BS 6319):	>50 MPa	

Chemical resistance

The cured Nitofill LV epoxy is resistant to oil, grease, fats, most chemicals, mild acids and alkalis, fresh and sea water. Consult Parbury Technologies Technical Department when exposure to solvents or concentrated chemicals is anticipated.

Specification clauses

Low viscosity crack injection system

The crack injection system shall be Nitofill LV. It shall be applied strictly in acordance with the application instructions given in the product data sheet.

Instructions for use

Surface preparation

All contact surfaces must be free from oil, grease, free standing water or any loosely adherent material. All dust must be removed.

Mixing the surface sealant

Lokset E is used to bond the injection flanges to the substrate and to seal the face of the crack. Pour all the contents of the Lokset E hardener pack into the base container. Mix using a slow speed mixer until homogeneous.

Nitofill LV: 6/1997

FOSROC

Application of the surface sealant

Immediately after mixing apply a small amount of product to the underside of each flange, making sure that the valve will not be blocked and place the flange centrally over the crack. Flanges should be placed between 200 mm and 500 mm apart dependent on crack size, along the length of the crack. Additional surface sealant should be applied around each flange edge and to the remainder of the crack between the flanges to ensure a resin tight seal to the substrate.

Where cracks can be sealed on one side only, flanges should be placed at centres which are 80% of the depth to which the resin is required to penetrate.

Application of the Nitofill LV injection resin can commence as soon as the Lokset E has fully hardened, (at least 12 hours at 20°C)

Injection of the Nitofill LV epoxy resin

The Nitofill LV static mixer/hose should be screwed onto the cartridge. The cartridge is then placed into the gun and the outlet end of the hose pushed onto the lowest flange using the adaptor.

The contents of the cartridge are then injected until the resin flows from an adjacent flange, or until firm and sustained hand pressure on the gun trigger signifies that no further resin will be accepted. Then pull the barb on the flange away from the base. Remove the liner strip out of the barb on the flange. Hold the base of the flange while removing the liner slip from the barb. This will ensure the flange is not accidentally removed from the substrate. The flange should be in the closed position when the liner slip is pulled totally away from the base. This will prevent material flowing out from the crack. The pressure should be released and the hose disconnected from the flange using the adaptor and tool.

The injection hose can then be refixed to an adjacent flange, and more Nitofill LV resin injected. Repeat the process until the entire length of crack has been injected.

In the case of cracks which go all the way through a wall or slab, the resin should be injected through alternate flanges on both sides where access is possible. In the case of slabs, injection from the underside takes precedence to top injection.

Making good

After the Nitofill LV injection resin has set, remove the flanges. These can be knocked off with a hammer. Make good any holes or voids with Lokset E.

The existing surface sealant can then be removed using a sharp broad-chisel or by grinding until the original substrate profile is restored.

Cleaning

All tools and equipment should be cleaned immediately after use with Fosroc Solvent 10.

Limitations

The Nitofill LV resin injection system should not be used for cracks where movement is expected to continue. Other measures should be taken to accommodate such movement, ie cutting and forming a movement joint.

Contact your local Parbury Technologies branch for further information.

Estimating

Nitofill LV resin:	450 ml pack (12 per carton)
Lokset E:	1.5 and 6 litre packs
Fosroc Solvent 10:	20 litre pails

Nitofill LV system accessory items

Nitofill LV Gun:	single item
Nitofill LV Flange:	50 per bag
Nitofill LV Adaptor:	10 per bag
Nitofill LV Static mixer/hose:	10 per bag
Nitofill LV Flange tool:	10 per bag

Storage

Nitofill LV resin, Lokset E and Fosroc Solvent 10 have a shelf life of 12 months if kept in dry conditions at 20°C.

Precautions

Fire

Fosroc Solvent 10 is flammable. In the event of fire extinguish with CO_2 or foam.

Health and safety

Nitofill LV resin and Lokset E contain resins which may cause sensitisation by skin contact. Avoid contact with skin and eyes and inhalation of vapour. Wear suitable protective clothing, gloves and eye/face protection. Barrier creams provide additional skin protection. Should accidental skin contact occur, remove immediately with a resin removing cream, followed by soap and water. Do not use solvent. In case of contact with eyes, rinse immediately with plenty of clean water and seek medical advice. If swallowed seek medical attention immediately - **do not** induce vomiting.

Fosroc Solvent 10: Flammable liquid.
Flash point: 27°C.

Keep away from sources of ignition - no smoking. Wear
suitable protective clothing, gloves and eye/face protection.
Use only in well ventilated areas.

A product Material Safety Data Sheet is available to users on
request to their nearest Parbury Technologies branch. Read
MSDS and product data sheet carefully before first use. In
emergency, contact any Poisons Information Centre.

Manufactured and sold under license from Fosroc International Limited,
England. Fosroc, the Fosroc logo, Nitofill and Lokset are trade marks of
Fosroc International Limited, used under license.

PARBURY
TECHNOLOGIES

PARBURY TECHNOLOGIES PTY LTD
A.C.N. 069 961 968

33 Lucca Road
NORTH WYONG, N.S.W. 2259
Tel (02) 4350 5000
Fax (02) 4351 2024

Sales Offices:

St Peters, Sydney	(02) 9519 4722
Wetherill Park, Sydney	(02) 9604 9399
Archerfield, Brisbane	(07) 3255 5666
Gold Coast	(07) 5539 3822
Townsville	(077) 254 394
Gladstone	(079) 726 499
Adelaide	(08) 8293 2222
Perth	(08) 9356 2533
Melbourne	(03) 9326 3100

7 days a week, 24 hour   1800 817 779
Technical Support Hotlines :   1800 812 864

Important note

Parbury Technologies products are guaranteed against defective materials and manufacture and are sold subject to its standard terms and conditions of sale,
copies of which may be obtained on request. Whilst the company endeavours to ensure that any advice, recommendation, specification or information it may
give is accurate and correct, it cannot, because it has no direct or continuous control over where or how its products are applied, accept any liability either
directly or indirectly arising from the use of its products, whether or not in accordance with any advice, specification, recommendation or information given
by it.

AUS/121/97/B

APPENDIX E

Risk Assessment

Description of hazard	Hazard Category	People at Risk	Injury Type	Risk level	Risk Management
Cuts when assembling cages	Sharp objects	People cutting, bending or tying reinforcement (1-2 people)	Cuts to hands and arms	Low	Hold reinforcement in vice when cutting, take care when assembling cages
Slipping on wet floor when casting	Gravity	All in area (up to 6 people)	Could injure any part of body	Low	Avoid too much spillage of concrete, Wear boots with slip resistant or good grip sole
Test beams falling over when loading, post tensioning, moving, or curing	Gravity	People within 1m of beams (up to 6 people)	Crushing of legs or feet	High	Wear steel capped boots, check support conditions, secure chains when moving, and avoid high stacks when curing
Lifting heavy objects (i.e. moving or positioning beams)	Gravity	Up to 6 people	Muscular injuries to back, legs, or arms	Moderate	Use lifting trolley or forklift to move beams, manual lifting only for final positioning (use correct lifting position)
Breaking or slipping of post tensioning rods	Mechanical Energy	All in area (up to 6 people)	Severe impact to any part of body	Very high	Check equipment thoroughly, no standing allowed behind either end of the rods when loaded, erect warning signs when post-tensioning in progress
Contact with epoxy resin or crack sealant	Harmful Substance	People when applying adhesives (1-2 people)	Skin irritation, respiratory problems	Low	Wear gloves and long sleeve shirt, Follow MSDS handling instructions
Removal of Lokfix E sealant	Harmful Substance	People grinding sealant off (1-2 people)	Respiratory problems	Low	Wear dust mask when grinding sealant